The Statistical Properties of the Particle Radial Diffusion in the Presence of the Magnetic Field Irregularities

Maluckov, Aleksandra A.

DOCTOR OF PHILOSOPHY

Department of Fusion Science
School of Mathematical and Physical Science
The Graduate University for Advanced Studies

2001 (School Year)

Acknowledgements

First of all, I would like to thank Professor M. Okamoto whose elaborate guidance and advices in discussion benefit me throughout my graduate study. Moreover, I wish to thank him for providing me opportunity to study plasma physics in School of Mathematical and Physical Science, Graduate University for Advanced Studies (GUAS) in Japan.

I express my gratitude to Dr N. Nakajima for his valuable suggestions and elaborated guidance based on the remarkable understanding in physics throughout my doctor course.

My appreciation to Dr S. Murakami and Dr R. Kanno for continuing support and valuable discussions.

I am also thankful to Dr M. Yokoyama, Dr K. Ichiguchi and Dr R. Ishizaki who helped me to understand complexity of plasma physics.

Abstract

The purpose of this study is to clarify the statistical properties of the particle radial diffusion in an radially bounded magnetic field region with irregularities, where the collisional (statistical) stochasticity and the magnetic (deterministic) stochasticity coexist. Note that, contrary to other works, the boundedness of the magnetic stochastic region is included and the statistical properties of the magnetic stochasticity are not postulated.

By analyzing the statistical quantities, the radial diffusion is recognized as one of the following three processes:

(a) The Wiener process (standard Brownian motion) characterized by a power-law autocorrelation coefficient, normal diffusive behaviour, Gaussian distribution, Markovianity, and statistical non-stationarity

(b) the uniform mixing process characterized by an exponentially vanishing autocorrelation coefficient, non-diffusivity, uniform distribution, Markovianity, and statistical stationarity

(c) the strange diffusive process characterized by a power-law autocorrelation coefficient, subdiffusivity or non-diffusivity, neither Gaussianity nor uniformity, and statistical non-stationarity. The strict justification of Markovianity remains open problem.

Extensive numerical analyses are performed in two dimensional $(s_b/s_{bc}, \nu/\nu_t)$ parametric space, where s_b and ν are the strength of the magnetic field perturbation and the collision (deflection) frequency, respectively. The normalization parameter s_{bc} corresponds to the islands overlapping criterion, and ν_t is the characteristic frequency of the passing particle motion. In conclusion, the following is shown.

(1) The radial diffusion only due to the collisional stochasticity in a regular magnetic field (neoclassical transport with $\nu \neq 0$ and $s_b = 0$)

  (i) is initialized in the velocity space by the pitch angle scattering which is a uniform mixing process

  (ii) develops as a Wiener type process in the configuration space .

  The statistical properties of the neoclassical radial diffusion are generically associated with the locality of the particle radial displacements.

(2) The radial diffusion only due to the magnetic field stochasticity ($\nu = 0, s_b \neq 0$)

  (i) appears as a strange diffusive process when $s_b/s_{bc} \geq 1$,

  (ii) appears as an uniform mixing process when $s_b/s_{bc} \gg 1$,

The statistical properties of the magnetic stochasticity are associated with the non-locality of the radial displacements of the stochastic magnetic field lines.

(3) The radial diffusion due to both the collisional (statistical) and the magnetic (deterministic) stochasticity ($\nu \neq 0$ and $s_b \neq 0$)

   (i) develops as a strange diffusive process in almost all parameter space,

   (ii) appears as the Wiener process only when the collisional decorrelation of particle orbits from magnetic field lines is strong enough.

   From the viewpoint of the locality of the particle radial displacements, the Wiener domain is reached when the locality is established by the enough effective collisions.

From above results, it may be concluded:

- The constant diffusion coefficient has sense only in the limited regions in the $(s_b/s_{bc}, \nu/\nu_t)$ parametric space, i.e. in the regions where the radial diffusion realizes as the Wiener type process.
- The particularity of the deterministic stochasticity have to be accounted.
- The particle radial diffusion should to be reconsidered from the viewpoint of the non-local transport.

Contents

1 Introduction

Being out of equilibrium, due to internal or external forces, a physical system relaxes to the state which is determined under given conditions by the requirements of the so called H-theorem, or S-theorem [1] (closed, and open system, respectively). In other words, the relaxation follows the simple rule which is contained in the formulation of the principle of minimum entropy production in stationary state [1]. Note that the entropy is adopted as a relative measure of the uncertainty of the statistical description of physical system.

Generally, the slow relaxation process is treated as a diffusion process [1]. According to this, the diffusion process is recognized as a characteristic of the final stage of relaxation towards equilibrium. However, such a determination assumes that the system relaxation may be described beyond several strictly distinct time (length) scales, among which that for a diffusion will be the longest one.

For example, in unified kinetic and hydrodynamic theory [1], the diffusion characteristic time, τ_d, the mean free path time , τ, and the characteristic time for the system to be described by statistical system, τ_{ph}, are ordered as

$$\tau_{ph} \ll \tau \ll \tau_d$$

The first one, τ_{ph}, is according to Krilov [2] clarified by the characteristic time of development of the dynamical (exponential) instability of motion per one particle within physically infinitesimal volume. Thus, unique definition of the border for an relaxation process to be treated as a diffusion is missing. In other words, the actual physical conditions determine conclusions about the type of the relaxation process. To describe the diffusion process theoretical approaches are based on analogy between the transport problem and the Gaussian random walk or standard Brownian motion theory and complementary kinetic approach [3, 4]. Briefly it can be illustrated starting with the classical diffusion of an ensemble of identical particles suspended in a fluid (plasma) which is based on two physical postulates: the net transport of the particles across a unit surface is proportional to the gradient of the particle density normal to the unit area, and in an unbounded medium the number of particles is conserved. Two mentioned concepts are modeled by the local Fick's law: $\vec{j} = -D\nabla n$, and the continuity equation

$$\frac{\partial n}{\partial t} + \nabla \vec{j} = 0$$

where $n = n(\vec{x}, t)$ is the number of suspended particles per unit volume at $\vec{x}$ and time t, D is the diffusion coefficient which is postulated to be constant, and $\vec{j}$ is the particle current, $\vec{j} = \vec{v}n$ with $\vec{v}$ the local velocity. Because of simplicity one dimensional examples are presented in the following. As a result the diffusion equation is obtained

$$\frac{\partial n}{\partial t} = D\frac{\partial^2 n}{\partial x^2},$$

or including streaming

$$\frac{\partial n}{\partial t} = D\frac{\partial^2 n}{\partial x^2} - v\frac{\partial n}{\partial x}.$$

The solution of the last equation subject to a sharp delta function initial condition $n(x,0) = \delta(x - x_0)$ in an unbounded medium is the propagating Gauss packet

$$n(x,t) = \frac{1}{(4\pi Dt)^{1/2}}\exp\left(-\frac{(x - x_0 - vt)^2}{4Dt}\right),$$

characterized with

$$\langle x\rangle = x_0 + vt, \quad \text{and} \quad \langle (x - \langle x\rangle)^2\rangle = 2Dt,$$

where $\langle x\rangle$ denotes average with respect to $n(x,t)$.

In the theory of Brownian motion a stochastic process is often characterized by the Bachelier-Smoluchowski-Chapman-Kolmogorov (BSCK) chain equation [3, 4, 5]

$$f(x_2,t_2|x_0,t_0) = \int_{-\infty}^{\infty} f(x_2,t_2|x_1,t_1)f(x_1,t_1|x_0,t_0)dx_1,$$

where $f(x_2,t_2|x_1,t_1)$ is the probability that a variable $x(-\infty < x < \infty)$ suffers a transition from x_1 to x_2 in time $t_2 - t_1$. In the statistical theory this is connected with Markov property. When moments exist for various transit probabilities the chain equation is easily converted into a Fokker-Plank differential equation similar to the diffusion equation. In the case of a translationally invariant stochastic process with

$$f(x_2,t_2|x_0,t_0) \equiv f(x_2 - x_0, t_2 - t_0)$$

adopting the Fourier transform

$$\hat{f}(k,t) \equiv \int_{-\infty}^{\infty} f(x,t)\exp(ikx)dx$$

and the convolution theorem for Fourier transforms BSCK equation yields

$$\hat{f}(k,t_2 - t_0) = \hat{f}(k,t_2 - t_1)\hat{f}(k,t_1 - t_0),$$

when it is apparent that the Gauss packet is one of the solutions. The last property is called self-similarity. Thus, equivalence between the classical diffusion and the Brownian motion (central limit theorem) is established.

In the terms of the random walk theory [3, 4, 6], the classical diffusion of random walker is observed. Defining, the probability density function, $n_j(x)$, of the position x_j of a walker after j steps and $f(x)$ the probability density function for the displacement of the walker at each step, the functions $[n_j(x)]$ are related through the recurrence formula

$$n_{j+1}(x) = \int_{-\infty}^{\infty} f(x - x')n_j(x')dx'$$

For a walker initially at the origin $n_0(x) = \delta(x)$ the propagating Gauss packet results after the random walk with successive equal displacements which occurred at regular

intervals. Corresponding characteristic (structure) function which appears in the random walk generating function [3]

$$\hat{f}(k) = 1 + ik\langle x\rangle - \frac{1}{2}k^2\langle x^2\rangle$$

is characterized by two non-vanishing cumulants

$$C_1(t) = \langle x\rangle, \qquad C_2(t) = \langle (x - \langle x\rangle)^2\rangle = 2Dt$$

i.e. it is Gaussian. The distribution of jump times of random walker is a Poisson like with at least

$$\langle t\rangle \approx \tau_{corr}$$

where τ_{corr} is the correlation time. The diffusion coefficient is constant

$$D = \frac{\langle \Delta x^2\rangle}{2\Delta t} \equiv \frac{dC_2(t)}{2dt}$$

Therefore, the classical diffusion is interpreted as a Markov, Gaussian, and normal diffusive stochastic process. As a consequence the Einstein relation from transport theory [2], which states that the mean square displacement is proportional to the time, with the proportionality coefficient equal to the diffusion coefficient is established.

The implementation of boundaries to the free diffusion of particles affects the statistical properties of the diffusion process [1]. Moreover, the recent developments in physics of systems out of equilibrium [6]-[9], e.g. transport in disordered systems, transport theory of Hamiltonian systems, turbulence theory, etc., treat the diffusive process as a synonym for a relaxation process. Actually, the strict distinction of the characteristic time (length) scale is not possible, i.e. the relaxation develops beyond many scales, but no one scale will be characteristic and dominate process [9]. For example, in order to describe the relaxation in disordered media, the continuous time random walk theory (CTRW) [3, 4] concerns with random walk generated by steps taken at regular time intervals $\tau, 2\tau, 3\tau, \ldots$. Actually, the particle may be trapped (stuck), and accelerated by the fractal structure of medium and it may happen that corresponding probability density function, $\psi(t)$, for pausing times between successive steps in the walk is characterized by the infinity first cumulant $\langle t\rangle \to \infty$, i.e. the characteristic time of process is absent. To understand the transport problem in complex system the non-Gaussian random walk, i.e. general Brownian motion theory, and complementary strange kinetic theory are adopted [6, 8, 9]. In other words, the standard approach based on Gaussianity, Markovianity, and normal diffusivity is naturally extended (so called generalized central limit theorem (CLT)). Simply, the self-similarity is showed to be property of the Levi-functions in space, and (or) time for which the second cumulant and (or) the first cumulant and higher cumulants, are infinite: these are distributions with long tail in space and (or) time. The physical system experiences the Levy-flights during the definite interval of time, thus the superdiffusivity is found [10]

$$C_2(t) = x^\alpha, \qquad \alpha > 1$$

It is interchanged with the trapping phases during which the diffusion is slowed down

$$\alpha < 1$$

and subdiffusivity is detected. The strange diffusive behaviour is generically connected with the apparent non-Gaussianty, and non-Markovianity (during the subdiffusive phases the system carries information from successively states). The usual definition of the diffusion constant is meaningless. There are some tendencies [8, 9] (generalized Fokker-Plank equation approach) for a process which is not smooth and homogeneous in x, t to use

$$\mathcal{D} = \lim \frac{|\Delta x|^{2\alpha}}{|\Delta t|^{\beta}}, \text{where} \quad \Delta x, \Delta t \to 0$$

instead of D. The problem is physical meaning of the coefficients α, and β. It seems that they are connected with the properties of the phase space of the system under consideration.

The particle radial diffusion is a problem of great importance in the context of the transport in a magnetically confined plasma. The earliest theoretical approaches [11]-[18] treat it as a classical diffusion with premise to determine the constant diffusion coefficient. Thus, the Gaussianity, Markovianity, and normal diffusivity of the collisional radial diffusion are assumed a priori. The usual diffusion constant is then obtained as the long time limit of the second cumulant (mean square displacement) under constraint that the diffusion is local. The locality constraint is necessity in order to treat the diffusion process in real system, which is usually inhomogeneous and bounded, from the viewpoint of the standard diffusion theory established for homogeneous and unbounded system. In the regular magnetic field with toroidally nested flux surfaces (domain of the neoclassical theory) the radial diffusion (in configuration space) is completely determined by the deterministic drift motion of particle guiding centers inherent in such a geometry and the stochasticity due to the Coulomb collisions in velocity space. The locality constraint is ensured with respect to the smallness of the particle displacement which is of the order $\rho_p/a \ll 1$, where ρ_p is the particle poloidal gyroradius, and a is the minor radius. The properties of the neoclassical radial diffusion are categorized quantitatively according to the relative magnitude between the characteristic frequency (time) of the stochasticity (Coulomb collision frequency) ν ($\tau_c = \nu^{-1}$), and those of the drift motion. In axisymmetric tokamaks, the deterministic drift motion of guiding centers has two types of characteristic frequency (times): the bounce frequency ν_b (τ_b), and the transit frequency $\nu_t(\tau_t)$. Thus three asymptotic regimes exist: collisionless banana regime, $\nu \ll \nu_{bc}(\tau \gg \tau_{bc})$; intermediate plateau regime, $\nu_{bc} \ll \nu \ll \nu_t(\tau_{bc} \gg \tau \gg \tau_t)$, and collisional Pfirsch-Schlüter regime, $\nu_t \ll \nu(\tau_t \gg \tau_c)$, where $\nu_{bc} = \nu_b \varepsilon$ is the effective bounce frequency with ε being the inverse aspect ratio. For each asymptotic regime, the diffusion coefficient ($\nu t \gg 1$) is obtained by using a variational approach [11], or a moment approach [12]. In this study, to investigate the statistical properties of the neoclassical radial diffusion the Monte Carlo technique

is used. The adopted magnetic field is an tokamak equilibria with perfect nested flux surfaces and the Coulomb collisions are introduced by the pitch-angle scattering in the velocity space. The neoclassical radial diffusion appears as a Wiener process which is associated with the locality of the particle radial displacements due to the particle drift motions and the Coulomb collisions. In other words, the assumptions of the neoclassical theory about the normal diffusivity, Gaussianity, and Markovianity of the particle radial diffusion are justified. Additionally, the time-independent neoclassical diffusion coefficient is obtained.

However, experimentally obtained diffusion coefficients are usually much greater than the neoclassical ones. As one of the reasons, the destruction of the regular magnetic surfaces due to MHD instabilities and error fields is suggested. Even if the amplitude of the magnetic field perturbations is small, they can change the topology of the magnetic field structure due to the resonance at their mode rational surfaces, namely, the magnetic islands and stochastic region are created [4, 13]. Usually, many Fourier modes of the magnetic perturbation can be simultaneously excited, and so the radially extended magnetic stochastic region appears after the overlapping of the magnetic island chains, i.e. the global magnetic stochasticity is created as the amplitude of the magnetic perturbation increases [4, 13]. Thus, with the increase of the stochasticity level, the particle radial diffusion in the stochastic magnetic field region comes to be prescribed by the statistical properties of the stochastic magnetic field lines themselves.

In order to estimate the diffusion coefficient of the static highly stochastic magnetic field, the correlation of the radial component of the perturbed magnetic field between two different points (Eulerian correlation) is specified by two characteristic lengths of the stochastic magnetic field lines: the parallel $L_{\|}$ and perpendicular length $L_{\perp}$ to the equilibrium magnetic field lines [14]. Moreover, the stochastic magnetic field is characterized by another characteristic length, radial Kolmogorov length L_K, which is associated with the fast exponential divergence of the stochastic magnetic field lines in the radial direction [15]-[17]. Depending on the relative magnitude of these three characteristic lengths: $L_{\|}, L_{\perp}$ and L_K, the various types of diffusive regimes are defined. The most famous one is the quasilinear regime, where the relation

$$L_{\|} \ll L_K \ll L_{\perp} < L$$

holds, and L is the length of the stochastic region. In this limit, the constant diffusion coefficient of the stochastic magnetic field lines is derived by postulating that in a radially unbounded stochastic magnetic field region ($L \to \infty$), the magnetic field stochasticity appears as a radially homogeneous, Gaussian random process with $L_{\|} \ll L_{\perp} \to \infty$. The quasilinear diffusion coefficient is proportional to the square of the amplitude of perturbation. It is worth to mention, frequently discussed percolation diffusive regime

defined by

$$L_{\|}\left|\frac{\delta\vec{B}}{B}\right| \gg L_{\perp},$$

where $|\delta\vec{B}/B|$ is the magnitude of the magnetic perturbation [17]. The percolation diffusion coefficient is constant and proprtional to the magnitude of the perturbation. Note that the quasilinear limit can be written in equivalent form as

$$L_{\|}\left|\frac{\delta b}{B}\right| \ll L_{\perp}.$$

The radial unboundedness of the homogeneous stochastic region is equivalent of the locality constraint in the neoclassical particle radial diffusion in the regular magnetic field configuration. In the quasilinear regime, the evaluation of Lagrangian correlation, i.e. evaluation of the correlations along the magnetic field lines, is easily performed due to the feature of $L_{\perp} \to \infty$ [18]. When the perpendicular characteristic length $L_{\perp}$ is finite, the Corrsin approximation is used to evaluate the Lagrangian correlation [18]. However, this approximation is valid only for a homogeneous equilibrium magnetic field without a magnetic shear [19].

On the basis of the diffusion of the stochastic magnetic field lines, the diffusion coefficient of the radial heat (particle) transport is calculated under the influence of the Coulomb collisions. It is reasonably assumed that the particle displacements due to collisions appear as a standard (Gaussian) Brownian process with the mean free path λ_{mfp} as the characteristic length. Thus, depending on the relative magnitude of four characteristic lengths: $L_{\|}, L_{\perp}, L_K$, and λ_{mfp}, several asymptotic diffusive regimes are obtained. In the pioneering paper [15], both the collisionless and collisional limits are considered in the quasilinear regime of the magnetic field stochasticity. For both of them, the time independent diffusion coefficient is found, which means that the particle radial diffusion is a normal diffusive process like a standard Brownian motion. However, the particle diffusion coefficient becomes time-dependent in the absence of any perpendicular motion to the stochastic magnetic field lines. This case corresponds to the subdiffusive process, where the diffusion coefficient decreases with time. The existence of subdiffusivity influenced extensive investigations of the particle radial diffusion in the highly stochastic magnetic field [20, 21, 22, 23]. For example, in paper [20] from the viewpoint of the standard diffusion theory the Langevin equation, hybrid, and kinetic methods, and in paper [21] the continuous time random walk theory are applied in order to describe the particle radial diffusion in the presence of the stochastic magnetic field. In this approaches the particles are tied to the magnetic field lines, i.e. the particles move in radial direction only as far as the field lines radially diffuse, and undergo so called parallel collisions with surrounding plasma. Namely, the magnetic stochasticity is a spatially homogeneous, static Gaussian process, the Coulomb collisions are modeled as a Gaussian process in velocity space and

the perpendicular drift motion is neglected. The results are the long time limit subdiffusivity, and time dependent diffusion coefficient independent on approach [20, 21]. But, the particle radial diffusion is characterized by the Gaussian profile and Markovianity from the viewpoint of the standard diffusion theory, while the CTRW describes it as a non-Gaussian and non-Markov process modeled by the non-Markov diffusion equation [3]. Thus, these are the first indications that the statistical approach based on the mean square displacement is insufficient in order to understand the physics of the particle radial diffusion. Inclusion of the perpendicular drifts leads system to the normal diffusive behaviour [22].

In all previous treatments of the particle radial diffusion in the highly stochastic magnetic field, it is worth to stress that the allowable analytical approaches assume unboundedness and inhomogeneity of the highly stochastic magnetic field and specify the statistical characteristics of the magnetic field perturbation. Thus, there are ambiguous points when such analytical results are applied to a realistic system as the ideal limits. Especially, the treatment of the statistical properties of the stochastic magnetic field in the radial direction leads to problems. In torus systems, generally, the equilibrium magnetic field is inhomogeneous in the radial direction due to the magnetic shear, and the magnetic stochastic region created by perturbed magnetic fields, e.g. due to MHD instabilities or error fields, is usually bounded in the radial direction. It means that the Corrsin approximation is not valid and the perpendicular characteristic length $L_\perp$ should to be treated as finite. From the technical point of view, due to the inhomogeneity and boundedness in the radial direction, the Fourier transformation is not applicable to the radial direction, which means that the approach to assume the Eulerian correlation function in the Fourier space may not be directly applicable to the systems with inhomogeneous and bounded stochastic region in the radial direction. Thus, in the realistic magnetic field configurations with radially bounded and inhomogeneous stochastic regions, the applicability of the previous analytical results is under question. As another aspect, it should be pointed out that the physical interpretation why the above mentioned subdiffusivity of the radial diffusion occurs is not so clear. The reason may not be unique depending on the situations which are investigated. However, in the present context as one of reasons, the non-locality of the particle radial displacements is considered. Up to now, the role of non-locality has not been properly mentioned.

On the other hand in the case before overlapping, near overlapping, and moderate overlapping, the magnetic field inside the stochastic region is generally neither entirely regular nor entirely irregular, but a complicated mixture of regular and irregular regions. In the regular island like regions, the magnetic field lines lie on tori or KAM surfaces [4, 13], while in irregular domains the magnetic field lines are apparently stochastic, or chaotic indicating the deterministic stochasticity [4, 13]. With stress on the enhancement of the time-independent diffusion coefficient of the collisional radial diffusion due to the magnetic

field destruction, the series of researches are developed [24, 25, 26]. To ensure locality, i.e. not to allow large particle displacements from the initial flux surface, the value of the diffusion coefficient is evaluated in the interval of the order of several collisional times. In these cases, the statistical treatment of the particle radial diffusion inside the partially destroyed magnetic field region is missing. However, the non-Gaussianity and strange diffusivity (supperdiffusivity and subdiffusivity) of the magnetic field stochasticity in the presence of regular structures are suggested from analogy with the standard mapping [27, 28, 29].

To avoid problems coming from the applicability of the analytical results in an idealized situation to a realistic one, to clarify the relationship between expected various diffusion processes and non-locality of the particle radial displacements, and to clarify the statistical properties of the various types of irregular magnetic field themselves, the statistical properties of the magnetic and particle radial diffusion have been examined for various values of the stochasticity parameter and the Coulomb collision frequency by using direct numerical calculations of the trajectories of magnetic field lines and Monte Carlo simulations of the particle radial diffusion. The adopted system consists of both an axisymmetric MHD equilibrium with perfect nested flux surfaces and a radially bounded irregular magnetic field created by superposing the three Fourier harmonics of a magnetic perturbation which resonate at their mode rational surfaces. By changing values of the strength of perturbation, which is treated as a stochasticity parameter, the level of stochasticity is controlled. Thus, four types of the radially bounded magnetic stochastic region are created: region with isolated island chains under the overlapping threshold, with weak overlapping of the magnetic islands, with moderate overlapping characterized by the mixture of regular and irregular domains, and with highly irregular stochastic magnetic field lines. The statistical properties of the magnetic stochasticity, which realizes within the radially bounded stochastic region, are not assumed, but examined by numerically calculating the Liapunov exponent [13], the cumulant up to the fourth order [30, 31], and the autocorrelation coefficient [5, 30]. It is found that as the level of stochasticity increases, the magnetic field stochasticity inside the radially bounded perturbed magnetic field region tends to appear as a uniform mixing process characterized by non-diffusivity, radially uniform distribution, statistical stationarity, and Markovianity. The uniform mixing process, which stems from both the radial boundedness of the stochastic region and fast exponential divergence of the magnetic field lines in the radial direction, is firstly mentioned in the context of the particle radial diffusion in the stochastic magnetic field. Note that the radial diffusion of the guiding center particles tied to the stochastic magnetic field lines without both the perpendicular drifts and Coulomb collisions is equivalent to the radial diffusion of the magnetic field lines.

After clarifying the statistical properties of the magnetic field stochasticity within the radially bounded magnetic field region, the effects of the perpendicular drift of guiding

centers and of the Coulomb collisions are investigated through the Monte Carlo technique. The perpendicular drifts qualitatively do not change the statistical properties of the particle radial diffusion, since the radial displacement due to the fast parallel drift motions along the stochastic magnetic field lines is dominant compared with that due to the slow perpendicular drift motions. Thus, the statistical properties of the collisionless particle radial diffusion in the radially bounded stochastic magnetic field are prescribed by those of the stochastic magnetic field, and the particle radial diffusion is non-local. The Coulomb collisions interrupt the fast parallel motions along the stochastic magnetic field lines. As the stochasticity parameter increases and collision frequency decreases, the particle radial diffusion appears as a strange diffusive process characterized by subdiffusivity, neither uniform nor Gaussian profile, statistical non-stationarity, reflecting the statistical properties of the magnetic stochasticity. The radial diffusion is still non-local in this regime. In the opposite limit with small stochasticity parameter and a high collision frequency, the radial exponential divergence of the magnetic field lines is suppressed, and the frequent collisions recover the locality of the diffusion, so that the diffusion appears as the Wiener process which is previously recognized in the neoclassical radial diffusion in the regular magnetic field [32]. It is clarified that non-locality of the particle radial displacements leads to non-diffusivity or subdiffusivity in a radially bounded stochastic magnetic field region. The stochastic parameter is interpreted as the indicator of the non-locality of the particle radial displacements, and the Coulomb collision frequency is recognized as the scattering rate of such the non-local displacements. Thus, as a result of the superposition of these two effects, the degree of the non-locality of the particle radial displacements is determined, leading to various types of diffusion process.

The organization of this study is as follows. In the present context, the particle radial diffusion is synonym of a relaxation of the magnetic (deterministic) stochasticity, and the collisional (statistical) stochasticity. To investigate statistical properties of such a complex problem in first section the basic concepts in theory of stochastic processes are shortly mentioned: random walk, probability concept, deterministic, and statistical stochasticity.

In section 2, the basic equations of the guiding center electrons, the numerical Monte Carlo method, and magnetic field configuration consisting of an axisymmetric MHD equilibrium and a radially bounded magnetic field region with irregularities are described. As the statistical measures the cumulant up to the fourth order, the diffusion coefficient and autocorrelation coefficient are defined in section 3. Additionally, the effective radial Liapunov exponent is introduced in connection with the magnetic stochasticity. By using these measures, the statistical analyses are performed in section 4 by comparing numerically obtained process with the fundamental diffusive process: the Wiener process in infinite domain; and the fundamental process from the viewpoint of the deterministic stochasticity: the uniform mixing in finite domain of configuration space. In section 4.1 the statistical properties of the collisional stochasticity in the velocity space and the

configuration space are investigated. It is shown that the particle radial diffusion in the regular magnetic field is the Wiener process due to the locality of the particle radial displacements according to the negligible small deviations of particle orbits from the starting flux surface due to perpendicular drift motions and the Coulomb collisions, compared with the minor radius which appears as a characteristic dimension of system. Section 4.2 is devoted to the statistical analysis of the magnetic field stochasticity which is meaningful in the region of so called global magnetic stochasticity initialized by the overlapping between two neighboring islands. One fitting equation is given for all mentioned stochastic levels in the region of global stochasticity, by which the saturated value of the effective radial Liapunov exponent is estimated. Additionally the number of the magnetic field lines with positive radial Liapunov exponent is taken as an indicator of the existence of the regular structures inside the stochastic region. In section 5.1, the effects of the perpendicular drift motions on the statistical properties of the radial diffusion in the radially bounded stochastic magnetic field region are presented. The statistical properties of the particle radial diffusion in the presence of both the magnetic field stochasticity inside the radially bounded perturbed magnetic field region and the collisional stochasticity due to the Coulomb collisions are investigated in section 5.2. The statistical properties are investigated in two-parameter space consisting of above mentioned four levels of stochasticity and for three collision frequencies corresponding to plateau, and Pfirsch-Schlüter region. In section 6, the characteristic lengths, the locality of diffusion, the second cumulant, and the ballistic phase in the highly stochastic magnetic field are discussed. It is shown that the present situation with radially bounded stochastic field is characterized by completely different ordering of the characteristic lengths from that in the quasilinear regime. Also, it is shown that the diffusion coefficient defined by the time derivative of the second cumulant has no clear physical meaning when the locality of the diffusion is not ensured. Moreover, the short time ballistic phase in the highly stochastic magnetic field is discussed associated with the dynamical relaxation to an equilibrium. Section 7 presents conclusions.

1.1 On random phenomena

The large scale random phenomena in their collective action may create strict non random irregularity [3]. Starting from this premise, the theory of probability goes beyond the traditional Brownian motion based on Gaussian central limit theorem [5, 6] to the fractal Brownian motion with whom the class of Levy-flight random walks [3, 10], and continuous time random walks [3, 4] are associated. Accordingly the generalized central limit theorem is adopted [6].

Let walker performs at each step a jump of length x_n independently chosen at each step according to a given distribution $f(x)$, which decreases for large x as $|x|^{-(1+\mu)}$ (with $\mu > 0$ to allow normalization). After N steps, its position is the sum of N independent

displacements

$$X_N = \sum_{n=1}^{N} x_n \tag{1}$$

Note that

$$\langle x^a \rangle = \int x^a f(x) dx \tag{2}$$

and

$$X_N^a = N\langle x^a \rangle \approx N \int_{x_c} x^a f(x) dx \tag{3}$$

where $x_c \approx N^{1/\mu}$ is the largest value among N terms of the sum (1) [6].

Then:

(i1) for $0 < \mu < 1$, X_N behaves typically as $N^{1/\mu}$ (or $N\ln N$ if $\mu = 1$). Note that $\langle x \rangle$ is infinite in this case;

(i2) for $1 < \mu < 2$, $\langle x \rangle$ is finite while the difference $X_N - \langle x \rangle N$ again behaves typically as $N^{1/\mu}$, (or as $\sqrt{N \ln N}$ for $N = 2$). Note that the variable $\overline{X_N^2} - \overline{X_N}^2$ is still infinite;

(i3) for $\mu \geq 2$, writing $t = n\tau$, $\langle x^2 \rangle$ is finite and $\overline{X_N} = Vt, \overline{X_N^2} - \overline{X_N}^2 = 2Dt$ where parameter τ is the time step, V is the velocity

$$V = \frac{\langle x \rangle}{\tau}$$

and D is the diffusion coefficient

$$D = \frac{\langle x^2 \rangle - \langle x \rangle^2}{2\tau}$$

Stated more precisely [6], the variable $Z_N = X_N / N^{1/\mu}$ for $0 < \mu < 1$, $(X_N - \langle x \rangle N)/N^{1/\mu}$ for $2 > \mu > 1$, has a limit distribution when $N \to \infty$ in the sense

$$\text{Probability}(u_1 < Z < u_2) \to_{N \to \infty} \int_{u_1}^{u_2} L_{\mu,\beta}(u) du$$

and when $\mu \geq 2$

$$\text{Probability}(u_1 \leq \frac{X_t - Vt}{\sqrt{2Dt}} \leq u_2) \to_{t \to \infty} \int_{u_1}^{u_2} G(u) du$$

The limit distributions $L_{\mu,\beta}$ and G ($G = L_{\mu=2,0}$) are defined by their characteristic functions (Fourier transforms) $\hat{f}(k)$

$$\hat{f}(k) = \int d^3x \exp(ikx) f(x) = \exp(-C|k|^\mu), \quad 0 < \beta \leq \mu \text{ and } C = \text{const.} \tag{4}$$

They are called Levy (Gaussian when $\mu = 2$) or "stable" laws of index μ. The last denotes the invariant property of the characteristic functions which may be written as

$$\hat{f}(a_1 k)\hat{f}(a_2 k) = \hat{f}(ak)$$

where $a_{1,2}$ are given positive constants and a is function of latter [4, 6]. Up to translations and dilatations the Levy laws are fully characterized by the two parameters μ and β ($0 < \mu \leq 2$, $-1 \leq \beta \leq 1$). The latter characterizes its degree of asymmetry [4, 6] which depends on the relative frequency of occurance of large positive and negative increments in the sum (1). In other words, the limit distributions $F_N(x)$ for the sum of N steps (1) have the same distribution $f(x)$ (up to scale factors) as the individual steps. The infinite value of the second moment of $f(x)$ when $\mu < 2$ means that there is no characteristic size for the random walk jumps, except in the Gaussian case of $\mu = 2$. It is just this absence of a characteristic scale that makes Levy random walks (flights) scale invariant fractals. Thus to employ Levy flights for trajectories, one introduces velocity through a coupled spatial-temporal probability density $\psi(x,t)$ for a random walker to undergo a displacement x in a time t [9, 10]

$$\psi(x,t) = \psi(x|t)f(x)$$

Putting for simplicity $\psi(x|t) \approx \delta(t - |x|/V(t))$, it may be seen that such random walks with explicit velocities (which can depend on the size of jump [10]), visit all points of the jump on the path between 0 and x. For various values of μ, that leads to the following different time dependencies of the mean square displacement

$$\langle x^2(t) \rangle \approx t^\alpha, \tag{5}$$

where with $\alpha > 1$ superdiffusive behaviour is associated.

On the other hand the random walk is characterized by the waiting time probability distribution function $w(t)$ (probability density of duration t between two successive steps of walker), and characteristic waiting time $\langle t \rangle$. The traditional Brownian motion is described by the waiting time probability which is in the long time limit given as

$$w(t) \approx \exp(-\frac{t}{\tau}) \tag{6}$$

and corresponding $\langle t \rangle$ is finite

$$\langle t \rangle = \tau \tag{7}$$

In the presence of trapping effects [1] in the real dynamic systems $\langle t \rangle$ may diverge what is manifested as subdiffusion [4, 9]. This divergence comes about by Levy-type waiting time distribution function with the long time behaviour (power-law like)

$$w(t) \approx \frac{\tau^\eta}{t^{1+\eta}}, \tag{8}$$

[1] **Trapping describes the occasional immobilization of the random walking test particle or a waiting time which defines the time span elapsing between the immobilization and the subsequent release of the test particle.**

where $0 < \eta < 1$, and τ is an intrinsic time scale of the waiting process. Such a random walk is treated by the theory of continuous time random walk (CTRW) [3, 4, 9], and it is proved that

$$\langle x^2 \rangle \approx t^{\alpha}, \tag{9}$$

where $0 < \alpha < 1$. The real physical systems may include both the enhanced diffusive behaviour (for example accelerating modes) and subdiffusive behaviour (due to trapping in space and time), what go beyond the traditional Brownian motion description [6, 9, 10].

If for any stochastic process the following condition are satisfied

(i) the distribution of the summed random events is not "too broad" (a sufficient condition is in particular, the finiteness of its second cumulant);

(ii) these random events must not be "long-range correlated" (in time and space)

the Gaussian central limit theorem applies (i3), and so called normal diffusion of the classical Brownian motion is observed. The process is described by the Markovian diffusion-convection equation [3, 4]. On the other hand the non-Markovian diffusion equation [3, 4] and so called fractal Fokker-Planck type equations [8] are used in order to described fractal Brownian motion, characterized by strange diffusion properties [9]. Therefore, the investigation of the actual physical process needs to identify measures which declare the validity of conditions (i) and (ii).

1.2 Characterization of stochastic processes

Let X be a stochastic variable with the probability density $F_X(x)$. Then, all quantities $Y(t)$ that are defined as functions of X by some mapping f are stochastic processes [30]

$$Y_X(t) = f(X, t) \tag{10}$$

On inserting for X one of its possible values x, a sample function or realization of the process is given by

$$Y_x(t) = f(x, t) \tag{11}$$

The probability density for $Y_X(t)$ to take the value y at time t, and the joint probability density that Y has the value y_1 at t_1, y_2 at t_2, .., and so on till y_n at t_n are

$$f_1(y, t) = \int \delta(y - Y_x(t)) F_X(x)\, dx, \tag{12}$$

and

$$f_n(y_1, t_1; y_2, t_2; \quad ...; y_n, t_n) = \int \delta(y_1 - Y_x(t_1))\delta(y_2 - Y_x(t_2))...\delta(y_n - Y_x(t_n)) F_X(x)\, dx, \tag{13}$$

respectively. They permit to compute all avreges

$$\langle Y(t_1)Y(t_2) \quad ...Y(t_n)\rangle = \int y_1 y_2 ... y_n f_n(y_1,t_1;y_2,t_2;...;y_n,t_n)\, dy_1\, dy_2 ... dy_n \tag{14}$$

The hierarchy of functions f_n obeys the following four "consistency conditions"

(i) $f_n \geq 0$;

(ii) f_n does not change on interchanging two pairs (x_k,t_k), and (x_i,t_i);

(iii)

$$\int f_n(y_1,t_1;...;y_{n-1},t_{n-1};y_n,t_n)\, dy_n = f_{n-1}(y_1,t_1;...;y_{n-1},t_{n-1})$$

(iv) $\int f_1(y_1,t_1)\, dy_1 = 1$

Each moment of the joint distribution of $Y(t_1), Y(t_2), ...$ [30, 33] can be found as the coefficient of the term with $k(t_1)k(t_2)...$ in the expression of the characteristic functional

$$G([k]) = \sum_{m=0} \frac{i^m}{m} \int k(t_1)...k(t_n)\langle Y(t_1)..Y(t_m)\rangle\, dt_1 ... dt_m$$

where $k(t)$ is an arbitrary test function. Similarly, the cumulants can be found from

$$\log G([k]) = \sum_{m=1}^{\infty} \frac{i^m}{m} \int k(t_1)...k(t_m)\langle\langle Y(t_1)...Y(t_m)\rangle\rangle\, dt_1 ... dt_m$$

where the double brackets denote cumulants. In the following the cumulants up to fourth order with respect to fixed t, and the second cumulant with respect to two different time instants are of interest. They are denoted by $C_n(t), n = 1,2,3,4$ and $\mathcal{A}(t,t')$, respectively. Thus

$$C_1(t) = \langle\langle Y(t)\rangle\rangle = \langle Y(t)\rangle \tag{15}$$

$$C_2(t) = \langle\langle Y(t)Y(t)\rangle\rangle = \langle Y^2(t)\rangle - \langle Y(t)\rangle \tag{16}$$

$$C_3(t) = \langle\langle Y^3(t)\rangle\rangle = \langle Y^3(t)\rangle - 3\langle Y^2(t)\rangle\langle Y(t)\rangle + 3\langle Y(t)\rangle^3 \tag{17}$$

$$C_4(t) = \langle\langle Y^4(t)\rangle\rangle = \langle Y^4(t)\rangle - 3\langle Y^3(t)\rangle\langle Y(t)\rangle - 3\langle Y^2(t)\rangle^2 + 12\langle Y^2(t)\rangle\langle Y(t)\rangle^2 - 6\langle Y(t)\rangle^4 \tag{18}$$

and

$$\mathcal{A}(t,t') = \langle\langle Y(t)Y(t')\rangle\rangle = \langle Y(t)Y(t')\rangle - \langle Y(t)\rangle\langle Y(t')\rangle \tag{19}$$

A process is stationary when the moments are not affected by a shift in time

$$\langle Y(t_1+\tau)Y(t_2+\tau)...Y(t_n+\tau)\rangle = \langle Y(t_1)Y(t_2)...Y(t_n)\rangle \tag{20}$$

for all n, τ and $t_1, t_2, ..., t_n$ [30]. In particular $\langle Y(t)\rangle = const.$ Thus, it is convenient to substract this constant from $Y(t)$, and deal with the zeroth-mean process $\tilde{Y}(t) = Y(t) - \langle Y\rangle$. At the same time $\langle Y^n(t)\rangle = const.$ and $\mathcal{A}(t,t') = \mathcal{A}(t'-t)$.

A process is called Gaussian process if all its f_n are Gaussian distributions

$$G([k]) = \exp\left(\mathrm{i}\int k(t_1)\langle Y(t_1)\rangle\, dt_1 - \frac{1}{2}\int\int k(t_1)k(t_2)\langle\langle Y(t_1)Y(t_2)\rangle\rangle\, dt_1 dt_2\right) \tag{21}$$

The conditional probability $f_{1|1}(y_2,t_2|y_1,t_1)$ is the probability density for Y to take the value y_2 at t_2, given that its value at t_1 is y_1 (transition probability). Additionally, the general conditional probability $f_{l|k}$, is defined by

$$f_{l|k}(y_{k+1},\ t_{k+1}\ ;\ldots;y_{k+l},t_{k+l}|y_1,t_1;\ldots;y_k,t_k) = \frac{f_{k+l}(y_1,t_1;\ldots;y_k,t_k;y_{k+1},t_{k+1};\ldots;y_{k+l},t_{k+l})}{f_k(y_1,t_1;\ldots;y_k,t_k)}$$

1.2.1 Markov property

The concept of Markovianity is established as the probabilistic analogy of the processes of classical mechanics, where the future development is completely determined by the present state and is independent of the way in which the present state is developed [33]. In stochastic (statistical) processes the future is never uniquely determined, but there are at least probability relations enabling to make predictions. Thus, a Markov process is defined as a stochastic process with the property that for any set of n successive times, $t_1 < t_2 < \ldots < t_n$,

$$f_{1|n-1}(y_n,t_n|y_1,t_1;\ldots;y_{n-1},t_{n-1}) = f_{1|1}(y_n,t_n|y_{n-1},t_{n-1}), \tag{22}$$

i.e the conditional probability density at t_n given the value y_{n-1} at t_{n-1} is uniquely determined (the whole hierarchy f_n can be constructed) and is not affected by any knowledge of the values at earlier time [5, 30, 33]. In other words, a Markov process is fully determined by the two functions $f_1(y_1,t_1)$, and $f_{1|1}(y_2,t_2|y_1,t_1)$ which obey two identities

(i) the Chapman–Kolmogorov equation

$$f_{1|1}(y_3,t_3|y_1,t_1) = \int f_{1|1}(y_3,t_3|y_2,t_2)\, f_{1|1}(y_2,t_2|y_1,t_1)\, dy_2 \tag{23}$$

(ii)

$$f_1(y_2,t_2) = \int f_{1|1}(y_2,t_2|y_1,t_1) f_1(y_1,t_1)\, dy_1 \tag{24}$$

Vice versa, any two non-negative functions f_1, $f_{1|1}$ that obey identities (equations (23) and (24)) define uniquely a Markov process.

Associating the conditional probability of a deterministic system to be in state $x = \phi(x_0, t-t_0)$ at t by

$$f_{1|1}(x,t|x_0,t_0) = \delta(x-\phi(x_0,t-t_0))$$

where x_0 is the position at t_0, the Markov property in statistical sense is applicable [30].

On the other hand, the randomness with respect to the dynamical instability of motion (exponential divergence of the close trajectories [2, 34]) may be a property of nonlinear deterministic systems (in some parametric regions): the deterministic stochasticity is created, and probability concept becomes applicable. Thus, neglecting the regular phase of the growth of exponential instability, that is neglecting the residual correlations, the Markov property is established.

1.3 On deterministic stochasticity

Nonlinear systems governed by perfectly deterministic laws of motion may behave in such a complex way as to simulate a random motion. This randomness is equivalent to the exponentially divergence of close trajectories (exponential instability) [2, 7, 13]. However, this does not imply an exponential correlation decay, nor even decay at all. The corresponding "anomalies" in the motion statistical properties, particularly, occur when the "chaos border" in the phase space is present which separates a chaotic and regular components of the motion. In order to illustrate mentioned behaviour here is considered a conservative Hamiltonian system with two degrees of freedom [13]: its phase space is 4D. The equation of motion in action-angle coordinates $\vec{J} = (J_1, J_2)$, $\vec{\theta} = (\theta_1, \theta_2)$ given by

$$\begin{aligned} \frac{d\vec{J}}{dt} &= -\frac{\partial H}{\partial \vec{\theta}} = \varepsilon \vec{f}(\vec{J}, \vec{\theta}) \\ \frac{d\vec{\theta}}{dt} &= \frac{\partial H}{\partial \vec{J}} = \frac{\partial H_0(\vec{J})}{\partial \vec{J}} + \varepsilon \vec{g}(\vec{J}, \vec{\theta}), \end{aligned} \tag{25}$$

($\vec{f} = -\partial H_1(\vec{J}, \vec{\theta})/\partial \vec{\theta}, \vec{g} = \partial H_1(\vec{J}, \vec{\theta})/\partial \vec{J}$ are the periodic functions of the angle variables) are derived from the Hamiltonian

$$H(\vec{J}, \vec{\theta}) = H_0(\vec{J}) + \varepsilon H_1(\vec{J}, \vec{\theta}), \tag{26}$$

which consists of so called unperturbed part $H_0(\vec{J})$, and small perturbation $\varepsilon H_1(\vec{J}, \vec{\theta})$ ($\varepsilon \ll 1$). The energy being conserved, the motion occurs along an orbit lying in the 3D energy hypersurface. If the orbits are bounded then by fixing one of the coordinates ($\theta_2 = const.$) a 2D Poincare surface of section ($J_1 - \theta_1$) may be considered [13]. The sequence of intersection points follows some mapping law which may be interrelated with a canonical transformation in the complete phase space.

So called twist mapping, which is area-preserving [13, 34], may be considered in the $J_1 - \theta_1$ (index is lost in the followings) choosing $\Delta t = 2\pi/\omega_2$ as time step which separates successive intersections with $J_1 = const.$:

$$\begin{aligned} J_{n+1} &= J_n + \varepsilon f(J_{n+1}, \theta_n) \\ \theta_{n+1} &= \theta_n + 2\pi\alpha(J_{n+1}) + \varepsilon g(J_{n+1}, \theta) \end{aligned} \tag{27}$$

Here the rotational number α is given by

$$2\pi\alpha(J) = \frac{\partial H_0}{\partial J} = \frac{\omega_1}{\omega_2} \tag{28}$$

The generalized standard mapping

$$\begin{aligned} I_{n+1} &= I_n + Kf^*(\theta_n) \\ \theta_{n+1} &= \theta_n + I_{n+1}, \mathrm{mod} 2\pi, \end{aligned} \tag{29}$$

with $K = 2\pi\alpha'\varepsilon f_{max}$ as a stochasticity parameter, $I = 2\pi\alpha'\Delta J_n$ and $f^* = f/f_{max}$ as the jump in the action, normalized to a maximum value of unity, is obtained from (27) putting $f = f(\theta)$, $g = 0$ and linearizing about a period 1 fixed point $J_{n+1} = J_n = J_0$ for which $\alpha(J_0)$ is an integer [13].

For the unperturbed system (27) any point on the circle $\alpha(J) = n/m$ is a fixed point of the mapping with period m. When the small perturbation is included the resonances at $\alpha(J) = n/m$ are seeds for eventually topological changes in the system. The KAM theorem [13] ensures the existence of an invariant torus $(\vec{J}, \vec{\theta})$ parametrized by $\vec{\xi}$ in the 2D Hamiltonian system (25)

$$\begin{aligned} \vec{J} &= \vec{J}_0 + \vec{v}(\vec{\xi}, \varepsilon) \\ \vec{\theta} &= \vec{\xi} + \vec{u}(\vec{\xi}, \varepsilon), \end{aligned} \tag{30}$$

where $\vec{u}$ and $\vec{v}$ are periodic in $\vec{\xi}$ and vanish for $\varepsilon = 0$ and $\dot{\vec{\xi}} = \vec{\omega}$ is the unperturbed frequency on the torus, provided conditions

1. the linear independence of the frequencies

$$\sum_i m_i \omega_i(\vec{J}) \neq 0$$

over some domain of $\vec{J}$ (sufficient nonlinearity), where the ω_i are the components of $\vec{\omega} = \partial H_0/\partial \vec{J}$ and the m_i are the components of the integer vector $\vec{m}$;

2. a smoothness condition on the perturbation (sufficient number of continuous derivatives of H_1);

3. initial conditions sufficiently far from resonance to satisfy

$$|\vec{m} \cdot \vec{\omega}| \geq \gamma |\vec{m}|^{-\tau}$$

for all $\vec{m}$, where τ is dependent on the number of degrees of freedom and smoothness of H_1, and γ is dependent on ε, on the magnitude of the perturbation Hamiltonian H_1, and on the nonlinearity of the unperturbed Hamiltonian H_0.

Thus, some of fixed points remain after the perturbation is adopted ($2km$ points). Due to area preserving property the Poincare-Birkhoff theorem proves they are of elliptic and hyperbolic type [4, 13]. Anyway, the topology of the phase space is deeply changed by the perturbation. Near every rational surface with $\alpha = n/m$, immediately, there appear closed regular orbits encircling the m elliptic points, forming a chain of m islands. The motion near the hyperbolic points (which are connected by separatrices) is much more complicated: it is this neighborhood that a chaotic layer starts [4, 13]. Nevertheless, for sufficiently small stochasticity parameter, the alternation of elliptic and hyperbolic points is a generic property of the system. Thus, according to the initial conditions and the value of stochasticity parameter (K for the standard mapping) there appear orbits having different topological properties: cycles (which correspond to the periodic motion), invariant KAM curves (island chains or trapped orbits, and KAM barriers or passing orbits), and chaotic (irregular) orbits whose intersection points densely fill a two dimensional region. Thus, the rational curves with growing K are immediately destroyed and replaced by island chains. The irrational are more robust: most of them subsist in the perturbed map as KAM barriers. Anyway, as K increases it reaches a value where the KAM curve changes its character [13]. Instead of a continuous curve it develops holes which transform it into fractal, so called cantori. These holes are possible "exit points" for a chaotic orbit which was formerly blocked by the KAM barrier. The various KAM barriers do not disappear at the same K: some occupy more and more area in the phase space until a final critical K_c is reached when the last KAM barrier is destroyed: global chaos (stochasticity). There still remain, however, regions bounded by islands, these regions shrinking as the stochasticity parameter increases.

The inclusion of a time variation in the perturbed Hamiltonian (26) introduces another degree of freedom into the observed system, such that the energy E is no longer conserved. Thus the resonance conditions is modified $\vec{m} \cdot \vec{\omega} + \omega_t = 0$ where ω_t is the frequency of time variations. Thus, the motion is allowed across the energy hypersurfaces and the phenomenon of Arnold diffusion appears [13].

From the statistical viewpoint, the irregular chaotic regions are characterized by the mixing [2, 7, 13]. Actually, the points (orbits) of the initial region M_0 (phase space region $(\vec{J}, \vec{\theta})$) tend to be uniformly distributed over the surface (3D volume) of the single valued integrals of motion (here energy E in the stationary case) as the time increases. It governs the system relaxation, and the probabilistic laws of the distribution [4, 13] of the states, which are independent of the initial state, may be adopted. In the transport theory of Hamiltonian systems [7, 8, 34] the independence of the initial conditions inside the irregular domains is then signed as the Markov property of them. Quantitatively it is measured by exponentially decreasing correlation function. The appearience of correlations is then recognized by the power-law correlation functions. Note that such

a deterministic stochasticity is signed by positive Liapunov exponent [2] and Kolmogorov entropy [3] [13].

On the other hand the complex structure of phase space makes the theory of fractal Brownian motion [9, 10] applicable. The orbit which starts in the chaotic region separated by cantori like boundary from the other chaotic region had to wait for a relatively long time before finding its way through a hole in the cantorus. Shortly, the orbit cannot wander at random to any point of phase space at any time. Rather, it sticks to a certain region near an island chain for a certain time then jumps to another region, where it sticks again for many iterations, etc.. The other possibility is to obtain so called accelerated modes, if the particle is trapped by the separatrix web formed by the separatrices overlapping of the neighboring island chains. Then it may be interchanged between them. Various mappings may model the various examples of deterministic stochastic motions [8, 13, 29]. Some of them are successively treated by the theory of CTRW and Levi random walk [9, 10, 29] (standard mapping) based on above briefly mentioned circumstances. The same mechanism is believed to be in the origin of the magnetic field stochasticity although the model treated here is much more complicated than simple standard mapping given by equation (29).

1.4 On the collisional stochasticity

In this study the test electron ensemble experiences the surrounding plasma (which is treated as a continuous medium) through the Coulomb collisions [4]. The particularity of the Coulomb collisions which dates from the long range nature of a Coulomb interparticle force is closely interrelated with the observation that the cumulative effect of the small deflections resulting from interactions with distant particles is more important than the effect of the occasional large deflections caused by relatively close encounters in plasma. Thus the diffusion type Fokker-Plank collisional operator is established in order to model the energy conserved test particle-plasma background interaction

$$\frac{\partial f(\lambda,t)}{\partial t} = \frac{\nu}{2}\frac{\partial}{\partial \lambda}\left((1-\lambda^2)\frac{\partial f(\lambda.t)}{\partial \lambda}\right), \tag{31}$$

where $f(\lambda,t) = f(\vec{r},t,\lambda)$, $\vec{r}$–fixed. Note that the particles redistribute in the velocity space due to the pitch angle scattering, staying all time at the same energy surface ($E = const.$): mixing property in v-space [13]. In other words, statistically collision is treated as a process of transition of a group of particles from an initial state to a final state having the same total momentum and energy. This process is completed during a negligably short time $\tau_c(=\nu^{-1})$ and in a region of negligably small size l_c, i.e. it is a quasi-instanteous,

[2] The Liapunov exponent of given trajectory measures the mean exponential rate of divergence of trajectories surrounding it.

[3] The Kolmogorov entropy h is defined as the integral over a specified region of phase space of sum over all positive Liapunov exponents.

and quasi-pointlike event. As a result, the particle evolution is no longer described as a dynamical process but rather as a succession of separate transitions characterized by a transition probability $f(\vec{r}, t, \lambda)$. The collisional stochasticity is a statistical stochasticity [4]. Actually, the Fokker-Plank equation (31) with the initial condition

$$f(\lambda, t = 0) = \delta(\lambda - \lambda_0) \tag{32}$$

is valid for the conditional (transition) probability $f_{1|1}(\lambda, t|\lambda_0, 0)$ identifying $f(\lambda, t = 0) = f_{1|1}(\lambda, 0|\lambda_0, 0)$, and $f(\lambda, t)$ with $f_{1|1}(\lambda, t|\lambda_0, 0)$.

Adopting such a model the Markov property is established in the sense developed in section 1.2.1.

2 Establishment of model

The particles diffuse being tied to the magnetic field lines which diffuse themselves, and due to external collisional stochasticity. In other words, the particle diffusion is governed by two stochasticity origins: the magnetic field stochasticity and collisions.

The test particle radial diffusion is evaluated by solving the gyro-phase averaged Boltzmann equation with the linearized pitch angle scattering due to the Coulomb collisions. The last one describes the unidirectional background plasma-test particle interaction. Note that the pitch angle scattering operator is used instead of the full collision operator which changes both the energy and pitch of particles. It is justified by the physics of the neoclassical and transport due to asymmetries which are determined primarily by the varying depth of particle trapping in the magnetic wells which exist along the field lines. The last is changed only by the pitch angle scattering. Additionally, the uniformity of the plasma background is implicitly assumed, and the test particle ensemble of the high number of independent electrons is prepared. The orbit part of Boltzmann equation, i.e. the equation of particle motion in the guiding center approximation is derived adopting the Littlejohn approach [35]. The magnetic Boozer coordinates based on the equilibrium toroidally nested magnetic field are applied. Such a choice is fully justified by assuming that the magnetic field is destroyed only locally. The form of perturbation is chosen with premise that the topological changes are of interest, and that in the tokamak environment such changes are dominately influenced by the resistive instability [36].

The numerical Monte Carlo model is established following reference [26]. Under assumption that the energy is conserved, the pitch angle scattering operator is numerically obtained starting from the binomial distribution.

2.1 The guiding-center equations

In order to find the Hamiltonian guiding-center equations the variational method of Littlejohn [35], i.e. so called hybrid Hamiltonian-Lagrangian method is adopted. Such a variational approach have the advantages of being invariant under arbitrary coordinate transformations, and that the invariance associated with symmetries follows transparently from the independence of the Lagrangian of the corresponding symmetry coordinates (Noether's theorem).

The variational principle in the general form is given by

$$\delta \int \Lambda = 0 \tag{33}$$

where Λ is a non-degenerate 1-form in the extended phase space $(\vec{p}, \vec{q}, t)$. In the Lagrangian approach

$$\Lambda \equiv L dt \tag{34}$$

where L is the particle Lagrangian

$$L(\vec{z},\dot{\vec{z}},t) = \vec{\gamma}\cdot\dot{\vec{z}} - H, \tag{35}$$

written in an arbitrary coordinate system or phase space $\vec{z} = \vec{z}(\vec{q},\vec{p},t) = (z_\mu, \mu = 1,...,6)$, $\vec{\gamma} = (\gamma_\mu, \mu = 1,...,6)$, and H are functions of $\vec{z}$ and t, given by

$$\begin{aligned} \vec{\gamma}(\vec{z},t) &= \vec{p}\cdot\frac{\partial\vec{q}}{\partial t} \\ H(\vec{z},t) &= H_{can} - \vec{p}\cdot\frac{\partial\vec{q}}{\partial t} \end{aligned} \tag{36}$$

where H_{can} is the usual Hamiltonian in terms of canonical variables $(\vec{q},\vec{p}) = (q_i, p_i, i = 1,2,3)$.

The equations of motion in the Littlejohn approach follow by varying the integral of $L(\vec{z},\dot{\vec{z}},t)dt$, considering the variations of all six phase space coordinates $\vec{z}$ independent during the variational process.

For a particle in an electromagnetic field, the canonical Hamiltonian is

$$H_{can}(\vec{q},\vec{p},t) = \frac{1}{2m}\left(\vec{p} - \frac{e}{\varepsilon}\vec{A}(\vec{q},\varepsilon t)\right)^2 + e\Phi(\vec{q},\varepsilon t), \tag{37}$$

where ϵ is the adiabatic ordering parameter which physically represents the ratio of gyroradius to scale length (it is written $\epsilon = 1$ at the end of calculations). Note that adiabatic ordering assumes the slow change of the corresponding parameter. Let $\vec{z} = (\vec{x},\vec{v})$, where $\vec{x} = (x_i,\ i = 1,2,3)$ is the particle position, and $\vec{v} = (v_i,\ i = 1,2,3)$ is the particle velocity

$$\vec{x} = \vec{q}, \qquad \vec{v} = \frac{\vec{p}}{m} - \frac{e\vec{A}(\vec{q},\varepsilon t)}{m\varepsilon} \tag{38}$$

Then, the particle Lagrangian is

$$L = \left(\frac{e}{m\varepsilon}\vec{A}(\vec{x},\varepsilon t) + m\vec{v}\right)\cdot\dot{\vec{x}} - \left(e\Phi(\vec{x},\varepsilon t) + \frac{mv^2}{2}\right) \tag{39}$$

Note that $\vec{v}$ is considered independent of $\dot{\vec{x}}$, even though $\vec{v} = \dot{\vec{x}}$ follows from the equation of motion. This is because the variational principle selects the physical motion out of all conceivable motions, as the one to make the action integral stationary.

The basic idea of Littlejohn is that the Lagrangian for the guiding center equations is the gyroaverage of the exact (particle) Lagrangian. It is realized by combining the coordinate transformations according to the Darboux theorem [37], and the gauge transformations based on observation that equations of motion (Lagrange-Euler equations) are invariant under transformation

$$L' = L - \frac{dS}{dt}, \tag{40}$$

where $S = S(\vec{z},t)$ is arbitrary scalar function.

At first step the particle velocity $\vec{v}$, and position $\vec{x}$ are decomposed according to

$$\vec{v} = u\hat{b} + w\hat{c}, \quad \text{and} \quad \vec{x} = \vec{X} + \frac{\epsilon w\hat{a}}{B},$$

where $u, \hat{b}, w$ are purely averaged in the lowest order, (i.e. $u = U_{||}, w = U_n$), $\hat{c}$ is a perpendicular unit vector which is purely oscillatory, $\vec{X}$ is the guiding center position, $\vec{U} = (U_{||}, U_n)$ is the guiding center velocity,

$$\begin{aligned} \hat{b} &= \hat{e_1} \times \hat{e_2} \\ \hat{c} &= -\sin\gamma\hat{e_1} - \cos\gamma\hat{e_2} \\ \hat{a} &= \hat{b} \times \hat{c} = \cos\gamma\hat{e_1} - \sin\gamma\hat{e_2}, \end{aligned}$$

γ is the instantaneous gyrophase, and $\hat{e}_{1,2}(\vec{x}, \epsilon t)$ are arbitrary chosen unit vectors. So, after the first step the six independent phase space coordinates are $\vec{z} = (\vec{X}, u, \gamma, w)$.

At second step a gauge transformation in phase space

$$L \to L + \frac{dS}{dt}, \tag{41}$$

i.e.

$$\vec{\gamma} \to \vec{\gamma} + \frac{\partial S}{\partial \vec{z}}, \qquad H \to H - \frac{\partial S}{\partial t},$$

with $S = S(\vec{z}, t)$ an arbitrary scalar, gives possibility to write the oscillatory part of the particle Lagrangian approximately as a total time derivative

$$L - \langle L \rangle = \frac{eB}{m}\frac{\partial S}{\partial \gamma} \approx \frac{dS}{dt} + O(\epsilon), \tag{42}$$

so that this oscillating part can be eliminated term by term from the Lagrangian. The result is

$$L'(\vec{X}, \dot{\vec{X}}, U_{||}, \mu, \gamma) = \langle L \rangle = e\vec{A}^* \cdot \dot{\vec{X}} + \frac{m}{e}\mu\dot{\gamma} - H', \tag{43}$$

where

$$H' = e\Phi + \mu B + \frac{m}{2}U_{||}^2, \qquad \mu = \frac{mU_n^2}{2B}$$

and $\vec{A}^*$ is the effective magnetic potential

$$\vec{A}^* = \vec{A} + \rho_{||}\vec{B}, \qquad \rho_{||} = \frac{mU_{||}}{eB} \tag{44}$$

defined by the pseudo-magnetic field $\vec{B}^* = \nabla \times \vec{A}^*$. The quantity $\rho_{||}$ is the parallel gyroradius.

The Euler-Lagrange equations for the six independent variables $\vec{z} = (\vec{X}, U_{||}, \gamma, \mu)$ are given by

$$\frac{\delta L}{\delta \vec{z}} = \frac{d}{dt}\left(\frac{\partial L}{\partial \dot{\vec{z}}}\right) - \frac{\partial L}{\partial \vec{z}} = 0, \tag{45}$$

i.e. explicitly the set of the drift equations is

$$\begin{aligned} \dot{\vec{X}} &= \frac{U_{||}}{B_{||}^*}(\vec{B} + \frac{m}{e}\nabla \times (U_{||}\frac{\vec{B}}{B})) \\ \dot{\vec{X}}\hat{n} &= U_{||} \\ \dot{\mu} &= 0 \\ \dot{\gamma} &= \frac{eB}{m} \end{aligned} \tag{46}$$

where $\hat{n} = \vec{B}/B$, and $B^*_{||} = B + \vec{n} \cdot \nabla \times (\vec{n} m U_{||}/e)$.

The total magnetic field is assumed to be of the form [24]

$$\vec{B}_t = \vec{B} + \delta\vec{B}, \tag{47}$$

where $\vec{B}$ is the equilibrium magnetic field, and

$$\delta\vec{B} = \nabla \times (b\vec{B}) \tag{48}$$

is the slow perturbation [24], i.e. $|\delta\vec{B}/\vec{B}| \ll 1$, and $1/\Omega \cdot \partial|\delta\vec{B}/\vec{B}|/\partial t \ll 1$. Note that the first condition corresponds to the term small perturbation. Then, the total modified potential is

$$\vec{A}^*_t = \vec{A} + (\rho_{||} + b)\vec{B},$$

and the vector form of the drift velocity is given by

$$\vec{v} \equiv \dot{\vec{X}} = \frac{v_{||}(\vec{B} + \nabla \times ((\rho_{||} + b)\vec{B}))}{B + \hat{n} \cdot \nabla \times ((\rho_{||} + b)\vec{B})} \tag{49}$$

where $v_{||} \equiv U_{||}$ is the parallel velocity to the equilibrium magnetic field $\vec{B}$, $\rho_{||} = v_{||}/\Omega$, and Ω is the gyrofrequency.

The toroidal topology of the unperturbed magnetic field determined the establishment of the model in the Boozer coordinates (ψ, θ, ζ) [38]: ψ is the label of a flux surface defined as the toroidal flux/2π, θ is the poloidal, and ζ is the toroidal angle. Thus, the covariant, and contravariant form of the static unperturbed magnetic field in Boozer coordinates are written as

$$\vec{B} = I\nabla\theta + J\nabla\zeta + \beta_*\nabla\psi, \tag{50}$$

and

$$\vec{B} = \nabla\psi \times \nabla\theta - \iota\nabla\psi \times \nabla\zeta, \tag{51}$$

respectively, where $2\pi J(2\pi I)$ are the poloidal (toroidal) current outside (inside) the flux surface. Following the assumptions of Boozer [39] that β_* does not change ψ position of particle (according to $\beta_* \approx J_{PS}$–Pfirsch-Schlüter current), and focusing attention on the topology changes to a magnetic configuration, the term $\beta_*\nabla\psi$ is neglected in the following. When the slow perturbation $\delta\vec{B}$ is included the same premise is adopted. Actually, the term β_* appears in combinations $\rho_{||}\beta_*$, and $b\beta_*$ in the system Jacobian which determines how long a particle trajectory takes to cover different parts of its trajectory [39]

$$\mathcal{J} = \frac{v_{||}}{B^*} =$$
$$\frac{J + I\iota}{B}\left(J\left(1 + (\rho_{||} + b)(I' - \frac{\partial\beta_*}{\partial\theta})\right) - I\left(-\iota + (\rho_{||} + b)(J' - \frac{\partial\beta_*}{\partial\zeta})\right)\right)^{-1}$$

and $(\vec{v})_{\theta,\zeta}$ components, i.e. β_* does not change ψ position of particle.

Hence, the drift velocity (equation (49)) can be written as

$$\vec{v} = \frac{(J + \epsilon I)U_{||}\left(\nabla\psi \times \nabla\theta - \epsilon\nabla\psi \times \nabla\zeta + \nabla \times (\rho_{||} + b)(J\nabla\zeta + I\nabla\theta)\right)}{B\left(J + \epsilon I + (\rho_{||} + b)(JI' - IJ')\right)} \tag{52}$$

in the Boozer coordinate system which is chosen in such a way that B_r, A_r vanish : canonical magnetic coordinate system [39, 40].

Note that two pairs of the canonical conjugate coordinates ($\beta_* = 0$) are

$$(\phi, \rho_c), \qquad (\theta_c, \psi),$$

where $\phi = J\theta - I\zeta, \rho_c = \rho_{||} + b$, and $\theta_c = \theta - \epsilon\zeta$[40].

2.2 The Monte Carlo model of the test particle diffusion

2.2.1 Model equations

The test particle transport in the presence of destroyed magnetic surfaces is evaluated by the solution of the gyro-phase averaged Boltzmann equation [41]

$$\frac{\partial f}{\partial t} + \vec{v} \cdot \nabla f = C(f), \tag{53}$$

where $f = f(t, \vec{r}, E, \mu)$ is the particle distribution function, and $C(f)$ is the linearized pitch-angle scattering due to Coulomb collisions. The energy E of each guiding center particle is conserved, and only the magnetic moment μ is changed by the Coulomb collisions.

In the magnetic field $\vec{B}_t$ of the form given by equation (47), the test particle drift velocity $\vec{v}$ is given by equation (49).

Instead of solving equation (53) directly, the Monte Carlo technique is used [26]. Equations for each guiding center particle equivalent to equation (53) consist of two parts: orbit, and collision part. Without the Coulomb collisions the characteristic equations of equation (53) are obtained from [26]

$$\dot{\xi} \equiv \frac{d\xi}{dt} = \vec{v} \cdot \nabla\xi, \tag{54}$$

where $\xi = (\psi, \theta, \zeta, \rho_c)$. Hence, the equations of the guiding center in the Boozer coordinates become

$$\dot{\psi} = -\frac{1}{\gamma}\left[\delta\left(J\frac{\partial B}{\partial\theta} - I\frac{\partial B}{\partial\zeta}\right) - \frac{e^2B^2}{m}\rho_{||}\left(J\frac{\partial b}{\partial\theta} - I\frac{\partial b}{\partial\zeta}\right)\right] \tag{55}$$

$$\dot{\theta} = \frac{\delta}{\gamma}J\frac{\partial B}{\partial\psi} + \frac{e^2B^2}{\gamma m}\rho_{||}\left[\epsilon - \rho_c J' - J\frac{\partial b}{\partial\psi}\right] \tag{56}$$

$$\dot{\zeta} = -\frac{\delta}{\gamma}I\frac{\partial B}{\partial\psi} + \frac{e^2B^2}{\gamma m}\rho_{||}\left[1 + \rho_c I' + I\frac{\partial b}{\partial\psi}\right] \tag{57}$$

$$\dot{\rho}_c = -\frac{\delta}{\gamma}\left[\left(\epsilon - \rho_c J'\right)\frac{\partial B}{\partial\theta} + \left(1 + \rho_c I'\right)\frac{\partial B}{\partial\zeta}\right] + \tag{58}$$

$$+\frac{m\Omega^2\rho_{||}}{\gamma}\left[\left(\epsilon - \rho_c J'\right)\frac{\partial b}{\partial\theta} + \left(1 + \rho_c I'\right)\frac{\partial b}{\partial\zeta}\right],$$

and

$$\gamma = e\left[J + I\iota + \rho_c(JI' - IJ')\right] \tag{59}$$

$$\delta = \mu + \frac{e^2 B}{m}\rho_{\|}^2 \tag{60}$$

To investigate the structure of the magnetic field lines, similar equations are constructed as follows. By neglecting the particle drift motion the equation (49) becomes

$$\vec{v} = v_{\|}\frac{\vec{B}_t}{\vec{B}_t \cdot \hat{n}} \tag{61}$$

Substituting equation (61) into equation (54) the equivalent of equation (54) can be written in the form of the magnetic field line equation

$$\frac{d\psi}{\vec{B}_t \cdot \nabla\psi} = \frac{d\theta}{\vec{B}_t \cdot \nabla\theta} = \frac{d\zeta}{\vec{B}_t \cdot \nabla\zeta} = \frac{v_{\|}dt}{\vec{B}_t \cdot \hat{n}}, \tag{62}$$

where the time t can be taken as an independent variable. The equation (62) can be identified as the equivalent of the equations of the guiding center by putting $\delta = 0$ and $\rho_c = b$ in equations (55), (56), and (57), namely

$$\dot{\psi} = \frac{m\Omega^2\rho_{\|}}{\gamma}\left(J\frac{\partial b}{\partial\theta} - I\frac{\partial b}{\partial\zeta}\right), \tag{63}$$

$$\dot{\theta} = \frac{m\Omega^2\rho_{\|}}{\gamma}\left(\iota - \frac{\partial(Jb)}{\partial\psi}\right), \tag{64}$$

$$\dot{\zeta} = \frac{m\Omega^2\rho_{\|}}{\gamma}\left(1 + \frac{\partial(Ib)}{\partial\psi}\right), \tag{65}$$

where

$$\gamma = e\left(J + \iota T + b(JI' - J'I)\right) \tag{66}$$

The equations (63)-(65) are solved under the condition that $v_{\|} = const.$ and $\mu = 0$.

The pitch angle scattering in equation (53) is expressed as

$$\frac{\partial f}{\partial t} = C(f) = \frac{\nu}{2}\frac{\partial}{\partial\lambda}\left((1-\lambda^2)\frac{\partial f}{\partial\lambda}\right) \tag{67}$$

where the pitch angle $\lambda = v_{\|}/v$ is used instead of μ, and ν is the deflection frequency [26]. Knowing the solution of equation (67) with the initial condition $f(\lambda, t = 0) = \delta(\lambda - \lambda_0)$ a Langevin equation giving the same mean value of λ and standard deviation σ is constructed

$$\frac{d\lambda}{dt} + \nu\lambda = W(t) \tag{68}$$

where the collisional effect from the plasma background is splited up into two parts: a systematic part $\nu\lambda$, representing dynamical friction experienced by the particle and fluctuation part, $W(t)$ which is modeled as a white noise source

$$\langle W(t)\rangle = 0, \qquad \langle W(t)W(t')\rangle = D\delta(t - t') \tag{69}$$

According to (67) the constant D is chosen to be $D = (1 - \lambda_0^2)\nu$. The general solution of the Langevin equation (68) is

$$\lambda(t) = \lambda_0 e^{-\nu t} + e^{-\nu t} \int_0^t W(t') e^{\nu t'} dt' \tag{70}$$

Corresponding the average value $\langle \lambda(t) \rangle$ (the first cumulant), and the mean square displacement (the second cumulant) are given by

$$\langle \lambda(t) \rangle = \lambda_0 e^{-\nu t}, \tag{71}$$

$$\sigma^2 = \langle \lambda^2(t) \rangle - \langle \lambda(t) \rangle^2 = \frac{1 - \lambda_0^2}{2} \left(1 - e^{-2\nu t}\right), \tag{72}$$

In the limit $\nu t \ll 1$ equations (71) and (72) become

$$\langle \lambda(t) \rangle \approx \lambda_0 (1 - \nu t) \tag{73}$$

$$\sigma^2(t) \approx (1 - \lambda_0^2)\nu t \tag{74}$$

For a discrete time step Δt satisfying $\Delta t \nu \ll 1$, λ is then changed as

$$\lambda(t_n) = \lambda(t_{n-1})(1 - \nu \Delta t) \pm \sqrt{(1 - \lambda^2(t_{n-1}))\nu \Delta t}, \tag{75}$$

for one step from $t_{n-1} = (n-1)\Delta t$ to $t_n = n\Delta t$ [26]. The symbol $\pm$ indicates that the sign is to be chosen randomly, but with equal probability for plus and minus.

The magnetic field stochasticity and pitch angle scattering due to Coulomb collisions introduce stochasticity in the system, so that the particle ensemble allows statistical treatment.

2.2.2 The structure of magnetic field

In the Boozer coordinates contravariant form of the equilibrium magnetic field $\vec{B}$ is expressed by equation (51). Hence, topology of the magnetic field is torus consisting of nested toroidal flux surfaces. In the small perturbation given by equation (48), the function b, which has unit of length, is used to represent the structure of destroyed magnetic field $\vec{B}_t$, i.e. the islands and stochastic regions. Its Fourier representation is

$$b(\psi, \theta, \zeta) = \sum_{m,n} b_{mn}(\psi) \cos(m\theta - n\zeta + \zeta_{m,n}), \tag{76}$$

where $\zeta_{m,n}$ is the phase and $|b_{mn}|/a \ll 1$. The form of $b_{mn}(\psi)$ is given by

$$\frac{b_{mn}(\psi)}{a} = s \exp\left(-\frac{(\psi - \psi_{mn})^2}{\Delta\psi^2}\right), \tag{77}$$

where parameter s indicates the strength of perturbation, called hereafter stochasticity parameter. The parameter $\Delta\psi$ is noted as the width of perturbation.

The equations of the magnetic field lines are given by equation (62). Thus, by using equations (51), (48), and (70), the topological changes of the magnetic configuration are dominated by

$$\left|\frac{\delta\vec{B}\cdot\nabla\psi}{\vec{B}\cdot\nabla\zeta}\right| = \sum_{m,n}(mJ-nI)b_{mn}(\psi)\sin(m\theta-n\zeta+\zeta_{m,n}) \tag{78}$$

According to section 1.3, in the presence of small perturbation near every rational surface with $\iota = n/m$, closed regular orbits appear encircling the m elliptic points, and forming a chain of m islands. The elliptic points are separated by hyperbolic points which are connected by separatrices. The island width [42] is approximately given by

$$w_{m,n} = W_{m,n}\sqrt{s}, \qquad W_{m,n} = \left(4q\sqrt{\frac{aR}{q'}}\right)_{r=r_{m,n}}, \tag{79}$$

where $r_{m,n}$ is the radial position of the rational surface with $q = m/n$, $q' = dq/dr$, and a and R are minor and major radii, respectively.. The most irrational surfaces subsist as KAM barriers among the island chains. As the stochasticity parameter increases it reaches value at which the KAM curve changes its character from a continuous to curve with holes. Thus, the KAM curve is transformed into so called cantory [4]. Previously blocked by the KAM barriers chaotic motion could be continued through the formed holes. Different KAM barriers disappear at different value of stochasticity parameter, some occupy more and more area in phase space. Finally at a critical parameter the last KAM barrier is destroyed: overlapping is started. Roughly, the value of stochasticity parameter at which the overlapping starts is estimated from equality of the separation between two selected neighboring rational surfaces Δr to the sum of the half widths of the corresponding islands

$$\frac{w_{m,n}+w_{m',n'}}{2} = \frac{W_{m,n}+W_{m',n'}}{2}\sqrt{s} \tag{80}$$

Thus, the threshold value for overlapping is

$$s_c \approx \left(\frac{2\Delta r}{W_{m,n}+W_{m',n'}}\right)^2, \tag{81}$$

However, there still remain regions bounded by islands which shrink as the stochasticity parameter increases. Thus, according to initial conditions and value of stochasticity parameter orbits of different topology appear (section 1.3).

As a magneto-hydrodynamic (MHD) equilibrium an axisymmetric flux conserving tokamak (FCT) with regular nested flux surfaces is adopted. The boundary is circular, $B = 3T$, and major and minor radii are $R = 3$m, and $a = 1.01$m, respectively. The profile of the rotational transform is specified as

$$\iota = 0.9 - 0.5875\left(\frac{r}{a}\right)^2, \tag{82}$$

the aspect ratio is given by

$$\varepsilon = \frac{a}{R} = \frac{1}{3}, \tag{83}$$

and β =(kinetic pressure/magnetic pressure)= 0.

The Fourier harmonics of the magnetic field perturbation are chosen to be

$$\frac{n}{m} = \frac{7}{10}, \frac{2}{3}, \frac{7}{11},$$

$\zeta_{nm} \equiv 0$ and $\Delta\psi/\psi_a = 0.1$. The relative magnitude of the perturbation is given by $s_b \equiv |\delta\vec{B} \cdot \hat{r}|/B \approx ms/(r/a) = 4.8s$. Thus, according to equation (81), the critical value of s_b is

$$s_{bc} \approx 7 \times 10^{-5} \tag{84}$$

2.3 Numerical model

2.3.1 Monte Carlo equivalent of the pitch angle scattering

The Monte Carlo equivalent to the pitch angle scattering operator (67) is numerically constructed starting with the binomial distribution [26]. Actually, the broadening of f is supposed to be due to a large number of steps in λ of equal value but of random sign. It is then derivable from the binomial distribution for obtaining m plus values in n trials with equal probability for plus and minus

$$P(m) = \frac{1}{2^n}\frac{n!}{m!(n-m)!} \tag{85}$$

In the limit $n \gg 1$, the binomial distribution can be written as [26]

$$P(j) = \frac{1}{\sqrt{2\pi n}}\exp(-\frac{j^2}{2n}), \tag{86}$$

with respect to the number of pluses minus the number of minuses, $j = 2m - n$. Thus, it resembles an Gaussian distribution with the standard deviation $\sigma_j = \sqrt{n}$. In the language of λ the square of the standard deviation of f (distribution of pitch angles) is

$$\sigma = \sqrt{\langle\lambda^2\rangle - \langle\lambda\rangle^2}, \tag{87}$$

where the moments $\langle\lambda\rangle$ and $\langle\lambda^2\rangle$ can be derived from equation (67) putting $\langle\lambda\rangle = \int_{-1}^{1}\lambda f d\lambda$

$$\frac{d\langle\lambda\rangle}{dt} = -\nu\langle\lambda\rangle \tag{88}$$

$$\frac{d\sigma^2}{dt} = \nu(1-\lambda_0^2) \tag{89}$$

If after short time t is expected f to be a Gaussian, then $\lambda = \lambda_0(1-\nu t)$ with standard deviation $\sigma = ((1-\lambda_0^2)\nu t)^{1/2}$. The standard deviation $\sigma = ((1-\lambda_0^2)\nu t)^{1/2}$ is equivalent to $\sigma_j = \sqrt{n}$ after n steps in λ, choosing λ step of magnitude $((1-\lambda_0^2)\nu\tau)^{1/2}$ with τ the

length of time between the steps (note that then $t = n\tau$). With respect to the above discussion it is possible to write

$$\lambda_n = \langle\lambda\rangle \pm \sigma_\lambda \tag{90}$$

Clearly, if the pitch is changed from λ_0 to λ_n after a time step of length τ with

$$\lambda_n = \lambda_0(1 - \nu\tau) \pm ((1 - \lambda_0^2)\nu\tau)^{1/2}, \tag{91}$$

then the effects of the Lorentz scattering operator will be reproduced if $\nu\tau \ll 1$ which is equivalent to equation (69).

With such a procedure if $|\lambda_0| < 1$, then $|\lambda_n| < 1$ [25]. Clearly, $|\lambda_0|$ must be near one for a problem to occur, so let $\lambda_0 = 1 - \delta$, with $\delta \ll 1$. The largest λ_n can be

$$\lambda_n = 1 - (\delta + \nu\tau) + (2\delta\nu\tau)^{1/2} \tag{92}$$

The maximum value of λ_n as δ is varied occurs at $\delta = \nu\tau/2$, so

$$|\lambda| < 1 - \frac{1}{2}(\nu\tau)$$

To have a good representation of the pitch angle scattering operator $\nu\tau \ll 1$.

2.3.2 Numerical procedure

The numerical code named *DCOM* [43] is used in order to model equation (53) according to discussion in section 2.2. The calculations are started ($t = 0$) by introducing the monoenergetic ($E = 3$keV) test electron ensemble of $N = 10000$ independent electrons with randomly distributed poloidal, toroidal, and pitch angle, $(\theta, \zeta \epsilon [0, 2\pi], \lambda \epsilon [-1, 1])$ at flux surface with $r/a = 0.63(\iota = 2/3)$. Each of the ensemble electrons evolutes independently according to equations (55-58) which are solved by the 6th order Runge-Kutta procedure [43]. To satisfy the energy constraint condition $E = const.$, the numerical step is chosen to be $dt = 5 \times 10^{-9}$s. This corresponds to the maximum numerical error of order $10^{-4}\%$, which is detected in the low collisional regimes (parameter set in section 4.1.2). In all other circumstances the maximum error is of order $10^{-6}\%$.

When the magnetic field line diffusion is investigated (section 4.2) the test field line ensemble is initially loaded at $\iota = 2/3$ with randomly distributed θ, ζ. The magnetic field line, i.e. the electron ($E \equiv m_e v_{th}/2 = 3$keV) which is tied to the magnetic field line ($\mu = 0, \rho_{||} = v_{th}/\Omega$), is followed numerically solving equations (63-65).

After each particle orbit step the Monte Carlo equivalent pitch angle operator is applied. The particularity of such a Monte Carlo procedure requires the checking of its validity. Therefore, the results of paper [44] are taken as the referent ones. In the neoclassical domain the system has two types of characteristic frequencies associated with the particle dynamics: the transit frequency of passing particles ν_t and the bounce frequency of trapped particles ν_b. The characteristic times are $\tau_t (= \nu_t^{-1})$ for passing and $\tau_b (= \nu_b^{-1})$

for trapped particles, respectively. According to the relative magnitude among above characteristic frequencies (times) associated with particle dynamics and the deflection collision frequency ν (collision time, $\tau_c = \nu^{-1}$) due to the Coulomb collision associated with stochasticity, there are three types of collisionality regime:

$$\begin{aligned}
&\nu \ll \nu_{be} \ll \nu_t \quad \text{or} \quad \tau_c \gg \tau_{be} \gg \tau_t \quad : \text{ banana regime} \\
&\nu_{be} \ll \nu \ll \nu_t \quad \text{or} \quad \tau_{be} \gg \tau_c \gg \tau_t \quad : \text{ plateau regime} \\
&\nu_{be} \ll \nu_t \ll \nu \quad \text{or} \quad \tau_{be} \gg \tau_t \gg \tau_c \quad : \text{ Pfirsch- Schlüter regime,}
\end{aligned} \tag{93}$$

where $\nu_{be} \equiv \epsilon\nu_b = \tau_{be}^{-1}$ is the effective bounce frequency. Thus, in the presence of collisions the characteristic frequencies and times at the initial flux surface are [44]

$$\begin{aligned}
\nu_t &= \frac{\epsilon v}{\pi R} &&= 2.21 \times 10^6 \text{ s}^{-1} \quad : \quad \tau_t = \nu_t^{-1} &&= 4.35 \times 10^{-7} \text{ s} \\
\nu_b &= \left(\frac{r}{R}\right)^{3/2} \nu_t &&= 2.30 \times 10^5 \text{ s}^{-1} \quad : \quad \tau_b = \nu_b^{-1} &&= 4.52 \times 10^{-6} \text{ s}
\end{aligned} \tag{94}$$

where $v = \sqrt{2E/m}$.

In the simulation of the neoclassical radial diffusion, the different collisional regimes are treated by choosing the parameter ν/ν_t to be 0.0045, 0.45 and 4.5, which correspond to the banana, plateau and Pfirsch-Schlüter regime, respectively. On the other hand, being interested in the qualitatively new effects from collisions in the presence of the magnetic field irregularities the chosen collisional frequencies are:$\nu/\nu_t = 0.45, 4.5$, and 45, respectively.

3 Establishment of the statistical approach

In this study the radial diffusion is synonym for the relaxation of the collisional stochasticity, and the magnetic field stochasticity. According to section 1.4 the collisional stochasticity is of the statistical type beyond the time scale with step τ_c. The smallness of the particle radial displacement due to collisions in regular magnetic field, $\delta r/a \approx \rho_p/a \approx 10^{-4}$, ($\rho_p$ is the poloidal gyro-radius of electron), allows to assume that particle wanders across the infinity domain. On the other hand, the magnetic stochasticity (section 1.3) is generated by the exponential (dynamical) instability and realizes inside the finite domain in configuration space. Thus, the statistical analysis of the radial diffusion is established on comparison with the fundamental diffusion process: the Wiener process in infinity domain; and the uniform mixing process in finite domain.

3.1 Statistical measures

The statistical measures are defined with respect to the particle radial displacement

$$\delta r(t) = r(t) - r(0)$$

adopting ensemble average

$$\langle Y \rangle = \frac{1}{N} \sum_{i=1}^{N} Y_i \tag{95}$$

where N is the number of particles in the observed particle ensemble.

3.1.1 The cumulant coefficients

The dimensionless n-th cumulant coefficient γ_n [5, 31] is given by

$$\gamma_n(t) = \frac{C_n(t)}{C_2^{n/2}(t)} \tag{96}$$

where $C_n(t)$ is n-th cumulant. Up to the 4th order it is calculated as (section 1.2)

$$C_1(t) = \langle \delta r(t) \rangle, \tag{97}$$

$$C_n(t) = \langle (\delta r(t) - \langle \delta r(t) \rangle)^n \rangle, \qquad n = 2, 3 \tag{98}$$

$$C_4(t) = \langle (\delta r(t) - \langle \delta r(t) \rangle)^4 \rangle - 3C_2^2(t). \tag{99}$$

The first cumulant is a measure of the advective effect or convective diffusion [5, 30]. This advective effect is eliminated from the higher cumulants by definitions (equations 98,99).

The second cumulant is the dispersion around $\langle r(t) \rangle$, and a measure of the conductive diffusion. Its time development indicates the type of diffusive behaviour [4, 9]. The normal diffusive behaviour is denoted by the linear increasing $C_2(t)$ in time. Accordingly,

the slower and faster than linear increasing in time are declared as the subdiffusivity and superdiffusivity of the observed stochastic process, respectively. In the power-law approximation

$$C_2(t) \approx t^{\alpha}, \tag{100}$$

the diffusion exponent α appears as a quantitative indication of the type of diffusive behaviour. The process with $\alpha < 1, = 1, > 1$ is a subdiffusive, normal diffusive, or superdiffusive process, respectively.

It is proved [31] that the only physically acceptable random process with a finite number of nonvanishing cumulant coefficients is Gaussian with $\gamma_{n>2} = 0$. Therefore, the cumulant coefficients $\gamma_{n>2}$ generically carry information about non-Gaussianity (section 1.2). The degree of asymmetry around $\langle r(t) \rangle$ and relative peakedness or flatness of a particle distribution, with respect to Gaussian, are characterized by γ_3 (skewness), and γ_4 (kurtosis), respectively. A positive (negative) value of skewness signifies a distribution with an asymmetric tail extending out towards $r(t) > \langle r(t) \rangle$ ($r(t) < \langle r(t) \rangle$). On the other hand, a positive (negative) value of kurtosis indicates more peaked (flated) distribution than the Gaussian one, i.e. the importance of the tails of the distribution is enhanced (reduced), respectively.

3.1.2 Effective diffusion coefficient

Under assumption that the diffusion is local

$$\frac{\delta r}{a} \ll 1, \tag{101}$$

the parameter

$$D(t) = \frac{dC_2(t)}{2dt}, \tag{102}$$

and power-law equivalent

$$D_{pw}(t) = \frac{C_2(t)}{2t}, \tag{103}$$

can be considered in order to indicate the type of diffusive behaviour: normal diffusivity, $D(t) \equiv D_{pw}(t) = const.$; subdiffusivity, $D(t) \neq D_{pw}(t)$, and both of them decrease in time; superdiffusivity, $D(t) \neq D_{pw}(t)$, and both of them increase in time. Additionally, the relative displacement $D(t)$ from $D_{pw}(t)$ is checked calculating

$$\Delta D(\%) = \lim_{t>\tau} \frac{|D(t) - \alpha D_{pw}(t)|}{D(t)} 100, \tag{104}$$

where τ is the characteristic time of treated process. Note that $\Delta D = 0$ for a normal diffusive process.

The parameter $D(t)$ is called the effective diffusion coefficient, and D_{pw} is noted as the power-law equivalent of the effective diffusion coefficient. For a practical purpose only the constant $D(t)$ is meaningful.

3.1.3 The autocorrelation coefficient

In order to estimate the time correlations between two states of system, the autocorrelation coefficient [30, 33] is given by

$$A(t,t') = \frac{\langle(\delta r(t) - \langle\delta r(t)\rangle)(\delta r(t') - \langle\delta r(t')\rangle)\rangle}{\sqrt{\langle(\delta r(t) - \langle\delta r(t)\rangle)^2\rangle\langle(\delta r(t') - \langle\delta r(t')\rangle)^2\rangle}}. \tag{105}$$

The system autocorrelation time is uniquely determined under condition

$$A(t,t') = A(t'-t)$$

when it is identified with the time instant after which the value of $A(t'-t)$ vanishes, i.e the events are uncorrelated. This condition is called the covariance stationarity [5]. Note that vanishing of the autocorrelation (decorrelated two events) is weaker criterion than statistical independence.

Usually, the system relaxation beyond some proper time scale follows exponential law. However, the relaxation in disordered media has given another opportunity [9, 31]: the power-law decreasing correlations. In other words the residual correlations are detected during the relaxation process (section 1).

In the physics of system near equilibrium, the statistical approach is usually developed with premise of the covariance stationarity. Therefore, the standard approaches are not enough precise in order to clarify the processes which evaluate in time, and corresponding autocorrelations are functions of the time instant $t(\text{or}\,t')$ and time interval $\tau = t' - t$.

3.1.4 Statistical stationarity

The statistical stationarity of the particle radial diffusion is defined as (according to (20))

$$\begin{aligned} C_{1,2}(t+T) &= C_{1,2}(t) \\ \gamma_{3,4}(t+T) &= \gamma_{3,4}(t) \\ A(t,t') &= A(t'-t) \end{aligned} \tag{106}$$

with arbitrary T. Corresponding diffusion exponent is zero, and $D(t) = 0$: the non-diffusive behaviour. In the absence of external forces the system is relaxed to the equilibrium. In other words, when the cumulant, and autocorrelation coefficients are not affected by a shift in time the stochastic process is statistically stationary. Note that the covariance stationarity is defined in section 3.1.3 as the independence of autocorrelation on shift in time.

3.1.5 Effective Liapunov exponent

In the context of the radial diffusion the degree of stochasticity for the magnetic field lines is additionally indicated by the effective radial Liapunov exponent. Thus, in the following magnetic field line is the equivalent of the particle trajectory.

Generally, the Liapunov exponent of i-th trajectory (magnetic field line), for given initial conditions (position and initial orientation of the infinitesimal displacement) indicates the exponential rate of divergence of trajectories (magnetic field lines) surrounding it [13]

$$l_{ei}(\vec{x}_0, \vec{w}, t) = \frac{1}{t} \ln \frac{d_i(\vec{x}_0, t)}{d_i(\vec{x}_0, 0)}, \tag{107}$$

where $\vec{x}_0 = (r, \theta)$ is the initial position, $\vec{w} = \Delta\vec{x}_0/|\Delta\vec{x}_0|$ is the infinitesimal displacement between two initially close magnetic field lines, $t \sim \zeta$, and $d(\vec{x}_0, t)$ is the norm of the tangent vector $\Delta\vec{x}(t)$, i.e. distance between close trajectories at time t. The positive value of the Liapunov exponent $l_{ei} > 0$ denotes exponential separation between i-th trajectory and initially neighboring one. On the other hand $l_{ei} \leq 0$ corresponds to regular motion during which i-th trajectory and initially neighboring trajectories are stuck to each other ($l_{ei} < 0$) or they are separated linearly with time ($l_{ei} = 0$). In the theory of stochastic processes the finite long time value of Liapunov exponent is of interest. On the other hand, in the context of the particle radial diffusion the interest is also in the time development of the radial Liapunov exponent which is given by

$$l_{ei} \equiv l_{ei}(\vec{x}_0, t) = l_{ei}(\vec{x}_0, \vec{e}_r, t) \tag{108}$$

where $\vec{e}_r \equiv (\partial\vec{w}/\partial r)/(|\partial\vec{w}/\partial r|)$.

The effective radial Liapunov exponent is defined as averaged radial Liapunov exponent with respect to different initial conditions i (magnetic field lines)

$$\langle l_e(t) \rangle = \frac{1}{N} \sum_{i=1}^{N} l_{ei}(t). \tag{109}$$

Note that for the trajectories in M dimensional phase space there is an M dimensional basis of $\vec{w}$ such that for any $\vec{w}$, l_e takes on one of the M (possible nondistinct) values which are ordered by size as

$$l_{e1} \geq l_{e2} \geq .. \geq l_{eM}$$

They are independent of the choice of metric for the phase space. Furthermore, the higher-order Liapunov exponents [13] are introduced in order to describe the mean rate of exponential growth of a p-dimensional volume in tangential space, $p \leq M$.

The Liapunov exponents are closely linked with the Kolmogorov-Sinai entropy (K-entropy) [13, 34] which represents production and growth of uncertainty in the stochastic process

$$K \approx \sum_{l_{ei}>0} l_{ei}$$

3.2 The Wiener process

The Wiener process in unbounded domain is fundamental to the study of diffusion processes [5, 30]. In the theory of Gaussian Brownian motion it describes the positions of the

independent particles on a coarse time scale of step $d\tau$, which is enough small with respect to the observation time, but nevertheless so large that in two successive time intervals $d\tau$, the movements executed by one and the same particle can be thought of as events which are independent of each other. Thus, of particular importance is statistical independence of the increments in the Wiener process. More precisely, the Wiener process is a Markov process (section 1.2.1) beyond the time scale with step $d\tau$. It is described by the Langevin equation as the integral of the white noise, $W(t)$

$$\frac{dx}{dt} = W(t), \tag{110}$$

with

$$\langle W(t) \rangle = 0, \qquad \langle W(t)W(t') \rangle = \mathcal{D}\delta(t - t')$$

where $\mathcal{D}$ is a constant and $x(t)$ is the particle position. Note that $x_i(t), i = 1, .., N$ (where N is the number of particles in the observed particle ensemble), and each $x_i(t)$ separately, are independent random events.

Corresponding Fokker-Plank equation is

$$\frac{\partial}{\partial t} f(x, t|x_0, 0) = \frac{\mathcal{D}}{2} \frac{\partial^2}{\partial x^2} f(x, t|x_0, 0)$$

Its solution is the Gaussian conditional (transition) probability $f(x, t|x_0, 0)$ with the initial condition $f(x, 0|x_0, 0) = \delta(x - x_0) \equiv f(x_0, 0)$. Thus, being of Markov type the Wiener process is totally determinated by the probability of any of its states (for example initial state , $f(x_0, 0)$) and the transition probabilities $f(x, t|x_0, 0)$ from the referent state to the i-th one (section 1.2.1).

Applying the statistical approach from section 3.1 the cumulant coefficients, diffusion exponent and autocorrelation coefficient are

$$C_1 = 0, C_2 = \mathcal{D}t, \alpha = 1 \tag{111}$$

$$\gamma_{3,4} = 0, \tag{112}$$

$$A(t, t') = \sqrt{\frac{t}{t'}}, t \leq t' \tag{113}$$

The autocorrelation coefficients satisfy relation

$$A(t, t")A(t", t') = A(t, t'), \qquad \forall t < (>)t" < (>)t' \tag{114}$$

Thus, from the statistical view point, the Wiener process is a normal diffusive, Markov, Gaussian, and statistically non-stationary process.

3.3 The uniform mixing process

Following Krilovs' definition [2]," a system is of a mixing type when any region, M_0, of the phase space of the system changes in accordance with the equations of motion in such a

way that, while retaining its measure (the volume according to the Liuville theorem) and its connectivity (by virtue of the continuity of the equations of motion), it is deformed so that the measure of that part of it, which finds itself in any prescribed region of a given layer of the phase space (the part of the phase space that is deliminated by the values of the single-valued integral of motion) tends to be proportional to the measure of this prescribed region as the time increases." A given layer is recognized as a part of phase space delimited by the values of the single-valued integrals of motion where the initial region M_0 is defined. In other words, the points of the initial region M_0 tend to be uniformly distributed over the surface of the single-valued integrals of motion as the time increases [2]. In the present context the allowable region for mixing is bounded in configuration space by impermeable KAM barriers around the destroyed magnetic field region (section 2.2.2). The uniform mixing is generically associated with the exponentially fast relaxation of distribution function to the uniform distribution

$$\lim_{t>\tau_{corr}} f(x,t) = \langle f(x,t) \rangle, \tag{115}$$

where τ_{corr} is the correlation time, i.e. the mixing relaxation time and exponentially vanishing correlations [2]

$$\lim_{t'-t>\tau_{corr}} C(g_1(t), g_2(t')) = 0, \tag{116}$$

where $C(g_1(t), g_2(t'))$ denotes arbitrary correlation function, and g_1, g_2 are arbitrary functions of the system states. Equivalently, it may be written by

$$\lim_{t_i-t_k>\tau_{corr}} f(x_k, t_k | x_i, t_i) = f(x_k, t_k) f(x_i, t_i), \tag{117}$$

where $f(x_k, t_k | x_i, t_i)$ is the transition probability. One of the exponentially vanishing correlations among the states of system may be expressed by the autocorrelation coefficients $(g_1(t) = g(t),\ g_2(t') = g(t'))$ as

$$A(t,t') \approx \exp\left(-\frac{t'-t}{\tau_{corr}}\right), \tag{118}$$

where τ_{corr} is the relaxation (correlation) time of mixing. The weaker concept of mixing, which allows slower than exponential decay [2, 7], is suggested in the physical systems recently. Generically it reflects the influence of chaoticity borders, i.e. regularly like structures inside the stochastic region where the mixing is expected to be realized. Thus, the exponentially fast mixing is declared as the uniform mixing process.

In the uniform mixing-type systems trajectories starting from two points laying close to each other diverge rapidly following an exponential law. It is described by the positive Liapunov exponent (section 3.1.5), and the positive Kolmogorov entropy (section 3.1.5). According to section 1.2.1 the Markov property of the mixing system is established with respect to the exponential divergence of initially neighboring trajectories.

The randomness with respect to the exponential instability of motion, i.e. the exponential divergence of the close trajectories [13], is called the deterministic stochasticity (section 1.3): the probability concept becomes applicable. Thus, the uniform mixing process which could be initialized by the exponential instability, appears as one of candidates to explain the statistical properties of the magnetic stochasticity.

In the actual problem the uniform mixing is bounded inside the irregular magnetic field regions. Thus, tendency to uniformization inside the 1D stochastic region: $x\varepsilon[a,b]$, is associated by

$$C_1 \to \frac{a+b}{2},\ C_2 \to \frac{(b-a)^2}{12},\ \gamma_3 \to 0,\ \gamma_4 \to -\frac{6}{5},\ \text{and}\ \alpha \to 0 \qquad (119)$$

Hence, the uniform mixing is a non-diffusive, Markov, uniform, and statistically stationary process in the time limit $t > \tau_{corr}$.

3.4 Strange diffusive process

If the radial particle diffusion is neither the Wiener nor uniform mixing process, then the long-range correlations in space and time, and long tail effects are suggested [6]. In such a case, various relaxation processes may exist. In the context of the radial particle diffusion in the radially bounded stochastic magnetic field region, however, the diffusive process, which is neither the Wiener nor the uniform mixing process in the long time limit, is categorized as subdiffusive or non-diffusive, profile neither uniform nor Gaussian, statistically non-stationary, and (maybe) non-Markov strange diffusive process.

3.5 Statistical criterions

In conclusion several definitions are adopted as the standing points for a declaration about the type of the relaxation process.

- Criterion I: The Wiener approximation is justified under the following conditions:
  - (i) $|\alpha - 1| \leq 0.1$ normal diffusivity [4]
  - (ii) the power-law autocorrelation coefficient fit to the Wiener one written in equation (113)
  - (iii) $|\gamma_{3,4}| \leq 0.1$, the vanishing third and fourth cumulant.
- Criterion II: The uniform mixing approximation is justified under the following conditions:
  - (i) $\alpha \leq 0.1$, $t > \tau_{corr}$ non-diffusivity, $(C_2 \sim w_{st}^2/12)$,

[4] A 10% error criterion.

(ii) the exponentially vanishing autocorrelation coefficient, τ_{corr} is finite

(iii) $|\gamma_3| < 0.1$ and $|\gamma_4 + 6/5| \leq 0.1$.

- Criterion III: Out of the domains of the Wiener, and uniform mixing approximation, the system relaxation associated by

  (i) strange diffusivity (subdiffusivity, superdiffusivity) or non-diffusivity,

  (ii) power-law autocorrelation coefficient,

  (iii) non-vanishing the third and fourth cumulants, and $|\gamma_3| > 0.1$, $|\gamma_4 + 6/5| > 0.1$

  is a strange diffusion process. Because of convinience the strange diffusive process which is non-diffusive and almost statistically stationary is denoted as a non-uniform mixing process.

Because of completeness two additional definitions are adopted:

- The Gaussian approximation is justified by the two following conditions (section 1.1): the particle distribution is not "too broad", and the particle motion is not "long-range correlated". In the present context it is equivalent to the statement: whenever the Wiener approximation is fully justified the Gaussianity is guaranteed.

- The Markovian approximation is justified whenever the correlations are being rapidly lost during the system relaxation: $\tau_{corr} \ll \tau$, where τ_{corr} is the correlation time (uniform mixing: the autocorrelation time; the Wiener process: $d\tau$), and τ is the observation time.

4 Statistical properties of the stochasticity origins

The present section is devoted to the statistical analysis of the collisional stochasticity, and the magnetic field stochasticity.

As it is said in section 1.4, the collisional (statistical) stochasticity is initialized in velocity space by the pitch angle scattering. In the regular magnetic field with nested toroidal surfaces, the collisional stochasticity realizes in configuration space through the particle drift motion: the neoclassical radial diffusion. Thus, the statistical analysis is done in two steps: the collisional stochasticity in velocity, and configuration space.

According to section 1.3, the magnetic field stochasticity is generated by the exponential instability in configuration space. It can be realized within the bounded configuration space region as isolated separatrix irregularity, mixture of regular and irregular domains, and highly developed magnetic field irregularities over all given region. As it was mentioned in section 1.3, the regular structures inside the stochastic region, and the boundaries of it, can change the statistical properties of the magnetic field stochasticity. Here the destruction of the magnetic field is done by involving properly chosen small resonant perturbation. Tables which are mentioned in this section are plotted on page 82.

4.1 Collisional stochasticity

4.1.1 Collisional stochasticity: velocity space

The statistical characteristics of the pitch angle scattering (velocity space stochasticity origin in the neoclassical radial diffusion) can be determined analytically by a conditional probability $f(\lambda, t|\lambda_0, 0)$ with the initial condition

$$f(\lambda, 0|\lambda_0, 0) = \delta(\lambda - \lambda_0) \tag{120}$$

satisfying the Fokker-Plank equation (67). Therefore, the pitch angle scattering is a Markov process, i.e. the knowledge of the general solution of equation (67) (the pitch angle conditional probability)

$$f(\lambda, t|\lambda_0, 0) = \sum_{n=0}^{\infty} \frac{2n+1}{2} P_n(\lambda_0) P_n(\lambda) \exp\left(\frac{-n(n+1)\nu t}{2}\right) \tag{121}$$

where $P_n(\lambda)$ is the Legendre polynomial [45], fully determines the pitch-angle scattering.

Using the orthonormallity relations of the Legendre polynomials

$$\int_{-1}^{1} d\lambda P_m(\lambda) P_n(\lambda) = \frac{2}{2n+1} \delta_{n,m}, \tag{122}$$

average with respect to $f(\lambda, t|\lambda_0, 0)$

$$\langle X(\lambda) \rangle = \int_{-1}^{1} d\lambda X(\lambda) f(\lambda, t|\lambda_0, 0), \tag{123}$$

and calculating the statistical measures with respect to $\lambda(t)$, the values of the first and second cumulants (equations (15) and (16), or (97) and (98)) are

$$C_1(t) = \lambda_0 e^{-\nu t} \tag{124}$$

and

$$C_2(t) = \lambda_0^2(e^{-3\nu t} - e^{-2\nu t}) + \frac{1}{3}(1 - e^{-3\nu t}) \tag{125}$$

The straightforward calculations (equation (96)) give the values of cumulants in the limit $\nu t \gg 1$

$$C_1 = 0, \qquad C_2 = \frac{1}{3}, \qquad \gamma_{2n+1} = 0, \qquad \gamma_4 = -\frac{6}{5}, \tag{126}$$

and

$$\gamma_{2n} \neq 0, \quad n = 1, 2, .. \text{and} \quad \alpha = 0 \tag{127}$$

Note that $\lambda \epsilon [-1, 1]$.

The calculations of two time autocorrelation functions give

$$\begin{aligned} \langle (\lambda(t) - \langle \lambda(t) \rangle)(\lambda(t') - \langle \lambda(t') \rangle) \rangle &= (\lambda_0^2 - \frac{1}{3}) e^{-\nu(t'+2t)} + \frac{1}{3} e^{-\nu(t'-t)} \\ &- \lambda_0^2 e^{-\nu(t+t')} \end{aligned}$$

Hence, the autocorrelation coefficient according to equation (105) is

$$A(t, t') = e^{-\nu(t'-t)}, \qquad t' \geq t \quad \text{when} \quad \nu t \gg 1, \tag{128}$$

where $\tau_{corr} = \nu^{-1}$ is the autocorrelation time. Since the cumulant coefficients are constants, and $A(t, t')$ is the function only of $t' - t$, the pitch angle scattering is a statistically stationary process (section 3.1.4).

According to criterion II (section 3.4) the pitch angle scattering is the uniform mixing process in velocity space.

The analytically predicted statistical properties of the pitch angle scattering are checked by the same numerical procedure as that established for the treatment of the radial diffusion. The numerical calculations are started with ensemble of $N = 10000$ independent particles, whose pitch angle distribution is obtained by uniform random number generator. For a fixed parameter ν, at each time step ($\Delta t = 0.5 \times 10^{-8}$s) the pitch angle of each particle is changed by the Monte Carlo procedure (equation (75)). The statistical procedure in section 3.1.1 gives the values of cumulants which are scattered around the analytical ones (equation (126,127))

$$C_1(t) = (0.0 \pm 10^{-6}), \quad C_2(t) = (\frac{1}{3} \pm 0.002), \quad \gamma_3(t) = (0.0 \pm 0.01), \tag{129}$$

$$\gamma_4(t) = (-\frac{6}{5} \pm 0.01), \quad \text{and} \quad \alpha = 0, \tag{130}$$

where the second number in brackets shows maximum discrepancy from the analytical estimations.

Additionally, the calculations of the autocorrelation coefficients give

$$A(t,t') \approx \mathrm{e}^{-(t'-t)/t_{corr}}, \qquad t' \geq t \tag{131}$$

where the correlation time is $t_{corr} = \nu^{-1}$.

Therefore, the numerically obtained statistical properties of the pitch angle scattering are consistent with the analytical ones.

4.1.2 Collisional stochasticity: configuration space

Since the collisional stochasticity in the regular magnetic field (the neoclassical radial diffusion) is realized by the synergetic effect between particle drift motion [deterministic part] and Coulomb collision (in our case, pitch angle scattering) [stochastic part], it is expected that the temporal behaviour of statistical properties changes beyond the slowest time scale among that of the trapped and passing particle orbits, and stochastic pitch-angle scattering. Thus, a system characteristic time is according to formula (94)

$$\tau_s \sim \begin{cases} \tau_c & \text{for banana regime} \\ \tau_{be} & \text{for plateau regime} \\ \tau_{be} & \text{for Pfirsch-Schlüter regime} \end{cases} \tag{132}$$

It is considered that the system is in transient phase for $t \leq \tau_s$, and the time region $t \gg \tau_s$ is specified as the asymptotic time region.

In the standard neoclassical theory, the radial diffusion is treated as the normal diffusive process. For each collisionality regime, the analytical diffusion coefficient is given by [44]

$$\begin{aligned} D_{PS} &= D_p \frac{\nu}{\nu_t} && : \text{for } \nu_t \ll \nu \\ D_p &= 0.64 \times \frac{\rho^2 v}{2\pi R} = 1.24 \times 10^{-2}\ \mathrm{m^2/s} && : \text{for } \nu_{be} \ll \nu \ll \nu_t \\ D_b &= D_p \frac{\nu}{\nu_t} && : \text{for } \nu \ll \nu_{be} \end{aligned} \tag{133}$$

where $\rho = mv/(eB)$ is the Larmor radius. In figure 1 the analytical diffusion coefficient is plotted as the function of parameter ν (solid line). In the followings, the stochastic properties of the relaxation of the collisional stochasticity in configuration space, i.e. the radial diffusion are numerically analyzed for each collisionality regime. The corresponding collision frequencies are shown in figure 1: $\nu/\nu_t = 0.0045, 0.45$, and 4.5 for banana, plateau, and Pfirsch-Schlüter collisionality regime, respectively. The ratios among various characteristic times are given, using equation (95), by

$$\begin{aligned} \tau_s = \tau_c : \tau_{be} : \tau_t &= 1 : 0.0425 : 0.00435 && \text{banana regime} \\ \tau_s = \tau_{be} : \tau_c : \tau_t &= 1 : 0.218 : 0.095 && \text{plateau regime} \\ \tau_s = \tau_{be} : \tau_t : \tau_c &= 1 : 0.095 : 0.0218 && \text{Pfirsch-Schlüter regime.} \end{aligned} \tag{134}$$

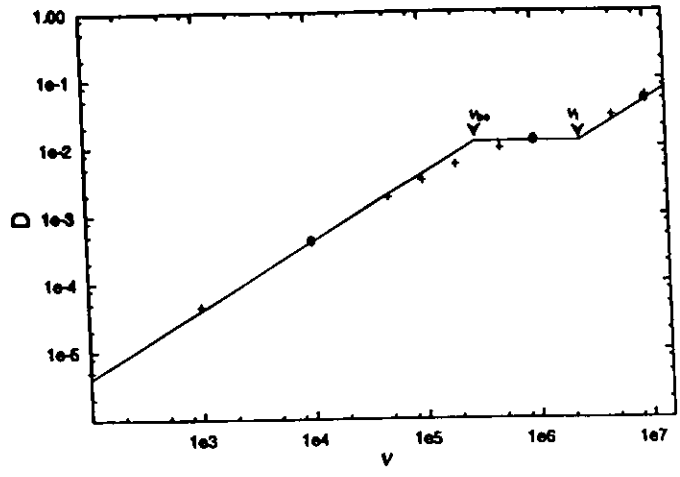

Figure 1: The comparison of the numerically and the analytically calculated neoclassical diffusion coefficients (solid and dotted curve, respectively) for starting particles position $r/a = 0.63$ is shown. The values ν_{be} and ν_t correspond to the effective bounce frequency and transit frequency, respectively. The axes are plotted in log-log proportion.

The type of diffusive behaviour

The normal diffusivity of the radial diffusion is proved by the numerical calculations of the second cumulant (equation (98)), and the diffusion coefficient (equation (102)). In figure 2, $C_2(t)$ is plotted with respect to t. The normal diffusive response of system

$$C_2(t) \approx t \tag{135}$$

in all collisional regimes is clarified by the value of the diffusion exponent α: $\alpha \approx 1$. It is followed by the saturation of the effective diffusion coefficient, and its power-law equivalent (figure 3)

$$D = D_{pw} \approx const., \qquad t > \tau_s \tag{136}$$

Estimations give $D = (0.0004, 0.013, 0.056)\mathrm{m}^2\mathrm{s}^{-1}$ for the banana, plateau, and Pfirsch-Shlüter regimes, respectively. These are consistent with the analytical neoclassical results indicated in figure 1 (open circles on the curve).

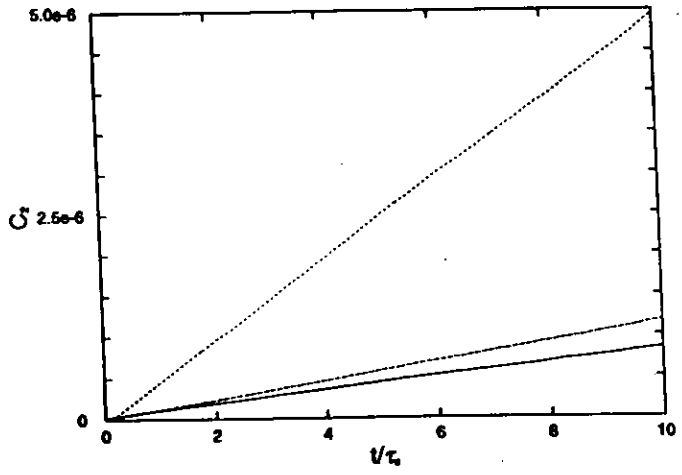

Figure 2: The 2nd cumulant time development for $\nu/\nu_t = 0.0045, 0.45$, and 4.5, is plotted by solid, dashed, and dotted curve, respectively. Time is normalized with respect to the system characteristic time τ_s.

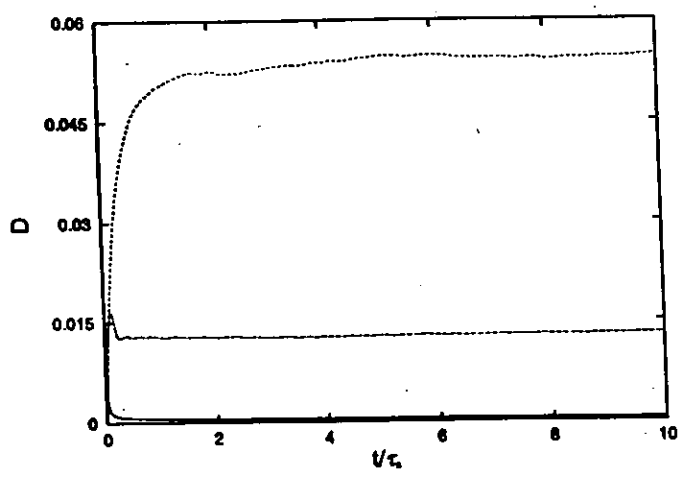

Figure 3: The diffusion coefficient vs time normalized with τ_s. In the long time limit $t/\tau_s \gg 1$ values of $D \equiv D_{pw}$ are estimated as $D = 0.0004, 0.013$, and $0.056\mathrm{m}^2\mathrm{s}^{-1}$ for $\nu/\nu_t = 0.0045$ (solid curve), 0.45 (dashed curve), and 4.5 (dotted curve), respectively.

The autocorrelation coefficient

In figures 4(a), 4(b), and 4(c) the autocorrelation coefficients $A(t,t')$ given by equation (105) are plotted with respect to $\tau = t' - t$, and starting time, t, chosen to be $(2\times10^{-3}, 1.6, 3.2, ..., 12.8)\tau_s$, $(4\times10^{-3}, 1, ..., 8)\tau_s$, and $(2\times10^{-2}, 1, ..., 8)\tau_s$, for the radial diffusion in the banana, plateau, and Pfirsch-Schlüter regimes (solid lines), respectively. As t increases the form of $A(t,t')$ curves changes (figures 4(a), 4(b), and 4(c)). The fine structures are observed in the power-law like autocorrelation curves. In the collisionless (banana) regime (figure 4(a)) they are the result of the characteristic trapped and passing particle periodic motions, which are weakly affected by rare stochastic events ($\tau_s = \tau_c \gg \tau_{be} > \tau_t$). As the stochastic small particle deflections from the regular drift orbits become more frequent ($\tau_s = \tau_{be} > \tau_c, \tau_t$, the collisional regimes), the autocorrelation curves become more smooth (figures 4(b), and 4(c)).

Additionally, in figures 4(a), 4(b), and 4(c) the autocorrelation coefficients $A(t,t')$ for the radial diffusion in the banana, plateau and Pfirsch-Schlüter regime (solid curves) are compared with the Wiener ones (dotted curves) which are given by equation (113). The time behaviour of the autocorrelation coefficients is well approximated by the Wiener process with the increase in t in all collisional regimes. This is more clear with the increase in $\tau = t' - t$. According to the absence of any time correlation effect in the Wiener process the deviations of $A(t,t')$ in the asymptotic time limit from the Wiener ones may be related to the existence of the short time correlations. Also, figures (4(a),4(b), and 4(c)) show that tendency of the radial diffusion $A(t,t')$ curves to fit to the Wiener ones is slower in the collisionless than in the collisional regimes. It appears since the particle orbit motion is less affected by collisions in the banana regime with $\tau_c \gg \tau_{be} > \tau_t$ than in the plateau and Pfirsch-Schlüter regimes with the characteristic time ordering $\tau_{be} > \tau_c > \tau_t$ and $\tau_{be} > \tau_t > \tau_c$, respectively.

In order to confirm above observations from figure 4, the coefficient y, associated with equation (114), is calculated

$$y = \frac{A(t,t'')A(t'',t')}{A(t,t')} - 1, \quad t < t'' < t' \tag{137}$$

For a Wiener process $y = 0$. The numerical values of $A(t,t')$ are collected on time scale whose unit step and starting time are $\Delta t = 0.1\tau_s$ and $t = (0.5, 1, 2, 3, 5)\tau_s$, respectively. Therefore, $t'' = t + m\Delta t$ and $t' = t'' + n\Delta t$, where $m, n = 1, 2....$ In table 1 the maximum values of $|y|$ are shown for the banana ($\nu/\nu_t = 0.0045$), plateau ($\nu/\nu_t = 0.45$), and Pfirsch-Schlüter ($\nu/\nu_t = 4.5$) regime, respectively. The radial diffusion process in the plateau regime is the best approximated by a Wiener process ($\tau_s = \tau_{be} > \tau_c > \tau_t$).

Generally, the values of $|y|_{max}(t)$ decrease as the starting time t increases and average values of deviations, $\langle y \rangle$, given in table 2 tend to the Wiener one $\langle y \rangle = 0$ in all collisional regimes. Thus, in the long time limit $t \gg \tau_s$ the radial diffusion $A(t,t')$ curves fit nicely to the Wiener ones.

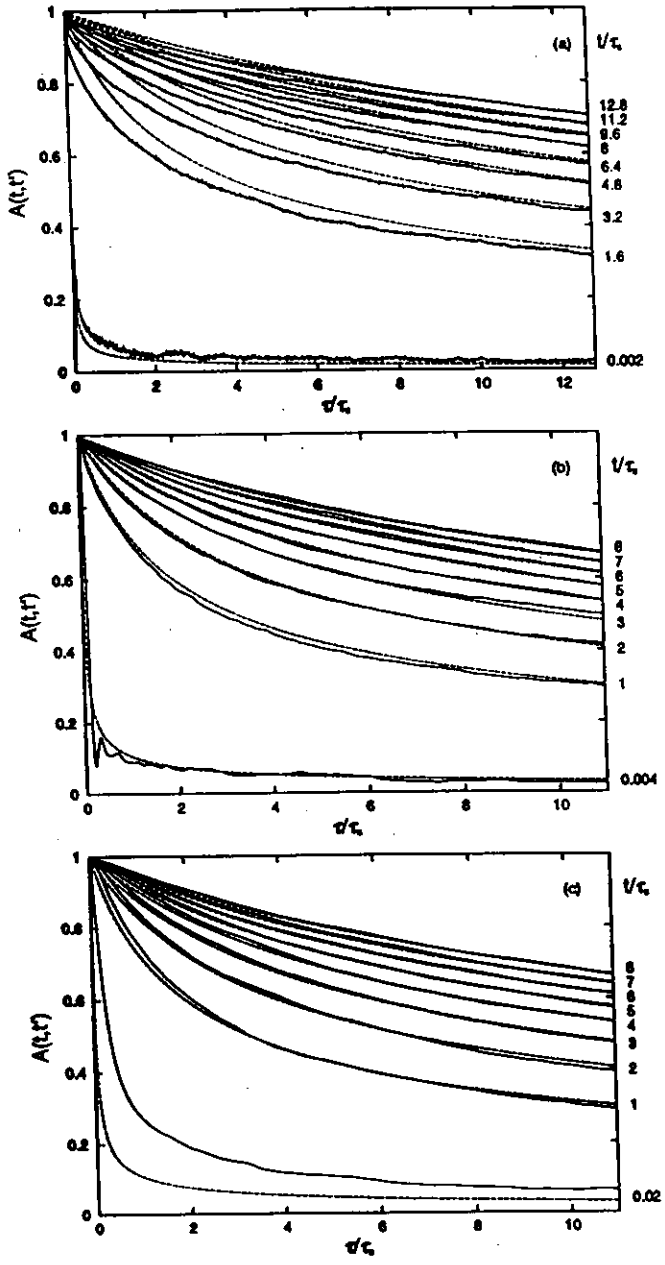

Figure 4: The $A(t,t')$ vs τ/τ_s. Different curves are obtained with respect to different starting time t/τ_s. The values of t/τ_s are written on the right: (a) $\nu/\nu_t = 0.0045$, (b) $\nu/\nu_t = 0.45$, (c) $\nu/\nu_t = 4.5$. Corresponding Wiener curves are plotted by dashed curves.

The cumulant coefficients

The calculations of $C_1(t)$ (equation (97)) show that the convective effect is irrelevant ($|C_1(t)| = |\langle \delta r(t) \rangle| \approx 10^{-5} a \approx \rho_{||}$) in all collisional regimes.

The time behaviour of skewness (γ_3), and kurtosis (γ_4) is investigated in order to see relation with Gaussianity. The values of skewness tend to $|\gamma_3| \approx 0.02$ ($t \gg \tau_s$) in figure 5, which indicates a highly symmetric particle radial distribution with respect to $\langle r(t) \rangle \approx r(t=0)$ in all collisional regimes. The normalized drift widths of passing Δ_p/a and trapped Δ_t/a particles (electrons) at the initial magnetic surface are given by

$$\frac{\Delta_p}{a} = \frac{\rho_{||}}{\epsilon a \sqrt{\epsilon}} = 9.2 \times 10^{-5}$$

and

$$\frac{\Delta_t}{a} = \frac{\rho_{||}}{\epsilon a} = 2.0 \times 10^{-4}$$

where $\epsilon = r(t=0)/R = 0.21$. These values are so small that electrons could not feel asymmetry of the system, even if their orbits are asymmetric around their initial magnetic surfaces. Figure 6 shows tendency of kurtosis to reduce to $|\gamma_4| \approx 0$ in asymptotic time

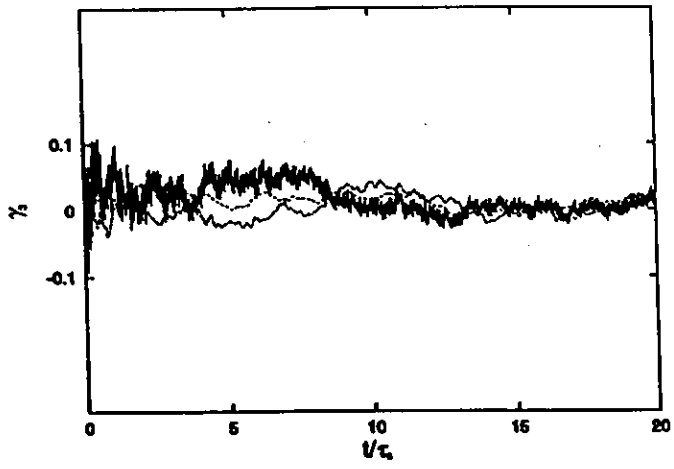

Figure 5: The third cumulant time developments for $\nu/\nu_t = 0.0045, 0.45$, and 4.5, are illustrated by solid, dashed, and dotted curve, respectively.

region, $t \gg \tau_s$, or more strictly, $t > 20\tau_s$ in the collisionless, and $t > 5\tau_s$ in the collisional regimes. Thus, the obtained time behaviour of γ_4 illustrates the particularity of the collisionless regime, or generally, of the time regions where the stochastic scatterings weakly affect the particle orbit motion (transient time regions in all collisional regimes). The particle orbit effects strongly affect the radial diffusion in the collisionless regime by slowing down relaxation of kurtosis to $\gamma_4(t) \approx 0$. The transient positive value of kurtosis in the collisionless banana regime (solid line in figure 6) indicates a more peaked (at $r(t) = \langle r(t) \rangle$) distribution function than Gaussian (rare stochastic scatterings yet can not produce the significant radial displacement of ensemble constituent majority from the regular drift

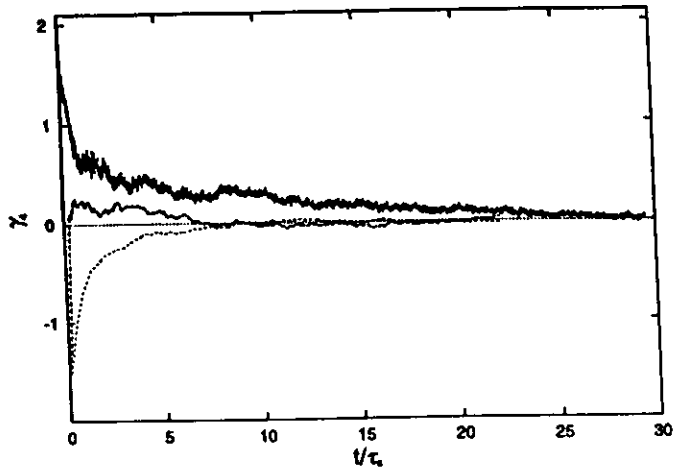

Figure 6: The fourth cumulant time developments for $\nu/\nu_t = 0.0045, 0.45$, and 4.5, are illustrated by solid, dashed, and dotted curve, respectively.

surfaces). On the other hand, the negative transient values of kurtosis observed in the collisional Pfirsch-Schlüter regime (dotted curve in figure 6), correspond to a more flated distribution than Gaussian (particles wander across areas in the neighborhood of the earlier regular drift surfaces).

The short time ballistic phase

The short time , $t \approx \tau_t \ll \tau_s$, ballistic phase characterized by

$$C_2(t) \approx t^2 \tag{138}$$

and the diffusion exponent $\alpha \approx 2$, is detected in all collisional regimes (figure 7). During it particles "freely" follow corresponding regular drift orbits. The collisional effects, which introduce stochasticity in the system, can not enough affect the particle motions as long as τ_c is higher or the same order as τ_t, and the ballistic phase is observed. In the banana ($\tau_c = 10^{-4}$s), plateau ($\tau_c = 10^{-6}$s), and Pfirsch-Schlüter ($\tau_c = 10^{-7}$s) regimes, $\tau_c \gg \tau_t$, $\tau_c > \tau_t$, and $\tau_c \approx \tau_t$, respectively. Hence, the short time ($t \approx \tau_t$) ballistic behaviour is found in all collisional regimes, but can not influence the long time behaviour of the particle diffusion.

Thus in the limit, $t \gg \tau_s$, according to the criterion I in section (3.4) the neoclassical radial diffusion is a Wiener type process.

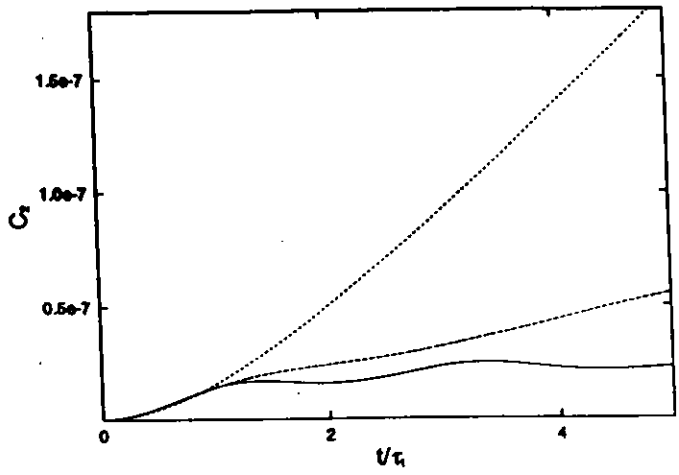

Figure 7: The short time behaviour of C_2 for banana, plateau, and Pfirsch-Schlüter regimes (solid, dashed, and dotted curve, respectively).

4.1.3 Type of the statistic process: the long time limit

- The collisional stochasticity is developed as a non-diffusive, Markov, uniform, and statistically stationary process, i.e. the uniform mixing in velocity space. The correlations exponentially vanish after the correlation time, $\tau_{corr} = \tau_c$.

- The collisional stochasticity is realized in configuration space as a radial diffusion which is a normal diffusive, Markov, Gaussian, and statistically non-stationary process, i.e. the Wiener type process.

4.2 Statistical properties of the magnetic field stochasticity

To investigate the statistical properties of the magnetic field structure, namely the cumulant, diffusion coefficient, diffusion exponent, and autocorrelation coefficient, equations of the magnetic field line given by (63)-(65) are solved under the condition of $\mu = 0, E = 3\text{keV}$, for various values of s_b (section 2.2.2). In this treatment the time t is used as independent variable, so that the direct comparison of statistical quantities of the magnetic field structure with those of particles under Coulomb collision becomes possible. Moreover, obtained statistical properties are interpreted as those of guiding center particles without perpendicular drift motion and Coulomb collisions. To create various types of magnetic field structure, s_b/s_{bc} is chosen as 0.33 (before overlapping), 1.3 (near overlapping), 3.3 (moderate overlapping), and 33 (highly overlapping). The critical value of s_b corresponding to the overlapping condition: s_{bc} is given by equation (84).

The magnetic field stochasticity appears in the configuration space through the growth of irregular domains. Thus, as long as the overlapping of neighboring islands (developing of the global magnetic stochasticity) has not been started the irregularities are localized around the island separatrix regions, and the statistical treatment is meaningless. However, the values of the cumulant, and autocorrelation coefficients in the absence of the global magnetic stochasticity are mentioned because of completeness.

The magnetic field structures, for $s_b/s_{bc} = 0.33, 1.3, 3.3$, and 33, are the isolated island chain at $q = 3/2 (w_{3,2}/a = 0.024)$, overlapping among islands at $q = 3/2, 10/7, 11/7 (w_{st}/a \approx 0.14)$, stochastic sea ($w_{st}/a \approx 0.17$) with isolated island structures at $q = 10/7, 11/7$ ($w_{m,n}/w_{st} \approx 1/4$), and stochastic sea without structures ($w_{st}/a \approx 0.25$). The $w_{m,n}$ and w_{st} are the width of the island and stochastic region, respectively. In figures 8a-8d, the corresponding Poincare plots at the poloidal cross section with $\zeta = 2.4\text{rad}$ are shown. The time interval for sequential plotting is $100 \times dt \equiv 10^{-7}\text{s}$, and the test magnetic field lines are followed during the time interval of $0 \geq t \leq 1.5 \times 10^{-4}\text{s}$ for $s_b/s_{bc} = 0.33, 3.3$, and 33, and the time interval of $1.3 \times 10^{-3}\text{s} \geq t \leq 1.5 \times 10^{-3}\text{s}$ for $s_b/s_{bc} = 1.3$.

4.2.1 Effective Liapunov exponent

The effective radial Liapunov exponent given by equation (109) provides a quantitative measure of the degree of stochasticity for magnetic field lines. Note that the magnetic field line is identified by an electron tied to it (section 2.2). Thus, the effective radial Liapunov exponent is calculated for a sample of $N = 1000$ magnetic field lines (electrons). The numerical approach of reference [46] is adopted for the magnetic field line described by equations (63)-(65), where the toroidal angle ζ is treated as an independent variable instead of time t by combining equations as $d\psi/d\zeta$ and $d\theta/d\zeta$. The transformation to time is done by $t \sim c\zeta$ with $c \approx R/v_{\|}$, $v_{\|} = \sqrt{2E/m}$, and $E = 3\text{keV}$.

Under the threshold for overlapping, $s_b/s_{bc} < 1$, although the effective radial Liapunov

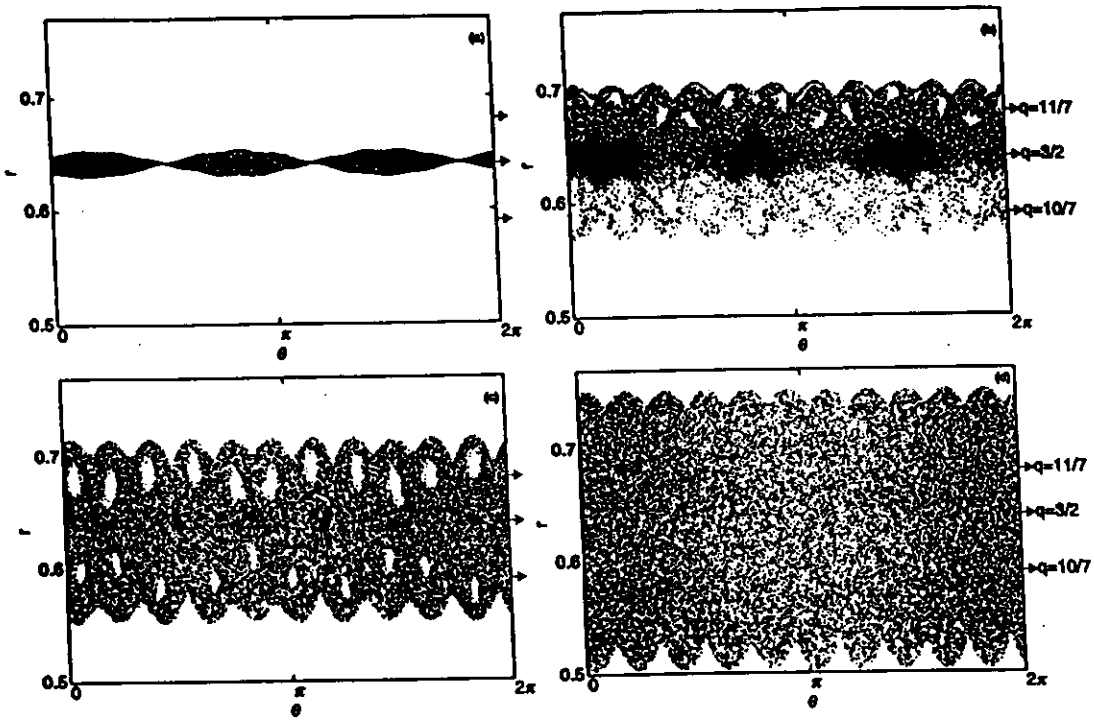

Figure 8: The Poincare plots of the test magnetic field line ensemble in (r, θ) plane at $\zeta = 2.4$: (a) $s_b/s_{bc} = 0.33$, (b) $s_b/s_{bc} = 1.3$, (c) $s_b/s_{bc} = 3.3$, (d) $s_b/s_{bc} = 33$. The arrows show position of the rational surfaces, $q = 10/7, 3/2, 11/7$.

exponent $\langle l_e(t)\rangle$ increases almost monotonically in time, it is always negative during the calculation tending to finite negative value $\langle l_e(t)\rangle c \approx -5 \times 10^{-3}$ after $t > 9 \times 10^{-5}$s (figure 9a). The corresponding number of the magnetic field lines with positive Liapunov exponent $N_p(t)$ is very few as indicated in figure 10a. On the other hand, in the region of the global magnetic stochasticity, $s_b/s_{bc} \geq 1$, the effective radial Liapunov exponent $\langle l_e(t)\rangle$ and the number of the magnetic field lines with positive Liapunov exponent $N_p(t)$ almost monotonically increase with time, as is show in figures 9b-9d and 10b-10d, respectively. The $\langle l_e(t)\rangle$ changes from negative to positive values, asymptotically leading to saturation. The $N_p(t)$ also shows the tendency to saturate, as time increases, and it saturates faster than the effective radial Liapunov exponent. A time t_d at which the effective radial Liapunov exponent becomes zero : $\langle l_e(t)\rangle$=0, is defined as a characteristic time for $s_b/s_{bc} \geq 1$. As is understood from figures 10b-10d, as s_b/s_{bc} increases, about half of the magnetic field lines are characterized by the positive Liapunov exponent ($l_{ei} > 0$) (diverge) at $t \approx t_d$. After t_d, $N_p(t)$ still continuously increases, and $\langle l_e(t)\rangle$ becomes positive, which means that the divergence of the magnetic field lines starts in the sense of the average. Thus, the time t_d is recognized as the decorrelation time of the stochastic magnetic field lines. Judging from figures 9b-9d, the simple analytical model expression of $\langle l_e(t)\rangle$ can be introduced as

$$\langle l_e(t)\rangle = \langle l_e\rangle \left(1 - \frac{t_d}{t}\right), \tag{139}$$

where $\langle l_e \rangle$ is asymptotic value of the effective radial Liapunov exponent which is determined by fitting the above expression to the numerically obtained one. The fitting curves are shown in figures 9b-9d by dotted lines, where good agreement between the numerical data and the model expression is found. From this good fitting it can be concluded that the time independent effective radial Liapunov exponent is indeed asymptotically obtained (in infinite time limit). Therefore, it is useful to introduce such a finite time t_s that indicates how the system is near a final relaxed state. In the present case, such time t_s is defined as $\langle l_e(t = t_s) \rangle = 0.9\langle l_e \rangle$, namely, $t_s = 10 \times t_d$. Note that t_s depends only on t_d, once the ratio $\langle l_e(t) \rangle / \langle l_e \rangle$ is determined. In the following the time t_s is interpreted as a relaxation time of the effective radial Liapunov exponent. Times t_d, t_s, and the estimated $c\langle l_e \rangle$ are denoted in figures 9 and 10, and are summarized as

$$\begin{aligned} &t_d \approx 1.2 \times 10^{-4}\mathrm{s}, t_s = 10 \times t_d, c\langle l_e \rangle = 5.4 \times 10^{-3} \quad , \quad \text{for } s_b/s_{bc} = 1.3, \\ &t_d \approx 2.0 \times 10^{-5}\mathrm{s}, t_s = 10 \times t_d, c\langle l_e \rangle = 3.7 \times 10^{-2} \quad , \quad \text{for } s_b/s_{bc} = 3.3, \\ &t_d \approx 1.8 \times 10^{-6}\mathrm{s}, t_s = 10 \times t_d, c\langle l_e \rangle = 4.5 \times 10^{-1} \quad , \quad \text{for } s_b/s_{bc} = 33. \end{aligned} \tag{140}$$

By assuming $\langle \ln d(t) \rangle \approx \ln \langle d(t) \rangle$, from the equations (107), (109) and (139),

$$\langle d(t) \rangle \approx \langle d(0) \rangle \exp\left(\langle l_e \rangle (t - t_d) \right), \tag{141}$$

is obtained. This relation means that the averaged distance $\langle d(t) \rangle$ between initially two neighboring trajectories exponentially grows after $t = t_d$. As one of the measures of the uniformity of process, the relative dispersion of the effective Liapunov exponent around mean value is defined as

$$\Delta l_e(t) \equiv \frac{\sqrt{\langle l_e(t)^2 \rangle - \langle l_e(t) \rangle^2}}{\langle l_e(t) \rangle}. \tag{142}$$

The relative dispersions $\Delta l_e(t)$ for $s_b/s_{bc} = 1.3, 3.3$, and 33 are $\Delta l_e(t \approx t_s) \approx 0.99, 0.27$, and 0.093, respectively. Thus, the uniform exponential divergence of magnetic field lines is obtained as s_b/s_{bc} increases.

From relation (140), the larger s_b/s_{bc} is, the shorter t_d, t_s and the interval $t_s - t_d$ become. Moreover, as it is shown in figures 10b-10d, approximately 0%, 80%, 98%, and 100% of magnetic field lines have a positive Liapunov exponent (magnetic field lines diverge) for $s_b/s_{bc} = 0.33, 1.3, 3.3$, and 33, respectively. The existence of magnetic field lines with a non-positive Liapunov exponent for $s_b/s_{bc} \geq 1$ is related to the presence of regular structures inside the destroyed magnetic field region. As long as the magnetic field lines are stuck to the regular structures (e.g. island like structures) their freely wandering is prohibited, leading to the negative or zero Liapunov exponent. Thus, as s_b/s_{bc} increases the importance of sticking to regular structures decreases, so that the time ordering from equation (140) becomes meaningful. The particularity of the overlapping threshold region, $s_b/s_{bc} = 1.3$, is very slow increase of Liapunov exponent and the number of exponentially diverging magnetic field lines in time after $t = t_d$. It is according to

fact that approximately 20% of magnetic field lines are prevented to wander by sticking to regular structures at $t \geq t_s$. Additional confirmation is obtained from the Poincare sections. Roughly, at $t \approx t_d$ the part of magnetic field lines started from flux surface with $q = 3/2$ can be transported into the region around $q = 11/7$, and additionally at $t \approx 5t_d$ transport into the region $q = 10/7$ starts. In other words, the magnetic field lines being temporary stuck by regular structures need long time to experience all allowable stochastic region (bounded by impermeable KAM surfaces around the destroyed magnetic field region) and slow saturation of the effective radial Liapunov exponent is observed.

As it is clear from the above argument, even if the overlapping condition of magnetic islands is satisfied ($s_b/s_{bc} \geq 1$), the statistical treatment of the magnetic field stochasticity is meaningless before $t = t_d$. Moreover, the statistical properties of the magnetic field stochasticity are thought to become uniquely clear after $t = t_s$. However, as it is shown in figures 10a-10d, the number of the magnetic field lines with positive Liapunov exponent becomes constant before $t = t_s$ for $s_b/s_{bc} = 3.3$, and 33. On the other hand, for $s_b/s_{bc} = 1.3$ it is not constant within calculation time, but similar tendency of Liapunov exponent to be constant is found. Since the magnetic field lines with positive Liapunov exponent have same expanding properties, once the number of magnetic field lines with positive Liapunov exponent becomes nearly constant, the statistical properties of the magnetic field stochasticity are considered not to change, at least qualitatively. Hence, the statistical properties of the magnetic field stochasticity are mainly examined after the number of the magnetic field lines with positive Liapunov exponent becomes constant, namely after $t = t_s$, in order to save the computational time. In the following calculations, this condition is satisfied for $s_b/s_{bc} = 3.3$, and 33, and it is weakly satisfied for $s_b/s_{bc} = 1.3$.

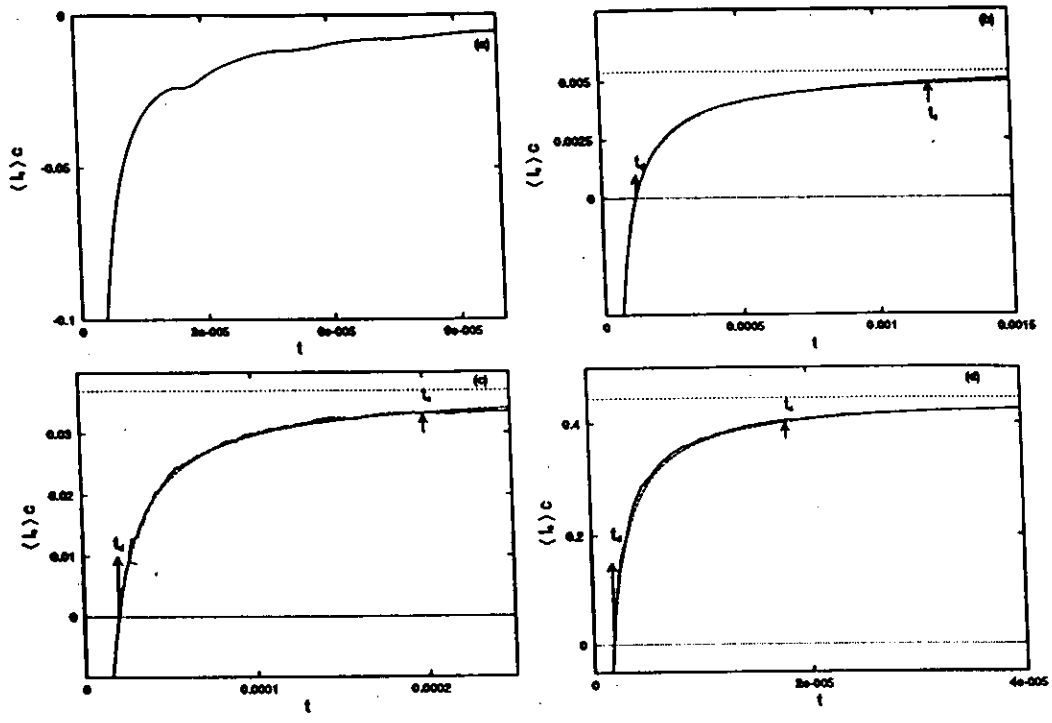

Figure 9: The time behaviour of the radial effective Liapunov exponent $\langle l_e \rangle c$ vs t for $s_b/s_{bc} = 0.33, 1.3, 3.3$, and 33 is plotted in figures (a),(b),(c), and (d), respectively.

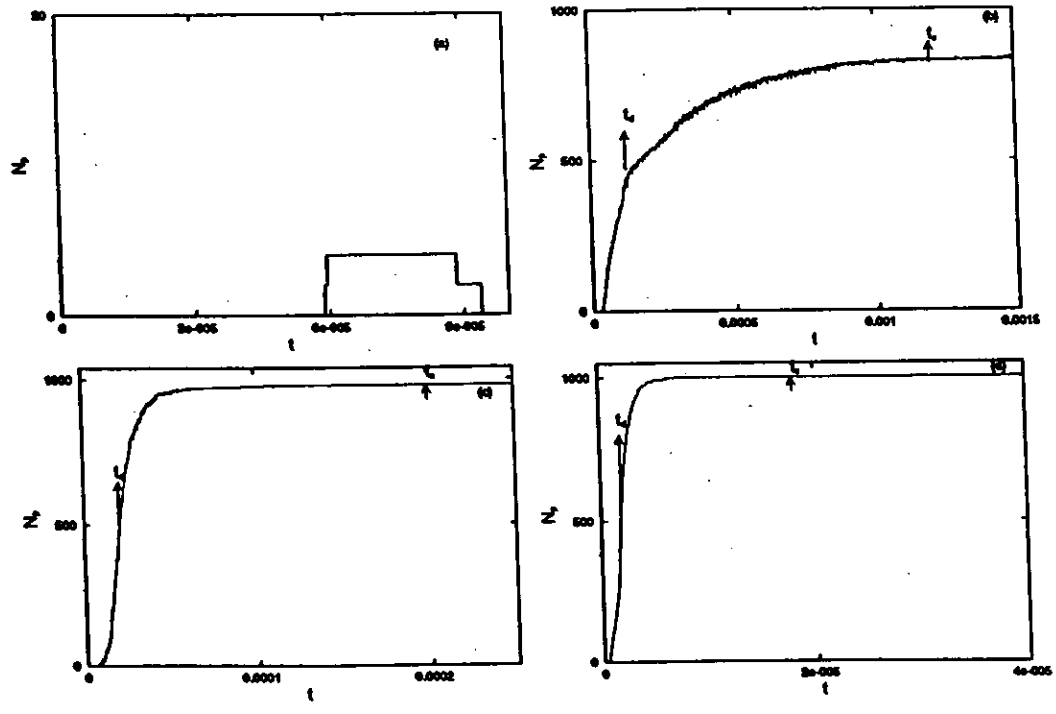

Figure 10: The number of magnetic field lines N_p with positive radial Liapunov exponent vs time t for $s_b/s_{bc} = 0.33, 1.3, 3.3$, and 33 is plotted in figures (a),(b),(c), and (d), respectively.

4.2.2 Type of diffusive behaviour

The case with isolated magnetic field irregularities ($s_b/s_{bc} = 0.33$) is characterized by the oscillatory behaviour of the second cumulant $C_2(t)$ around 2×10^{-5}, and corresponding oscillatory behaviour of the diffusion exponent, α around 0.

In figure 11 the time developments of the second cumulant in the region of global stochasticity ($s_b/s_{bc} \geq 1$) are shown for $s_b/s_{bc} = 1.3$, for $s_b/s_{bc} = 3.3$, and for $s_b/s_{bc} = 33$, respectively. After the transient phase ($t > t_d$), the second cumulants gradually increase. This behaviour is completely different from that of the Wiener process shown in figure 2. The corresponding diffusion exponent α, two types of diffusion coefficient $D(t), D_{pw}(t)$, and the relative difference $\Delta D(\%)$ in the long time limit are shown in tables 3 and 4 (the corresponding row is indicated by $\nu/\nu_t = 0 (v_{d\perp} = 0)$. In the case of $s_b/s_{bc} = 1.3$, the diffusion exponent α is fairly less than unity, but finite. Thus, it is understood that the radial magnetic field diffusion behaves as subdiffusive. In this case, the relative difference $\Delta D(\%)$ given by equation (104) between $D(t)$ given by equation (102) and $D_{pw}(t)$ given by equation (103) is not so large (table 4). The power-law approximation of the diffusion coefficient is not so wrong. However, in the stochastic sea with ($s_b/s_{bc} = 3.3$) and without structures ($s_b/s_{bc} = 33 \gg 1$), this difference becomes quite large (exp in table 4), and the diffusion exponent becomes significantly small. Thus, the radial magnetic field diffusion is considered to be non-diffusive.

After the overlapping of the magnetic islands, as s_b/s_{bc} increases, the type of diffusive behaviour changes from subdiffusivity to non-diffusivity in the long time limit. This tendency is natural in the considered magnetic field. The stochastic magnetic field considered here is bounded in the radial direction, namely outside of the stochastic region KAM surfaces exist. Thus, the maximum relative radial displacement $(\delta r(t) - \langle \delta r(t) \rangle)_{max}$ in the duration of the calculation is bounded by $w_{st}/2$ for each field line: non-locality of the radial displacements. Moreover, as s_b/s_{bc} increases, the magnitude of the effective radial Liapunov exponent $\langle l_e \rangle$ rapidly increases as it is shown in figure 9, so that majority of magnetic field lines reach the boundary of the stochastic region in a short time. Hence $C_2(t)$ rapidly increases up to the order of the bounded value $w_{st}^2/12$, which leads to the subdiffusive or non-diffusive behaviour in the long time limit. Indeed as it is shown in figure 4, $C_2(t)$ for $s_b/s_{bc} = 3.3$ and 33 is of the order of $w_{st}^2/12$ after $t = t_d$. In the long time limit, $C_2 \approx w_{st}^2/16$ for $s_b/s_{bc} = 3.3$ and $C_2 \approx w_{st}^2/12$ for $s_b/s_{bc} = 33$. The situation of the radial particle diffusion in the regular magnetic field investigated in section 4.1 is completely different. Although the system is bounded by the minor radius a, the relative radial displacement $\delta r(t) - \langle \delta r(t) \rangle$ is significantly small compared with a because of the quite small radial drift width, so that the particles never reach the plasma boundary in the observation duration, or the particles can not recognize the existence of the boundary. Therefore, the relative radial displacement can act as $\delta r(t) - \langle \delta r(t) \rangle \sim \sqrt{\nu t} c$ (c is positive constant) by the collisional effect, leading to the normal diffusion.

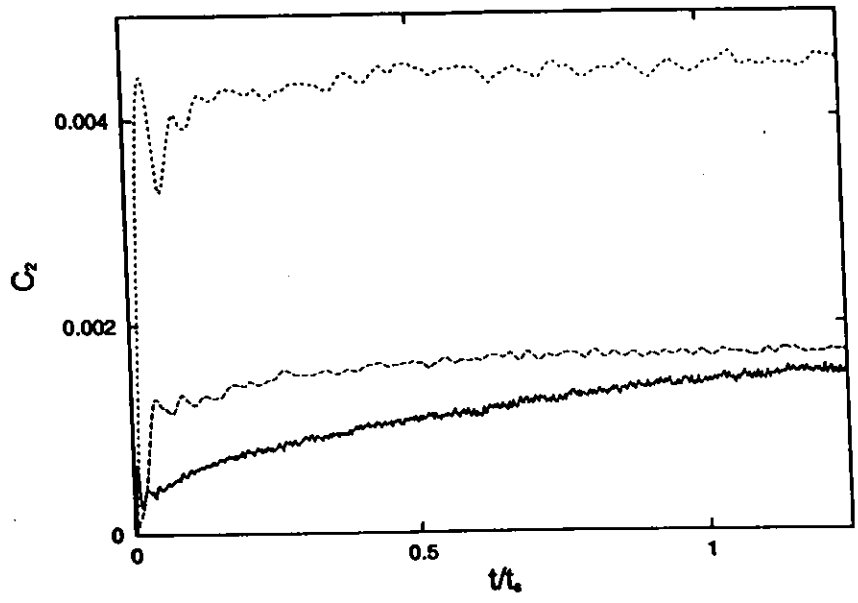

Figure 11: The second cumulant vs time for $s_b/s_{bc} = 1.3, 3.3$, and 33 are plotted by solid, dashed, and dotted curve, respectively. The time t is normalized with the relaxation time of the effective radial Liapunov exponent t_s.

4.2.3 Autocorrelation coefficient

The oscillatory behaviour of $A(t,\tau)$ with respect to τ is one of characteristics of the relaxation in the region of isolated island chain with $s_b/s_{bc} = 0.33$.

In figure 12, the autocorrelation coefficients $A(t, \tau = t'-t)$ vs τ are plotted at $t \approx 0.56t_s$ for $s_b/s_{bc} = 1.3$ (solid line), for $s_b/s_{bc} = 3.3$ (dashed line), and for $s_b/s_{bc} = 33$ (dotted line), respectively. The reminiscent oscillatory pattern on the power-law like envelope for $s_b/s_{bc} = 1.3$ (where overlapping between islands has just been started (figure 8b)) is the indication of the relative importance of the regular motion inside the stochastic region. It is indicated by P_{osc} in table 5. As s_b/s_{bc} increases, this oscillatory behaviour of $A(t,t')$ vanishes, and a stationary power-law like behaviour appears. For $s_b/s_{bc} = 3.3$, this stationary power-law like behaviour can be fitted as

$$A(t,t') \approx A(\tau) \approx \tau^{-0.87}, \tag{143}$$

for large τ (figure 12, dashed line), and is indicated by P_{st} in table 5.

In the presence of stochastic sea without structures ($s_b/s_{bc} = 33$), the exponentially fast vanishing autocorrelation coefficient (denoted by E in table 5) is obtained (figure 12, dotted curve). Since the autocorrelation coefficient is found to be independent of the starting time t, it may be expressed as

$$A(t,t') \approx A(\tau) \approx \exp\left(-\frac{\tau}{\tau_{corr}}\right), \tag{144}$$

where τ_{corr} is the autocorrelation time. The numerically evaluated τ_{corr} is around 2.4×10^{-6}s. This time corresponds to t_d given by equation (140).

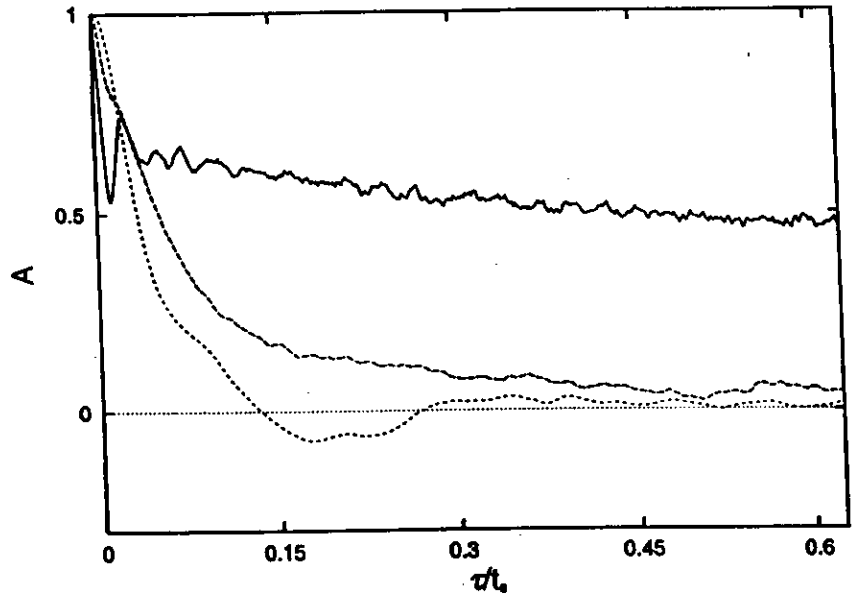

Figure 12: The autocorrelation coefficient $A(t,t')$ vs $\tau = (t'-t)/t_s$ for the starting time $t/t_s = 0.56$: $s_b/s_{bc} = 1.3$ solid curve, $s_b/s_{bc} = 3.3$ dashed curve, and $s_b/s_{bc} = 33$ dotted curve.

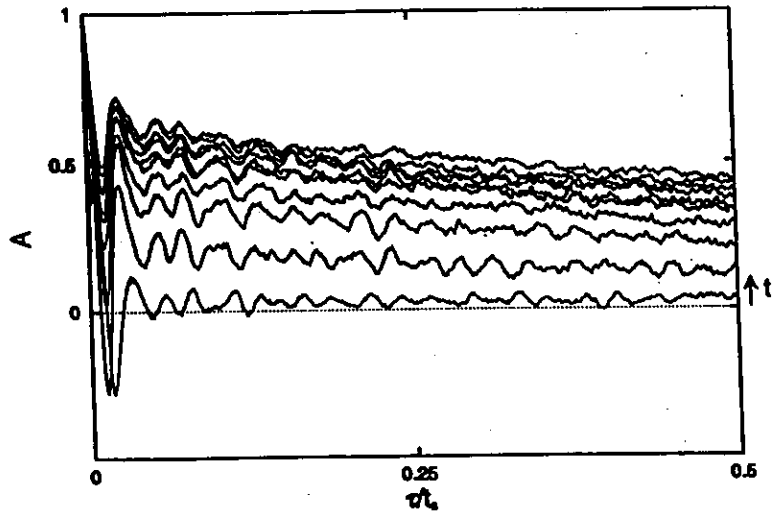

Figure 13: The $A(t,t')$ vs $\tau = (t'-t)/t_s$ for $s_b/s_{bc} = 1.3$ with respect to starting time $t/t_s = 8 \times 10^{-5}, 0.1, 0.15, ..., 0.45$. The arrow shows direction of the increasing t.

According to figure 12 and the above discussion, the larger s_b/s_{bc} is, the time correlations are lost faster, and the tendency of $A(t,t')$ to be stationary becomes stronger. For $s_b/s_{bc} \geq 1$, as it is shown in figure 9, some of magnetic field lines have a negative Liapunov exponent, which means that those field lines stick to the regular structures in the stochastic region (section 4.2.1). This sticking may be related with the slow relaxation of $A(t,t')$. As s_b/s_{bc} increases more, regular structures disappear, so that all of the magnetic field lines have a positive Liapunov exponent as is shown in figure 9d, leading to exponentially fast relaxation of $A(t,t')$ for $s_b/s_{bc} \gg 1$.

For $s_b/s_{bc} = 33 \gg 1$ the effective radial Liapunov exponent has a time independent positive value in the long time limit $t \geq t_s$. According to the value of relative dispersion of the effective radial Liapunov exponent $\Delta \approx 0.093$, this means that all the magnetic field lines with a positive radial Liapunov exponent have time-independent same magnitude of the Liapunov exponent in the average sense. In other words it is connected with ergodicity of the magnetic field lines. Hence, the autocorrelation coefficient $A(t,t')$ may become independent of time, namely stationary: $A(t,t') = A(\tau = t' - t)$, and the autocorrelation time as a time after which the time correlations vanish τ_{corr} for $s_b/s_{bc} \gg 1$ becomes similar to t_d with $\langle l_c(t_d) \rangle = 0$. In weaker sense the stationarity of the autocorrelation coefficient for $s_b/s_{bc} = 3.3$ can be considered from the same point of view. Note the absence of the autocorrelation time due to presence of regular structures inside the stochastic sea for $s_b/s_{bc} = 3.3$ which is indicated by the non-vanishing long time tail of the autocorrelation coefficient. On the other hand the stationarity of the autocorrelation coefficient for $s_b/s_{bc} = 1.3$ is absent as it is seen in figure 13, in which the $A(t,t')$ curves are plotted with respect to starting time $t/t_s = 0.8 \times 10^{-4}, 0.1, 0.15, ..., 0.45$.

4.2.4 Cumulant coefficients

Although the first cumulants C_1 show complicate temporal behaviours depending on s_b/s_{bc}, the magnitude normalized by the minor radius is always quite small independent on s_b/s_{bc}, as is indicated in table 6 for the long time limit.

Before island overlapping with $s_b/s_{bc} \ll 1$, as well as C_1 and C_2, both the skewness γ_3 and kurtosis γ_4 show oscillatory behaviours in time around $\gamma_3 \sim 0$ and $\gamma_4 \sim -0.4$, reflecting the regular motions in the magnetic islands.

After the overlapping with $s_b/s_{bc} \geq 1$, such oscillatory behaviours in time disappear, and the radial distribution of the stochastic magnetic field lines or particles strongly tied to them is completely different between the state near island overlapping threshold with $s_b/s_{bc} \sim 1$ and the more stochastic state with $s_b/s_{bc} > 1$. Near the threshold of island overlapping, both the skewness γ_3 and kurtosis γ_4 rapidly increase in the ballistic phase corresponding to the time $t < t_d$, and gradually decrease keeping the values positive, as is indicated in figures 14 and 15 by solid lines. Thus, the radial distribution is a peaked profile compared with Gaussian, and also the distribution has an asymmetric tail

extending out towards $\delta r > \langle \delta r \rangle$, which is consistent to the Poincare plot shown in figure 8b. In the moderate overlapping case with $s_b/s_{bc} > 1$, sticking of the magnetic field lines to O-points and around X-points of the magnetic island chain near the flux surface, from which magnetic field lines are started, is fairly released as is shown in figure 8c. Thus, except for such sticking regions and inside of the magnetic islands with different helicity, the Poincare plots of the field lines are almost uniform. Reflecting the results of the Poincare plots, the kurtosis γ_4 has a tendency to reach the values similar to the uniform mixing process: $\gamma_4 = -6/5$, as is shown in figure 15 by the dashed line. As s_b/s_{bc} increases more, the uniformity of the Poincare plots becomes stronger as is shown in figure 8d, so that within the ballistic phase ($t < t_d$), the kurtosis γ_4 almost reaches the value of the uniform mixing process, as is indicated in figure 15 by the dotted line. The skewness γ_3 of the moderate or highly overlapping case takes a small negative value within ballistic phase, and keeps the sign and the magnitude unchanged after $t = t_d$, as is shown in figure 14 by dashed and dotted lines. Thus, in these cases, the radial distribution of the stochastic magnetic field or particles strongly tied to them is fairly or almost the uniform distribution with a small asymmetric tail towards $\delta r < \langle \delta r \rangle$.

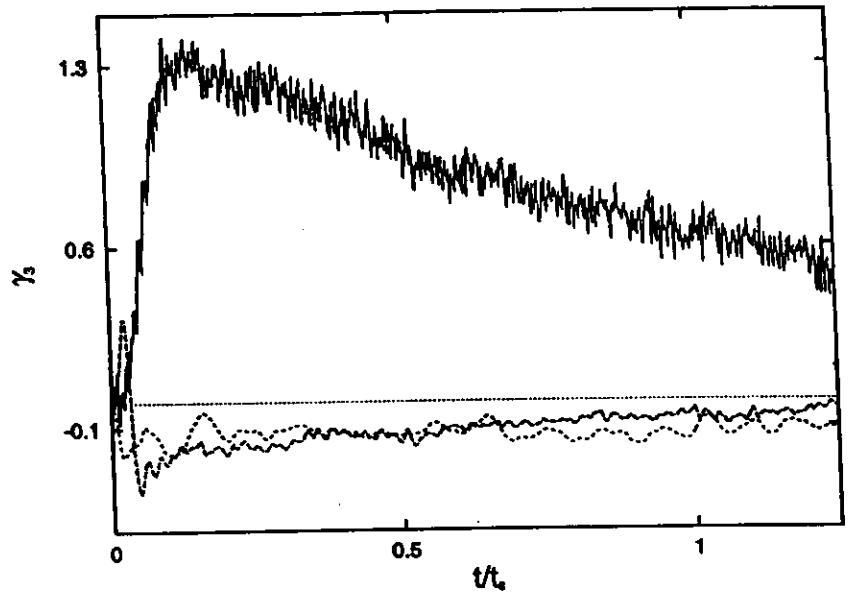

Figure 14: The skewness γ_3 vs t/t_e for $s_b/s_{bc} = 1.3$ (solid curve), $s_b/s_{bc} = 3.3$ (dashed curve), and $s_b/s_{bc} = 33$ (dotted curve).

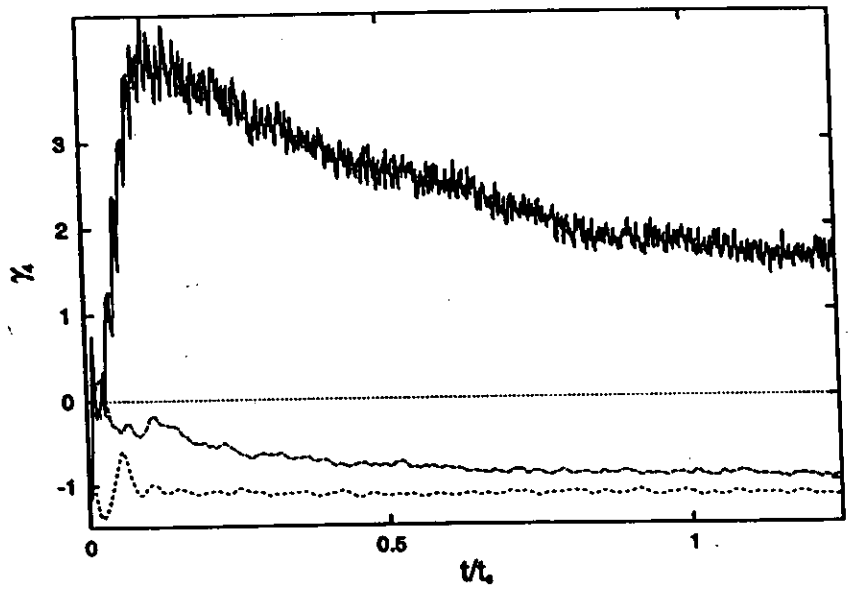

Figure 15: The kurtosis γ_4 vs t/t_e for $s_b/s_{bc} = 1.3$ (solid curve), $s_b/s_{bc} = 3.3$ (dashed curve), and $s_b/s_{bc} = 33$ (dotted curve).

4.2.5 Type of statistical process

Judging from the criteria given in section 3.5, in the partially destroyed magnetic field structure with mixture of regular and irregular regions ($s_b/s_{bc} \geq 1$) the magnetic field stochasticity appears in the long time limit with $t > t_s$ or $t \gg t_d$ as a strange diffusive process: subdiffusive ($s_b/s_{bc} = 1.3$) or non-diffusive (for $s_b/s_{bc} = 3.3$), neither Gaussian nor uniform, and statistically non-stationary ($s_b/s_{bc} = 1.3$) or almost stationary process ($s_b/s_{bc} = 3.3$). This strange diffusive process is symbolized by S in table 9. As s_b increases, the autocorrelation coefficient changes from power-law with oscillatory pattern for $s_b/s_{bc} = 1.3$ to power-law like behaviour given by equation (143) for $s_b/s_{bc} = 3.3$. Thus, in order to distinguish these properties, S_{osc} and S_{st} are used in table 9, respectively. Because of non-diffusivity and almost statistical stationarity the magnetic stochasticity for $s_b/s_{bc} = 3.3$ can be denoted as a relaxation process of non-uniform mixing type.

When $s_b/s_{bc} \gg 1$, the magnetic stochasticity in the long time limit with $t > \tau_{corr} \approx t_d$ appears as a uniform mixing process (criterion II): non-diffusive, uniform, Markov, statistically stationary process with exponentially vanishing autocorrelation coefficient. It is denoted by symbol U in table 9. Note that the criterion of the skewness γ_3 (admitting 10% error) is violated for uniform mixing process: $\gamma_3 = -0.13 < (-0.1)$ in table 7. This deviation of γ_3 from the uniform mixing process comes from the asymmetry of the system. Since the relative width of the stochastic region is fairly large ($w_{st}/a \approx 0.24$) and the equilibrium magnetic shear is not so small, asymmetry of the stochastic magnetic field is naturally created. However, this asymmetry does not affect other statistical properties, thus the highly overlapping case with $s_b/s_{bc} = 33$ is treated as a uniform mixing process.

The question about Markovianity remains open. Actually, the Markovian approximation (section 3.4) is justified whenever the correlations are being rapidly lost during the relaxation of the system. In the present case, the Markov approximation is applicable only to the case with highly developed magnetic field stochasticity ($s_b/s_{bc} \gg 1$) in the long time limit. In the partially destroyed magnetic field structure with mixture of regular and irregular domains ($s_b/s_{bc} \geq 1$), however, the non-uniformity, and power-law like or oscillatory like behaviour of the autocorrelation coefficient indicate that the space-time correlations remain in the time limit $t \geq t_s$ Thus, from the statistical point of view, it is considered that obstruction of the uniform mixing by sticking of test magnetic field lines to the local regular structures leads to non-Markovianity.

Thus:

- In the partially destroyed magnetic field region (mixture of regular and irregular domains) the magnetic stochasticity relaxes as a strange diffusive process: subdiffusivity or non-diffusivity, neither Gaussianity nor uniformity, power-law autocorrelation coefficient $A(t'-t)$, non-stationarity or almost stationarity, and non-Markovianity.
- In the totally destroyed magnetic field regions (stochastic sea without structures)

the magnetic stochasticity is realized as a uniform mixing process: non-diffusivity, uniformity, exponentially vanishing autocorrelating coefficient, statistical stationarity, and Markovianity.

The non-diffusivity and strange statistical properties are associated with the non-locality of the radial displacements of the stochastic magnetic field lines (particles strongly tied to the stochastic magnetic field lines).

5 Statistical properties of the particle radial diffusion

In the present section a systematic presentation of the statistical properties of the particle radial diffusion in the magnetic field with irregularities is done. Main task is to recognize the general tendencies of it beyond the $(s_b/s_{bc}, \nu/\nu_t)$ parametric space. Two accesses are allowable: start from the magnetic field stochasticity, and from the Wiener limit (neoclassical radial diffusion). Here the first one is selected. Thus, the particles are not tied to magnetic field lines which can be seen as a mixture of the regular and irregular structures, or the highly stochastic sea without structures, but they are additionally redistributed in configuration space by the collisionless drift decorrelation, and the collisional decorrelation from the magnetic field lines.

Interest is in the qualitative changes of the statistical properties of the particle radial diffusion by the collisionless, and collisional decorrelation from the magnetic field lines. Therefore, the values of parameter ν/ν_t are chosen to be $\nu/\nu_t = 0.45, 4.5$, and 45, i.e. the plateau, and Pfirsch-Schlüter neoclassical collisionality regimes.

Tables introduced in this section are presented on page 82.

5.1 Collisionless drift decorrelation

In section 4.2, the statistical properties of the magnetic field are examined from the view point of the radial displacement. As it is mentioned in 4.2, those properties are interpreted as the statistical properties of the radial particle diffusion without the perpendicular drift motion and Coulomb collision. In this section, the influences of the perpendicular drift motion on the statistical properties of the radial particle diffusion without Coulomb collision are investigated.

Even if the Coulomb collision does not exist, the particle can move from one magnetic field line to another due to the drift motion. This effect is called the collisionless drift decorrelation from the magnetic field line. However, since the drift velocity perpendicular to the magnetic field lines is much smaller than the parallel velocity, effects due to drift motion across magnetic field lines on the statistical properties are considered to be small. Indeed, although quantitative differences exist as shown in tables (3)-(9), qualitative

the magnetic stochasticity is realized as a uniform mixing process: non-diffusivity, uniformity, exponentially vanishing autocorrelating coefficient, statistical stationarity, and Markovianity.

The non-diffusivity and strange statistical properties are associated with the non-locality of the radial displacements of the stochastic magnetic field lines (particles strongly tied to the stochastic magnetic field lines).

5 Statistical properties of the particle radial diffusion

In the present section a systematic presentation of the statistical properties of the particle radial diffusion in the magnetic field with irregularities is done. Main task is to recognize the general tendencies of it beyond the $(s_b/s_{bc}, \nu/\nu_t)$ parametric space. Two accesses are allowable: start from the magnetic field stochasticity, and from the Wiener limit (neoclassical radial diffusion). Here the first one is selected. Thus, the particles are not tied to magnetic field lines which can be seen as a mixture of the regular and irregular structures, or the highly stochastic sea without structures, but they are additionally redistributed in configuration space by the collisionless drift decorrelation, and the collisional decorrelation from the magnetic field lines.

Interest is in the qualitative changes of the statistical properties of the particle radial diffusion by the collisionless, and collisional decorrelation from the magnetic field lines. Therefore, the values of parameter ν/ν_t are chosen to be $\nu/\nu_t = 0.45, 4.5$, and 45, i.e. the plateau, and Pfirsch-Schlüter neoclassical collisionality regimes.

Tables introduced in this section are presented on page 82.

5.1 Collisionless drift decorrelation

In section 4.2, the statistical properties of the magnetic field are examined from the view point of the radial displacement. As it is mentioned in 4.2, those properties are interpreted as the statistical properties of the radial particle diffusion without the perpendicular drift motion and Coulomb collision. In this section, the influences of the perpendicular drift motion on the statistical properties of the radial particle diffusion without Coulomb collision are investigated.

Even if the Coulomb collision does not exist, the particle can move from one magnetic field line to another due to the drift motion. This effect is called the collisionless drift decorrelation from the magnetic field line. However, since the drift velocity perpendicular to the magnetic field lines is much smaller than the parallel velocity, effects due to drift motion across magnetic field lines on the statistical properties are considered to be small. Indeed, although quantitative differences exist as shown in tables (3)-(9), qualitative

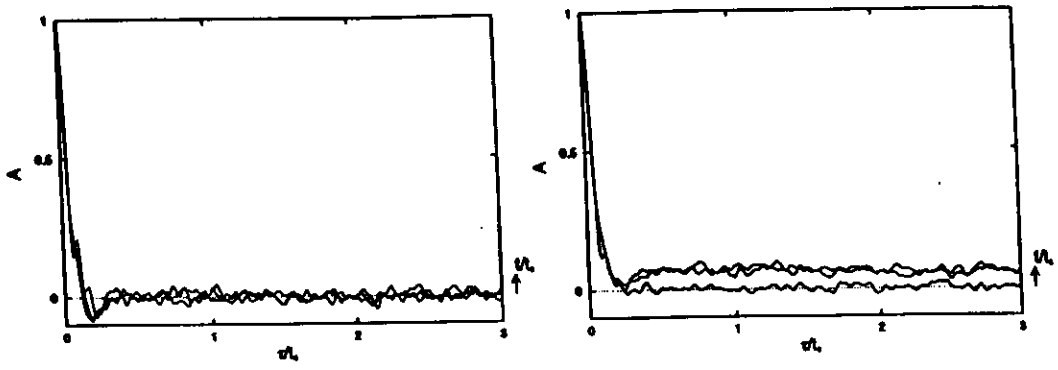

Figure 16: The $A(t,t')$ vs $\tau = t'-t$ for $s_b/s_{bc} = 33$ without (a) and with the perpendicular drift (b). Different curves correspond to starting time $t/t_s = 2.5 \times 10^{-3}, 0.75$, and 3.

differences are not seen except for the autocorrelation coefficient for $s_b/s_{bc} = 33 \gg 1$. In figure 16, the autocorrelation coefficients $A(t, \tau = t' - t)$ vs time interval τ/t_s are drawn for several starting times t: $t/t_s = (2.5 \times 10^{-3}, 0.75,$ and 3). Figures 16a, and 16b correspond to the case without perpendicular drift motion (section 4.2) and with perpendicular drift, respectively. In the presence of perpendicular drift, although the autocorrelation coefficients exponentially vanish independent of the starting time for $\tau/t_s \ll 1$, a finite correlation $A(t,t') \approx 0.05$ is recovered after the correlation time $\tau/t_s > \tau_{corr}/t_s \approx 0.1$, when the starting times are taken as large as $t/t_s > \tau_{corr}/t_s$. It is new quality with respect to the case without drift which is characterized by the exponentially vanishing $A(t,t')$ after $\tau/t_s \geq \tau_{corr}/t_s$ for all starting times. In other words, due to the perpendicular drift the particles are redistributed with respect to the case without drift which can be responsible to the finite correlations observed in figure 16b. However the physical reason is not clear. Such a case is denoted by E_{corr} in table 5 and U_{corr} in table 9.

As summary, although quantitative differences (and qualitative differences in the limited range of parameter s_b/s_{bc}) exist, the statistical properties of the radial diffusion without Coulomb collision are determined by those of the stochastic magnetic field.

5.2 Particle radial diffusion in the presence of both magnetic and collisional stochasticity

In this section the statistical properties of the radial particle diffusion in the presence of both magnetic field and collisional stochasticities are considered. Three cases of collisionality are chosen to be $\nu/\nu_t = 0.45, 4.5$, and 45, where $\nu_t = 2.21 \times 10^6 s^{-1}$ is the transit frequency of passing particles defined in the equilibrium magnetic field (eq. (94)). Thus, $\nu/\nu_t = 0.45$ corresponds to plateau collisionality regime, and $\nu/\nu_t = 4.5$, and 45 correspond to Pfirsch-Schlüter collisionality regime, respectively.

When the global magnetic stochasticity has not been developed ($s_b/s_{bc} < 1$), the particle radial diffusion is governed by the collisional stochasticity. In the collisionless

limit the test particles started inside the islands are prevented from escaping there into the regular KAM regions. Thus, the trapped particles inside islands execute periodic motion as long as they are tied to the magnetic field line. The characteristic time of this motion around O-point is estimated to be $t_b \approx 2\tau_t \approx 8.7 \times 10^{-7}$s, where $\tau_t = \nu_t^{-1} = 4.35 \times 10^{-7}$s is the characteristic time of passing particle motion (94). Thus, the long time limit in the presence of collisions is determined by

$$t > \max(\tau_c, \langle t_b \rangle), \tag{145}$$

where $\tau_c = \nu^{-1}$ is the collisional characteristic time and $\langle t_b \rangle = 1.8 t_b = 1.6 \times 10^{-6}$s is the averaged time of t_b, which is obtained by simple approximation of the motions in the magnetic islands as one dimensional pendulum. The ratios of $\langle t_b \rangle$ to τ_c are shown in table 10 for $s_b/s_{bc} = 0.33$. Since $\langle t_b \rangle > \tau_c$, the long time limit for $s_b/s_{bc} = 0.33$ is defined as $t \gg \langle t_b \rangle$.

In the region of global magnetic stochasticity with $s_b/s_{bc} \geq 1$ the relaxation time of the effective radial Liapunov exponent, t_s (section 4.2.1) is compared with the collisional characteristic time, and the long time limit is defined as

$$t > \max(\tau_c, t_s) \tag{146}$$

The ratios of t_d to τ_c are shown in table 10 for $s_b/s_{bc} = 1.3, 3.3$, and 33, respectively. Because of $t_s > t_d > \tau_c$, the long time limit for these cases is defined as $t \geq t_s$. However as well as the magnetic field structure in 4.2, once $t \gg t_d$ is satisfied, the statistical properties do not change qualitatively. Thus, to save computational time, the long time limit is treated as $t \geq t_s$ for $s_b/s_{bc} = 1.3$, and 3.3.

5.2.1 Type of diffusive behaviour

The collisional effects on the second cumulant (relative mean square displacement) $C_2(t)$ are shown in figure 17, (a) for $s_b/s_{bc} = 0.33$, (b) for $s_b/s_{bc} = 1.3$, (c) for $s_b/s_{bc} = 3.3$, and (d) for $s_b/s_{bc} = 33$. Before the island overlapping ($s_b/s_{bc} = 0.33$), $\langle l_c(t) \rangle$ is always negative as is discussed in 4.2.1. When the collisions are absent , $C_2(t)$ shows a superdiffusive phase due to the ballistic motion in the early time, where maxC_2 becomes of the order of that in the corresponding uniform mixing process: $C_2^{uniform} = (w_{2,3})^2/12 \sim 4.8 \times 10^{-5}$. After such the superdiffusive phase, $C_2(t)$ decreases and oscillates around a constant value, because of stickness to the regular structures inside of the magnetic islands ($\langle l_c(t) \rangle$ is always negative). When the collisions are introduced, such the superdiffusive phase and oscillatory behaviour are suppressed because of $\tau_c < \langle t_b \rangle$ as is shown in table 10, and C_2 comes to monotonically increase in time. As the collision frequency increases, the diffusive behaviour in the long time limit changes from subdiffusive for $\nu/\nu_t = 0.45$ to normal diffusive for $\nu/\nu_t = 4.5$ and 45 as is shown in table 3, and the magnitude of the diffusion coefficient decreases up to the level of the neoclassical diffusion in the regular

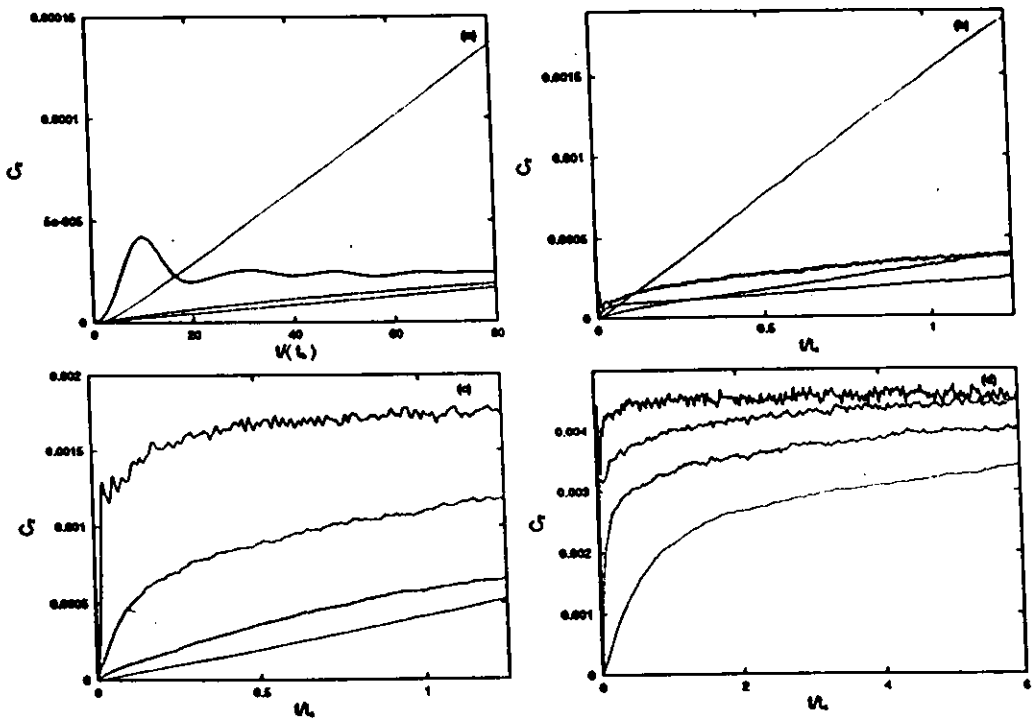

Figure 17: The $C_2(t)$ vs t/t_s for $s_b/s_{bc} = 0.33$ (a), $s_b/s_{bc} = 1.3$ (b), $s_b/s_{bc} = 3.3$ (c) and $s_b/s_{bc} = 33$ (d). In each figure solid curve corresponds to the case without collisions and perpendicular drift motion, and dashed, dot–dashed and dotted curve to $\nu/\nu_t = 0.45, 4.5$ and 45, respectively.

magnetic field, independent of the definition of the diffusion coefficient, as is indicated in table 4. The magnetic structure before overlapping considered here has both magnetic islands with small widths and quite tiny stochastic region around the separatrix. Thus, when the Coulomb collisions are fairly frequent ($\tau_c \ll \langle t_b \rangle$), particle orbits scattered by the collisions can not follow the magnetic field lines inside of small magnetic islands and of tiny stochastic region, leading to the normal diffusion with magnitude similar to that in the neoclassical diffusion. As the collision frequency decreases ($\tau_c < t_b$), particles can trace the magnetic field lines, which may lead to the subdiffusivity reflecting magnetic field structures. Note that the change of the magnitude of C_2 with respect to ν/ν_t is not monotonic. Since this behaviour is more clear for $s_b/s_{bc} = 1.3$, the reason is considered there.

Near the threshold of the island overlapping ($s_b/s_{bc} = 1.3$), the behaviour of C_2, and so, the behaviour of the diffusion exponent and the diffusion coefficient, are qualitatively similar to those before the island overlapping ($s_b/s_{bc} = 0.33$), as are shown in figure 17(b), and tables 3 and 4, namely with increasing in the collision frequency, type of diffusivity changes from the subdiffusive for $\nu/\nu_t = 0.45$ and 4.5 to the normal diffusivity for $\nu/\nu_t = 45$. As is similar to the case before overlapping, the change of the magnitude of C_2 with respect to ν/ν_t is not monotonic. In the absence of the Coulomb collision, a superdiffusive phase due to ballistic motion exist in the early time as well as before overlapping, where

$\langle l_e(t)\rangle$ is negative and maxC_2 becomes the order of that in the corresponding uniform mixing process: $C_2^{uniform} = (w_{st})^2/12 \sim 6.6 \times 10^{-4}$. After decreasing, $C_2(t)$ increases in time with oscillatory behaviour. It can be associated with the positive value of $\langle l_e(t)\rangle$ and increase of the number of field lines with positive effective radial Liapunov exponent as is seen in figures 9 and 10. When weak collisions with $\nu/\nu_t = 0.45$ are introduced, such the superdiffusive phase and oscillatory behaviour disappear according to $\tau_c < t_d$ as shown in table 10, and the magnitude of $C_2(t)$ decreases. This phenomenon is due to the interruption of the parallel free streaming by the pitch angle scattering. Since the mean free path is still long ($v_{\|}\tau_c \sim 32$m), however, the subdiffusivity due to the magnetic field is still strong. As the collision frequency increases more ($\nu/\nu_t = 4.5$), according to the reduction of the mean free path ($v_{\|}\tau_c \sim 3.2$m), the subdiffusive properties and the magnitude of $C_2(t)$ are more reduced. When the collision frequency becomes extremely large ($\nu/\nu_t = 45$), the mean free path becomes considerably short ($v_{\|}\tau_c \sim 0.32$m), so that the diffusion due to the stochastic magnetic field is lost and the normal diffusion due to the pitch angle scattering appear. This collisional effect is understood in terms of the relative average radial displacement of the stochastic magnetic field lines (eq. 141) in the duration of the collision time

$$\Delta d \equiv \frac{\langle d(\tau_c)\rangle - d(0)}{d(0)} \sim e^{\langle l_e\rangle \tau_c} - 1. \tag{147}$$

In the case with $s_b/s_{bc} = 1.3$, as is shown in figure 9b, $\langle l_e\rangle c$ is the order of 5.4×10^{-3}, so that $\Delta d \sim \langle l_e\rangle \tau_c \ll 1$, namely the relative average radial displacement of the stochastic magnetic field lines in the duration of the collision time is too small in the range of the collision frequency considered here, and the radial displacements due to collisions themselves become significant as ν increases. In the weak stochastic magnetic field with $s_b/s_{bc} \leq 1$, infrequent collisions reduce the relative mean square displacement C_2, however, frequent collisons enhance it in the long time limit.

In the moderate overlapping case with $s_b/s_{bc} = 3.3$, when the collision is absent, the relative mean square displacement C_2 becomes as large as the corresponding uniform mixing level in the early superdiffusive phase: $C_2^{uniform} = (w_{st})^2/12 \sim 2.4 \times 10^{-3}$. after that, C_2 does not decreases so much, but hold the level in the interval of $t < t_d$, where the effective radial Liapunov exponent $\langle l_e\rangle$ is still negative. Since the magnetic field is considerably stochastic compared with those for $s_b/s_{bc} \leq 1$, field lines or particles with only parallel drift spreading in the superdiffusive phase are considered not to return near the original position. After $t = t_d$, the effective radial Liapunov exponent becomes positive, and both $\langle l_e\rangle$ and the number of field lines with $\langle l_e\rangle > 0$ increase, so that C_2 gradually increases keep the level of the uniform mixing process. Weak collisions with $\nu/\nu_t = 0.45$ do not disturb so much the radial diffusion due to magnetic field stochasticity, as is understood from figure 17c, so that the relative average radial displacement of the stochastic magnetic field lines in the duration of the collision time is fairly large, e.g.,

$\Delta d \sim 0.31$ for $\langle l_c \rangle c = 2.5 \times 10^{-2}$. Hence, subdiffusivity stemming from the magnetic field stochasticity remains, and the level C_2 is in the range of the uniform mixing process. When the collision frequency increases as $\nu/\nu_t = 4.5$ and 45, Δd decreases and the property of subdiffusivity is gradually lost, and finally the normal diffusivity appears, as is shown in table 3. In the range of the collision frequency considered here, the magnitude of C_2 monotonically decreases as the collision frequency increases (figure 17c).

In the highly overlapped case with $s_b/s_{bc} = 33$, as well as the moderate overlapping, the relative mean square displacement C_2 becomes as large as the uniform mixing level in the early superdiffusive phase: $C_2^{uniform} = (w_{st})^2/12 \sim 5.2 \times 10^{-3}$. Since the stochastic magnetic field has no regular structures, t_d is quite small, and all of magnetic field lines have positive Liapunov exponent in a short time as is seen in figure 10d, then C_2 becomes almost constant with the level of uniform mixing process except for the small oscillatory behaviour. The relative average radial displacement of the stochastic magnetic field lines in the duration of the collision time Δd is 89., 0.58, and 4.7×10^{-2} for $\nu/\nu_t = 0.45, 4.5$, and 45, respectively. Thus, the collisional effects are so weak that the process always shows subdiffusivity due to the magnetic field stochasticity in the range of the collision frequency considered here, and the magnitude of C_2 monotonically decreases as the collision frequency increases (figure 17d).

5.2.2 Autocorrelation coefficients

The effect of collisions on the autocorrelation coefficient $A(t, t')$ is shown in figures 18a-d: (a) for $s_b/s_{bc} = 0.33$, (b) for $s_b/s_{bc} = 1.3$, (c) for $s_b/s_{bc} = 3.3$, and (d) for $s_b/s_{bc} = 33$, respectively. In each figure, the autocorrelation coefficients $A(t, t') = A(t, \tau = t' - t)$ are plotted as functions of the time interval $\tau = t' - t$ and the starting time t. Because of convinience τ is normalized with t_s ($\langle t_b \rangle$ for $s_b/s_{bc} = 0.33$). Two starting times $t = t_1 \ll t_s$ and $t = t_2 \approx t_s/2$ are specified. The starting time $t \equiv t_1$ corresponds to the early time: $t = 3.1 \times 10^{-3} \langle t_b \rangle$ for $s_b/s_{bc} = 0.33$, $t = 8.3 \times 10^{-4} t_s$ for $s_b/s_{bc} = 1.3$, $t = 2.5 \times 10^{-4} t_s$ for $s_b/s_{bc} = 3.3$, and $t = 2.8 \times 10^{-3} t_s$ for $s_b/s_{bc} = 33$; and the starting time $t = t_2$ corresponds to the late time: $t = 41. \langle t_b \rangle$ for $s_b/s_{bc} = 0.33$, $t = 0.56\, t_s$ for $s_b/s_{bc} = 1.3$, $t = 0.56\, t_s$ for $s_b/s_{bc} = 3.3$, and $t = 1.51 t_s$ for $s_b/s_{bc} = 33$. The dashed, dot-dashed, and dotted curves correspond to $\nu/\nu_t = 0.45, 4.5$, and 45, respectively and the corresponding Wiener cases are drown by solid curves. As the collision frequency ν/ν_t increases, independent of s_b/s_{bc}, the autocorrelation coefficient $A(t, \tau)$ has a tendency to become non-stationary power law like, whose values for a fixed t and τ are smaller than those of the corresponding Wiener process in the range of the collision frequency considered here. When the collision frequency ν/ν_t increases an d s_b/s_{bc} decreases, $A(t, \tau)$ finally becomes Wiener like. In table 5, the types of the behaviour of $A(t, \tau)$ as a function of t and τ are indicated, where P_W means that the behaviour of $A(t, \tau)$ is well approximated by the Wiener process in the whole starting time or in the long time limit, and P_f indicates the above mentioned

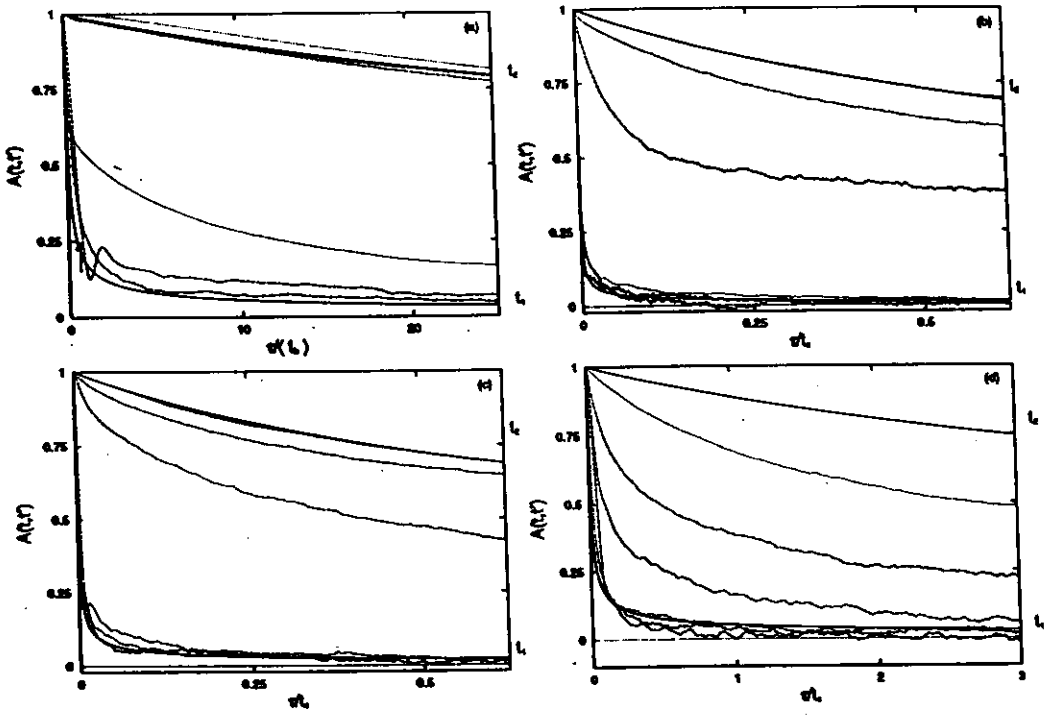

Figure 18: The $A(t,t')$ vs τ for two different starting times: $t_1 \approx 0.031\langle t_b\rangle, t_2 \approx 41.\langle t_b\rangle$ for $s_b/s_{bc} = 0.33$; $t_1 \approx 8.3 \times 10^{-4} t_s, t_2 \approx 0.56 t_s$ for $s_b/s_{bc} = 1.3$; $t_1 \approx 2.5 \times 10^{-4} t_s, t_2 \approx 0.56 t_s$ for $s_b/s_{bc} = 3.3$; $t_1 \approx 2.8 \times 10^{-3} t_s, t_2 \approx 1.51 t_s$ for $s_b/s_{bc} = 33$. The dashed, dot-dashed, and dotted curves correspond to $\nu/\nu_t = 0.45, 4.5$, and 45, respectively, and the Wiener case is drawn by solid curves. Times are normalized with respect to t_s for $s_b/s_{bc} \geq 1$ and $\langle t_b\rangle$ for $s_b/s_{bc} < 1$.

power-law like behaviour. These properties are understood as follows. The numerator of the autocorrelation coefficient $A(t,t')$ is expressed as

$$\begin{aligned} & \langle(\delta r(t) - \langle\delta r(t)\rangle)(\delta r(t') - \langle\delta r(t')\rangle)\rangle \sim \langle\delta r(t)\delta r(t')\rangle \\ = \; & \langle\delta r(t)^2\rangle + \langle(\delta r(t') - \delta r(t))\delta r(t)\rangle, \quad \text{for} \quad t' > t, \end{aligned} \tag{148}$$

where the first cumulant $C_1(t) = \langle\delta r(t)\rangle$ is neglected, because it is quite small as indicated in table 6. Thus, the starting time t appearing in $A(t,\tau)$ is interpreted as the common time interval between two trajectories $\delta r(t)$ and $\delta r(t')$ for $t' > t$. In the case of the Wiener process, as is understood from equation (110), the radial displacement is a superposition (time integration) of completely independent events created by the white noise. In this context, the pitch-angle scattering acts as the white noise (although both the pitch-angle scattering frequency and the width of perpendicular particle drifts determine the magnitude of the correlation of the white noise). Therefore, the correlation without common time interval vanishes, namely, $\langle(\delta r(t') - \delta r(t))\delta r(t)\rangle = 0$ in the above equation. In other words, the correlation is created within the common time interval t. For a fixed τ, the longer such the common time interval t becomes, the more the correlation persists. This property of the Wiener process is one of the characteristics of the particle radial diffusion by the Coulomb collision in the regular magnetic field [32], and is closely related to the locality of the particle orbits and particle diffusion in the radial direction . Partially because the drift width is quite small compared with the system size, and partially because the accumulation of small pitch-angle scatterings created in the velocity space gradually change the particle radial drift motions, the locality of the radial diffusion is ensured. Thus,the correlation indicating that the constituents of the particle ensemble stays near each other between two different times is increased, as the common time interval t or the starting time of $A(t,\tau)$ increases for a fixed τ.

On the other hand, the stochastic magnetic field in the radially bounded region shows the uniform mixing properties when $s_b/s_{bc}(\geq 1)$ increases, as discussed in 4.2. In these cases, the stochasticity of the magnetic field lines is characterized by the positive radial effective Liapunov exponent $\langle l_e\rangle(> 0)$, namely the ensemble of field lines or particles tied to the magnetic field lines have a tendency to exponentially spread in the radial direction. Thus, the knowledge that the field lines or particles stay near to each other is easily lost even if the common time interval t is large, so that the correlation between stochastic field lines or particle trajectories, comes to be rapidly lost independent of the common time interval or field lines makes fast loss of the correlations or fast decorrelation in the radial direction.

When the collisions are introduced to the particle radial diffusion in the stochastic magnetic field, the fast radial spreading of the particles along the perturbed field lines is interrupted. As a result, particles can stay nearer compared with the case without collisions, which means that the fast loss of the correlations by the stochastic magnetic field

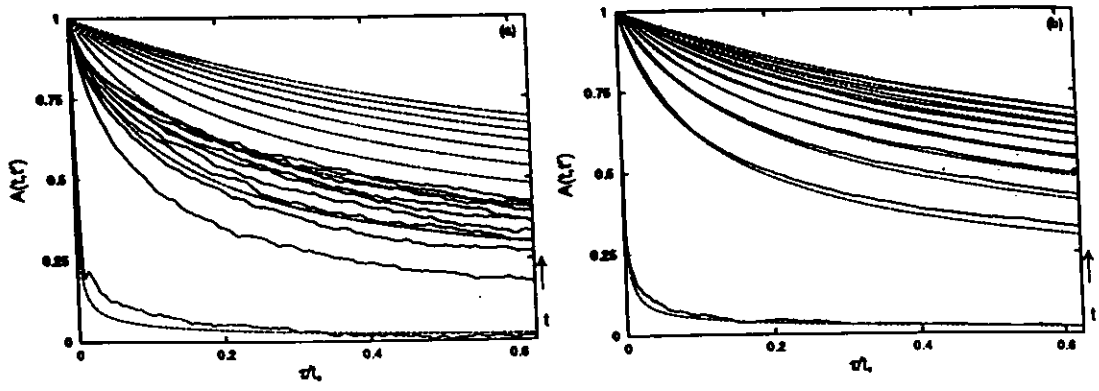

Figure 19: The $A(t,t')$ vs $\tau = t' - t$ for $s_b/s_{bc} = 3.3$ (solid curve): (a) $\nu/\nu_t = 0.45$, (b) $\nu/\nu_t = 4.5$, and (c) $\nu/\nu_t = 45$. Corresponding Wiener curves are plotted by dashed lines. The starting time t is chosen as $t = (3.6 \times 10^{-4}, 2.0 \times 10^{-2}, ..., 0.8)t_s$. In figure τ is normalized with respect to t_s.

is suppressed by the Coulomb collisions. The fact that the Coulomb collisions suppress the decorrelation due to the magnetic field stochasticity appears as the non-stationary power-law like behaviour of the autocorrelation coefficient. As s_b/s_{bc} increases, such the collisional suppression of the decorrelation is reduced, since $\langle l_c \rangle \tau_c = \lambda/L_K$ increases, where $\lambda = v_{\|}\tau_c$ and $L_K = v_{\|}/\langle l_c \rangle$ are the mean free path and the Kolmogorov length, respectively. Note that the Coulomb collisions themselves do not make the correlation, but suppress the decorrelation by the stochastic magnetic field. In the case of the neoclassical particle radial diffusion, perpendicular particle drifts are decorrelated by the Coulomb collisions and superposion of such random events leads to the Wiener process according to the central limit theorem [6]. In contrast with it, in the particle diffusion in the highly stochastic magnetic field, parallel particle drift along stochastic magnetic field lines leads to the decorrelation in the radial direction, and Coulomb collisions suppress such the decorrelation through the scattering of the parallel particle drift.

In figures 19a,b, $A(t,\tau)$ vs τ/t_s for $s_b/s_{bc} = 3.3$ is plotted by solid curve with respect to various starting times: (a) for $\nu/\nu_t = 0.45$, and (b) for $\nu/\nu_t = 45$, respectively. The corresponding $A(t,\tau)$ of the Wiener process is also drawn by dashed curve. The starting time is chosen as $t = (2.5 \times 10^{-4}, 6.2 \times 10^{-2}, ..., 0.56)\, t_s$. It is quite clear that the $A(t,\tau)$ becomes that of the Wiener process, as ν/ν_t increases.

5.2.3 The cumulant coefficients

As is shown in table 6, the convective effect indicated by C_1 is quite weak independent of both s_b/s_{bc} and ν/ν_t. Although the values of C_1 are larger that those in the neoclassical cases in [32], they are still too small compared with the minor radius a (C_1 is normalized by a).

As is mentioned in section 3, the both non-vanishing skewness γ_3 and kurtosis γ_4

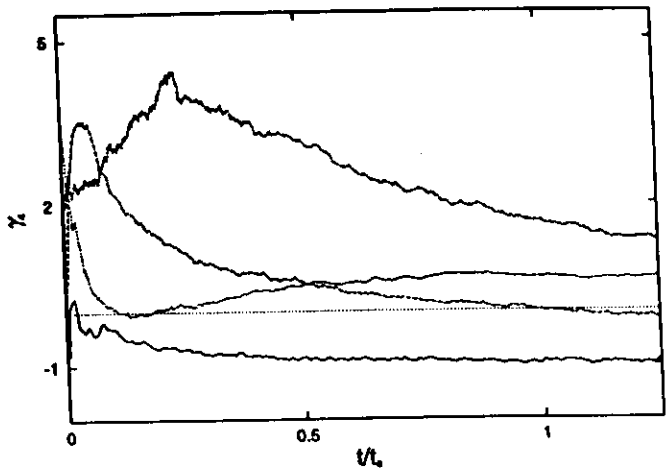

Figure 20: The time behaviour of kurtosis γ_4 for $s_b/s_{bc} = 1.3$ and different collisionalities: $\nu = 0$ (solid line), $\nu/\nu_t = 0.45$ (dashed line), $\nu/\nu_t = 4.5$ (dot-dashed line), and $\nu/\nu_t = 45$ (dotted line). Time is given as t/t_s.

indicate the deviation of the particle distribution from a Gaussian profile, and $\gamma_4 = -6/5$ corresponds to the uniform mixing process.

Before the island overlapping with $s_b/s_{bc} < 1$, the oscillatory behaviours coming from the particle regular motions, observed in the case without Coulomb collisions, are suppressed by the Coulomb collisions. Since the particle radial displacements stemming from the isolated magnetic island chain are quite small (particles are initially loaded at the corresponding rational surface), the radial displacements are mainly governed by the Coulomb collisions, leading to the distribution with vanishing both γ_3 and γ_4 (tables 7 and 8). Note that the vanishing of the skewness and kurtosis together with the previously mentioned normal diffusivity and the Wiener like autocorrelation coefficient (section 4.1) for $\nu/\nu_t = 4.5$ and 45 means that the particle distribution is Gaussian according to the criterion given in section 3.5.

In the highly overlapping case with $s_b/s_{bc} \gg 1$, the scattering due to the Coulomb collision of the parallel particle motion along the stochastic magnetic field lines is so weak that the particle radial distribution is similar to the corresponding uniform profile with $\gamma_4 = -6/5$, as is shown in table 8. As is mentioned in section 4.2, inhomogeneity of the equilibrium magnetic field due to the magnetic shear creates the finite skewness γ_3, but the values of γ_3 are similar to the cases without collisions.

The behaviour of γ_3 and γ_4 in the case near the island overlapping threshold and the moderate overlapping are fairly complicated. The reason may be due to the regular structures inside the stochastic sea, to or around which particles stick. The Coulomb collisions scatter particle motions: they sometimes scatter the particle from the stochastic field line to the particle stuck by regular structure and vice versa. The change of the temporal behaviours of γ_4 due to the Coulomb collisions is shown in figure 20 for $s_b/s_{bc} = 3.3$, where the change of the radial profile in the long time limit from a broad profile

($\gamma_4 < 0$) to a peaked one ($\gamma_4 > 0$) is understood as ν/ν_t increases.

5.2.4 Type of statistical process

The type of statistical process is summarized in table 11, being based on the results presented in 5.2, where U and W indicate the uniform mixing and Wiener process, respectively, and the symbol S denotes the strange diffusive process.

In the absence of the Coulomb collision, inside the bounded destroyed magnetic field region, as $s_b/s_{bc}(\geq 1)$ increases, the magnetic stochasticity or the particle radial diffusion with only parallel drift motion comes to appear as a uniform mixing process reflecting non-locality of orbits, which is a non-diffusive, uniform, statistically stationary, and Markov process after the exponentially fast relaxation of the autocorrelation coefficient. The Coulomb collisions interrupts the fast radial displacement of particles along the perturbed magnetic field lines, however, the locality is not obtained. Thus, the particle radial diffusion develops as a strange diffusive process in the long time limit: subdiffusive, non-uniform and non-Gaussian, and statistically non-stationary process, in almost all $(s_b/s_{bc}, \nu/\nu_t)$ parameter space. When the collisions are fairly frequent ($\nu/\nu_t \gg 1$) and uniformity of the magnetic field stochasticity is fairly lost, the locality of the particle motion is recovered, and the boundary effects become negligible during calculation time. Then the particle radial diffusion is governed as the Wiener process with normal diffusivity, Gaussianity, statistical non-stationarity, and Markovianity, as well as the neoclassical diffusion in the regular magnetic field.

The process corresponding to $s_b/s_{bc} = 3.3$ and $\nu/\nu_t = 45$ is similar to the Wiener process. However, only the kurtosis γ_4 does not satisfy the criterion given in section 3.5, and so this process is expressed by W_P in table 9. As is understood from this example and other cases recognized as the strange diffusive process in table 9, the various types of the strange diffusive process exist, e.g., even if the process shows a normal diffusivity: $\alpha \sim 0.92$ for $s_b/s_{bc} = 1.3$ and $\nu/\nu_t = 4.5$, the radial profile is broader than a Gaussian and the autocorrelation is not Wiener like. The significant point is not the detail differences in the diffusive process, but the overall tendency in two-parameter space $(s_b/s_{bc}, \nu/\nu_t)$. Table 9 shows that the change in the type of diffusive process is prescribed by the Coulomb collisional suppression of the non-locality of radial particle displacements due to the stochastic magnetic field.

The Markovianity in the strange diffusive process is still open question, which will be considered in future. However, adopting the viewpoint from section 3.5, the Markovianity is lost whenever the long space and time correlations are created. Considering them as the results of validation of criterions I and II (section 3.5) the non-Markovianity is natural property of the strange diffusion. Note that the usual transport analyses based on the locality of the particle motion have a sense only in the Wiener domain.

6 Discussion

Here, following several points are discussed.

6.1 Characteristic lengths of magnetic field lines

In this work, the several types of radially bounded stochastic magnetic field region are treated. On the contrary, in the most of previous works the statistical properties of the magnetic stochasticity are given a priori, mainly as a static, homogeneous Gaussian process which develops in the radially unbounded magnetic field region [14, 15, 16, 17, 18]. In other words, all these cases correspond to the parametric domain $s_b/s_{bc} \gg 1$ in actual model. In order to clarify the effects of the boundedness, three characteristic lengths associated with the magnetic field stochasticity are examined: the perpendicular correlation length $L_\perp$, the parallel correlation length $L_{||}$, and the Kolmogorov (Liapunov) length L_K. The most significant difference in the present context is connected with the perpendicular correlation length $L_\perp$. For example, in the quasi-linear approximation [14, 15, 16, 17, 18], in order to obtain a constant diffusion coefficient of the magnetic field lines, a radially unbounded, homogeneous stochastic region is used, where the perpendicular correlation length may be treated as infinity: $L_\perp \to \infty$. However, in present situation, $L_\perp$ is limited, namely, $L_\perp < w_{st}$, where w_{st} is radial width of the stochastic region. According to the discussion in 4.2.1, the parallel correlation length $L_{||}$ is recognized as a length which corresponds to the decorrelation time of the stochastic magnetic field lines t_d: $L_{||} = t_d v_{||}$. Indeed, such the decorrelation time is similar to the correlation time τ_{corr} of the autocorrelation coefficient in the highly stochastic case with $s_b/s_{bc} \gg 1$. The Liapunov length is obtained from the asymptotic value of the effective radial Liapunov exponent $\langle l_e \rangle$ as $L_K = v_{||}/\langle l_e \rangle$. Substituting the corresponding values to the three characteristic lengths, the following ordering is obtained for $s_b/s_{bc} \geq 1$:

$$L_\perp \ll L_K \ll L_{||}. \tag{149}$$

Note that ordering in the radially bounded stochastic magnetic field is completely different from other situations, especially from the quasi-linear approximation [15, 16, 17].

The ordering between the collisional mean free path λ_{mfp} and the characteristic lengths of the stochastic magnetic field lines for $s_b/s_{bc} \geq 1$ is summarized in table 11. As ν/ν_t decreases, and as s_b/s_{bc} increases, the collisional mean free path λ_{mfp} becomes comparable to the Liapunov length L_K, and finally larger than L_K and comparable to the parallel correlation length $L_{||}$. Thus, it is understood that the collisional effects becomes more significant as the level of stochasticity of the magnetic perturbation decreases or s_b/s_{bc} decreases. Moreover, it will be expected that in more collisionless cases with $L_{||} \ll \lambda_{mfp}$, whose condition will be established for banana collisionality regime, the statistical properties of the particle radial diffusion become closer to those of the magnetic field

stochasticity. In order to obtain the proper statistical properties in the parameter space considered here, all of calculations have been performed up to $z \gg L_{\|}$ or $t \sim t_s = 10 \times t_d \gg t_d$. In the case before overlapping with $s_b/s_{bc} < 1$, the ensemble averaged Liapunov exponent is always negative. Thus, L_K and $L_{\|}$ are interpreted as infinity, so that the ordering $L_\perp \ll \lambda_{mfp} \ll L_K$, $L_{\|} \to \infty$ holds, where $L_\perp$ is recognized as the width of the magnetic islands at $q = m/n = 3/2$: $w_{2,3}$. Note that the characteristic lengths and orderings discussed here have not strict sense in the inhomogeneous magnetic field stochastic region: the mixture of regular and irregular structures. In such a case, the stickness of the magnetic field lines to or around regular structures, indicated by the presence of magnetic field lines with a negative Liapunov exponent in the long time limit $t > t_s$ means the existence of many different scales [9]. To investigate more precise properties of the radial diffusion in such cases, the method of the continuous time random walk [3, 21] maybe suggested. However, in order to understand the general and global tendencies of the particle radial diffusion, the concept of characteristic lengths is useful for all $s_b/s_{bc} \geq 1$ cases, because both L_K and $L_{\|}$ are definitely determined by the effective radial Liapunov exponent $\langle l_e(t) \rangle$ in average sense without ambiguity..

6.2 Locality of the radial diffusion

In this section the relation between locality of the diffusion and the constant diffusion coefficient is investigated. In the standard theory of Brownian motion, according to the Gaussian central limit theorem [6], the spreading of the Gaussian is described by the diffusion coefficient given by

$$D \equiv \lim_{t\to\infty} D(t) = \lim_{t\to\infty} \frac{dC_2(t)}{2dt}. \tag{150}$$

Such a diffusion coefficient is analogy of that in the standard random walk [3, 6]

$$D = \frac{(\Delta x)^2}{\Delta t}, \tag{151}$$

where Δx, and Δt are the characteristic space and time steps of random walker, respectively. Following these developments, in the classical diffusion theory [3, 20], the diffusion process in an unbounded, homogeneous media is characterized by the diffusion coefficient. In the context of the confinement physics, it is ensured by the demand for locality of diffusion. In order to understand the meaning of the locality, the standard neoclassical radial diffusion treated in [41] is reconsidered. By integrating the linearized gyro-phase averaged Boltzmann equation given by equation (1) in the velocity space (in the present case, the energy E is a parameter , so that integration is done only over the magnetic moment μ), and by taking the flux surface average, the equation of continuity in the radial direction is obtained

$$\frac{\partial \langle n \rangle_F}{\partial t} = -\frac{1}{V'}\frac{\partial}{\partial r}\left(V' \langle \vec{\Gamma} \cdot \nabla r \rangle_F\right), \tag{152}$$

where $\langle Q(\vec{r},t)\rangle_F$ is the flux surface average of $Q(\vec{r},t)$, and $\langle Q(\vec{r},t)\rangle_F$ becomes a function with respect to r and t. Also, $\langle n\rangle_F$ is the flux surface averaged density, $\vec{\Gamma} = n(\vec{r},t)\vec{v}(\vec{r},t)$ is the particle flux, and $V' \equiv dV/dr$ with the volume V surrounded by the flux surface specified by an appropriate radial coordinate r. The diffusion coefficient D is introduced through the phenomenological Fick's law in the radial direction given by

$$\vec{\Gamma} \cdot \nabla r = -D(\vec{r},t)\frac{\partial n(\vec{r},t)}{\partial r}. \tag{153}$$

Since the radial diffusion is concerned, by assuming a weak poloidal and toroidal dependence (this is usually ensured by the strong magnetic field and the rotational transform), the flux surface averaged Fick's law becomes

$$\langle \vec{\Gamma} \cdot \nabla r\rangle_F = -\langle D\frac{\partial n}{\partial r}\rangle_F \sim -D(r,t)\frac{\partial \langle n\rangle_F}{\partial r} \tag{154}$$

where $D(r,t) \equiv \langle D\rangle_F$. As is clear from the form of the above equation, the standard Fick's law is based on the locality of the diffusion, since the particle flux at a position r is completely determined only by the diffusion coefficient D and the gradient of $\langle n\rangle_F$ at the same position r. By using the Fick's law, and defining the probability $f(r,t) \equiv \langle n(r,t)\rangle_F/N$ where N is the total number of the particles, the diffusion equation of the particles is obtained

$$\frac{\partial f(r,t)}{\partial t} = \frac{1}{V'}\frac{\partial}{\partial r}\left(V'D(r,t)\frac{\partial f(r,t)}{\partial r}\right). \tag{155}$$

Here, how to obtain the diffusion coefficient $D(r,t)$ by the Monte Carlo method is considered [26]. In the Monte Carlo method, the particles are initially loaded on a flux surface as $f(r,0) = \delta(r-r_0)$. Putting $\delta r = r - r_0$, from the equation (155),

$$\frac{dC_1}{dt} = \frac{d}{dt}\langle \delta r\rangle = \left\langle \frac{1}{V'}\frac{\partial}{\partial r}(V'D)\right\rangle, \tag{156}$$

where two partial integrations in r are done, assuming $f = \partial f/\partial r = 0$ at $r = 0$ and a. Similarly,

$$\frac{dC_2}{dt} = \frac{d}{dt}\langle(\delta r - \langle \delta r\rangle)^2\rangle = 2\langle D\rangle + 2\left\langle \frac{\delta r - \langle \delta r\rangle}{V'}\frac{\partial}{\partial r}(V'D)\right\rangle, \tag{157}$$

is obtained. Thus, when the particle distribution f does not spread so much in the radial direction (in this case the above boundary conditions are satisfied), namely the locality of the radial diffusion is ensured: $|\delta r|/L \ll 1$, where L is scale length of the equilibrium,

$$D(r_0,t) = \frac{1}{2}\frac{dC_2}{dt}, \tag{158}$$

is obtained, partially because the second term in the right-hand side of the equation (157) is neglected due to $|\delta r - \langle \delta r\rangle|/L \ll 1$, where $L \equiv |1/D \cdot \partial D/\partial r|^{-1}$ (note that the diffusion coefficient is determined by the equilibrium quantities), and partially because $\langle D\rangle \sim D(r_0,t)$ by the condition $|\langle \delta r\rangle|/L \ll 1$. The equation (157) means that the local

diffusion coefficient at the position where particles are initially loaded is obtained, when the locality of the diffusion is ensured.

From above consideration, it is known that

(a) The definition of the diffusion coefficient through the second cumulant given by the equation (102) has meaning, when the locality of the diffusion is satisfied. Note that the validity of this definition of the diffusion coefficient is not directly related to the time-dependence of the diffusion coefficient.

(b) The more significant point is that the concept of the diffusion process itself using the diffusion coefficient assumes the locality of the diffusion process as is seen in the standard Fick's law.

In the present parameter space $(\nu/\nu_t, s_b/s_{bc})$, except for the Wiener domain, the locality of the diffusion process does not hold, where the diffusion coefficient defined by equation (102) does not have clear meaning, and moreover, the standard local Fick's law may not hold. In such strange diffusive processes and a uniform mixing process, the diffusion coefficient defined by the equation (102) have to be understood as the time derivative of the second cumulant itself, and the particle radial transport must be treated as a non-local transport, which may be related to systems far from thermodynamical equilibria.

6.3 The second cumulant

It is discussed in section 6.2, the diffusion coefficient, introduced through the local Fick's law, have no clear physical meaning in the diffusive process without locality like a strange diffusive process and uniform mixing process. On the contrary, the second cumulant itself always has a clear physical meaning as the mean square displacement [4, 30]. The time dependence of the second cumulant $C_2(t)$ indicates how fast the radial dispersion of particles spread out as time increases. Thus, when the systems with time-dependent diffusion coefficient are compared in order to evaluate how long or how much particles are confined near their initial position, the temporal behaviour of C_2 must be evaluated instead of the diffusion coefficient.

6.4 Ballistic phase of uniform mixing process

The statistical properties of the uniform mixing process and the strange diffusive process observed in the highly stochastic magnetic field with $s_b/s_{bc} \gg 1$, are strongly affected by the fast exponential divergence of magnetic field lines in the radial direction. As is understood from figure 17d, as the collision frequency decreases, the magnitude of C_2 almost reaches the final state within the short time ballistic phase ($t < t_d$), which indicates that the process for particle to spread in the radial direction up to the level of the fast exponential divergence, is not regarded as a diffusive process, but as a dynamical

relaxation process. After such a ballistic phase or dynamical relaxation process ($t > t_d$), the uniform mixing properties of the magnetic field lines alone for $\nu/\nu_t = 0$ or together with the Coulomb collisions for $\nu/\nu_t \neq 0$, make the particle radial motions diffusive process. In contrast with it, in the case of Wiener process, although the ballistic phase exists in the early time, such a phase does not influence the time evolution of the system after that, or it does not prescribe the final state of the system, because of the locality of the particle orbits. Thus, the time evolution of the system showing the Wiener behaviour is treated as a diffusive process in almost all time. However, in the uniform mixing process and the strange diffusive process similar to that, created by the non-local particle motions, the ballistic phase almost prescribes the final state of the system. Hence, the time evolution of such non-local fast processes should be treated in the framework of a fast dynamical relaxation process of a system far from equilibria to an equilibrium.

7 Conclusion

In this study the statistical properties of the particle radial diffusion in the radially bounded magnetic field region with irregularities are investigated. The particle radial diffusion is treated as a realization of the collisional (statistical) stochasticity and the magnetic (deterministic) stochasticity.

The particle radial diffusion in the regular magnetic field with nested flux surfaces, i.e. the neoclassical radial diffusion is realization of the collisional stochasticity alone. In the absence of collisions the electron guiding centers draw periodic trapped and passing motions in the configuration space, whose drift width δr is at most the poloidal gyroradius ρ_p in the axisymmetric systems, hence $\delta r \sim \rho_p \ll a$. The collisional stochasticity due to the Coulomb collisions is created in the $\lambda(= v_{\|}/v)$ velocity space by the pitch-angle scattering as a uniform mixing process. The pitch-angle scattering acts as the white noise on the perpendicular drift motions (although the magnitude of the correlation of the white noise is determined by both the pitch-angle scattering and the drift width). Thus, due to the radial locality of the collisionless particle motion: $\delta r/a \ll 1$ a nd the accumulation effect of the small pitch-angle scattering acting as a white noise, the locality of the particle radial diffusion is ensured and the radial diffusion appears as a Wiener process with normal diffusivity, Gaussian distribution, statistical non-stationarity and Mark ovianity. The system characteristic time is estimated as the largest among the collisional characteristic time τ_c, the effective bounce time τ_{be}, and the characteristic time of passing particle motion τ_t.

The main effort in this study is to investigate the statistical properties of the particle radial diffusion in the presence of both the collisional and the magnetic stochasticity. Thus, the electron radial diffusion is investigated in a radially bounded stochastic magnetic field region existing in the axisymmetric torus MHD equilibrium. In order to

relaxation process. After such a ballistic phase or dynamical relaxation process ($t > t_d$), the uniform mixing properties of the magnetic field lines alone for $\nu/\nu_t = 0$ or together with the Coulomb collisions for $\nu/\nu_t \neq 0$, make the particle radial motions diffusive process. In contrast with it, in the case of Wiener process, although the ballistic phase exists in the early time, such a phase does not influence the time evolution of the system after that, or it does not prescribe the final state of the system, because of the locality of the particle orbits. Thus, the time evolution of the system showing the Wiener behaviour is treated as a diffusive process in almost all time. However, in the uniform mixing process and the strange diffusive process similar to that, created by the non-local particle motions, the ballistic phase almost prescribes the final state of the system. Hence, the time evolution of such non-local fast processes should be treated in the framework of a fast dynamical relaxation process of a system far from equilibria to an equilibrium.

7 Conclusion

In this study the statistical properties of the particle radial diffusion in the radially bounded magnetic field region with irregularities are investigated. The particle radial diffusion is treated as a realization of the collisional (statistical) stochasticity and the magnetic (deterministic) stochasticity.

The particle radial diffusion in the regular magnetic field with nested flux surfaces, i.e. the neoclassical radial diffusion is realization of the collisional stochasticity alone. In the absence of collisions the electron guiding centers draw periodic trapped and passing motions in the configuration space, whose drift width δr is at most the poloidal gyroradius ρ_p in the axisymmetric systems, hence $\delta r \sim \rho_p \ll a$. The collisional stochasticity due to the Coulomb collisions is created in the $\lambda(= v_{\|}/v)$ velocity space by the pitch-angle scattering as a uniform mixing process. The pitch-angle scattering acts as the white noise on the perpendicular drift motions (although the magnitude of the correlation of the white noise is determined by both the pitch-angle scattering and the drift width). Thus, due to the radial locality of the collisionless particle motion: $\delta r/a \ll 1$ a nd the accumulation effect of the small pitch-angle scattering acting as a white noise, the locality of the particle radial diffusion is ensured and the radial diffusion appears as a Wiener process with normal diffusivity, Gaussian distribution, statistical non-stationarity and Mark ovianity. The system characteristic time is estimated as the largest among the collisional characteristic time τ_c, the effective bounce time τ_{be}, and the characteristic time of passing particle motion τ_t.

The main effort in this study is to investigate the statistical properties of the particle radial diffusion in the presence of both the collisional and the magnetic stochasticity. Thus, the electron radial diffusion is investigated in a radially bounded stochastic magnetic field region existing in the axisymmetric torus MHD equilibrium. In order to

take account of the practical situation that magnetic field perturbations usually create a radially bounded stochastic region in the axisymmetric torus equilibria and avoid the assumptions related to the statistical properties of the stochastic magnetic field, a radially bounded stochastic magnetic field is created by superposing three Fourier harmonics of the perturbed magnetic field which resonate at the rational surfaces to a axisymmetric MHD equilibrium. Due to the radial boundedness, the statistical properties of such a stochastic magnetic field are completely different from those used in the previous works [15, 16, 17, 18, 20, 21]. Especially, the radially bounded stochastic magnetic field has a finite correlation length in the radial direction. It is opposite to the quasi-linear approximation [15, 16, 17] where usually the radial (perpendicular) correlation length is treated as infinity by assuming radially infinite homogeneous stochastic field.

By changing the amplitude of the perturbed magnetic field, several types of the radially bounded magnetic field region are created: region with isolated island chain before the overlapping threshold ($s_b/s_{bc} < 1$), region with overlapped magnetic islands near the overlapping threshold ($s_b/s_{bc} \sim 1$), stochastic sea with regular structures ($s_b/s_{bc} > 1$), and stochastic sea without structures ($s_b/s_{bc} \gg 1$). The stochasticity parameter s_b corresponds to the strength of perturbation, and s_{bc} is the value of the stochasticity parameter at the overlapping threshold. One aspect of the stochasticity of the resonantly perturbed magnetic field is understood from the temporal behaviour of the effective radial Liapunov exponent $\langle l_e(t)\rangle$ and the number of the magnetic field lines with the positive Liapunov exponent $N_p(t)$, where time t is used as the independent variable. The conversion into the length along the equilibrium field direction is performed as $z \sim R\zeta \sim v_{||}t$ with the major radius R and the parallel velocity of particle $v_{||}$ tied to the magnetic field line. Before overlapping with $s_b/s_{bc} < 1$, the number of the magnetic field lines with the positive Liapunov exponent $N_p(t)$ is zero or quite a few, and the effective radial Liapunov exponent $\langle l_e(t)\rangle$ is always negative. After, overlapping with $s_b/s_{bc} \geq 1$, i.e. in the region of global magnetic stochasticity, N_p almost monotonically increases with time, finally leading to the saturation. As $s_b/s_{bc}(\geq 1)$ increases, the saturated value of N_p increases, i.e. from $N_p < N$ for $s_b/s_{bc} \geq 1$ to $N_p = N$ for $s_b/s_{bc} \gg 1$, where N is the total number of observed field lines. The existence of the magnetic field lines with the negative Liapunov exponent for $s_b/s_{bc} \geq 1$ indicates importance of sticking to regular structures inside the stochastic region. Associated with the variation of $N_p(t)$, $\langle l_e(t)\rangle$ almost monotonically increases from negative to positive value, finally leading to asymptotic saturation, as time t increases. In spite of the various stochasticity levels depending on s_b/s_{bc}, after overlapping, the effective radial Liapunov exponent is for all $s_b/s_{bc} \geq 1$ described as $\langle l_e(t)\rangle = \langle l_e\rangle(1 - t_d/t)$, where t_d is the decorrelation time of the magnetic field lines satisfying $\langle l_e(t_d)\rangle = 0$, and $\langle l_e\rangle$ is the saturated value of $\langle l_e(t)\rangle$. In other words, the effective radial Liapunov exponent is characterized by two independent quantities t_d and $\langle l_e\rangle$. Recognizing $t_d v_{||}$ as the parallel correlation length of the magnetic field lines: $L_{||} \equiv t_d v_{||}$, and defining the

Liapunov length $L_K \equiv v_{||}/\langle l_e \rangle$, both the parallel correlation length $L_{||}$ and the Liapunov length L_K decrease as $s_b/s_{bc}(\geq 1)$ increases. Since the perpendicular (radial) correlation length of the magnetic field lines $L_\perp \approx w_{st}$, where w_{st} is the radial width of the stochastic region, $L_\perp \ll L_K \ll L_{||}$ holds independent of $s_b/s_{bc} \geq 1$ in the considered cases. Note that this ordering is different from that of the usual quasi-linear approximation. To obtain the statistically meaningful results, the calculations are performed up to $z \gg L_{||}$ or $t \sim t_s = 10 \times t_d \gg t_d$, where t_s is defined as a time satisfying $\langle l_e(t_s) \rangle / \langle l_e \rangle = 0.9$. The evaluation in the long time limit is done at $t > t_s$ for $s_b/s_{bc} \geq 1$ or at $t \gg \langle t_b \rangle$ for $s_b/s_{bc} < 1$, where $\langle t_b \rangle$ is a typical time of particle motion trapped by the islands. As $s_b/s_{bc}(\geq 1)$ increases, the dispersion of the effective radial Liapunov exponent Δl_e decreases, which means that all the magnetic field lines have a tendency to radially spread with almost same exponential divergence rate.

The statistical properties of the magnetic field stochasticity are examined by evaluating the cumulant coefficients up to fourth order, the effective diffusion coefficient, and autocorrelation coefficient $A(t,t')$ between two different times t and t'. Due to the above mentioned fast exponentiation of the magnetic field lines in a radially bounded stochastic magnetic field region, the relaxation of the magnetic field stochasticity or particles tied to magnetic field lines without the perpendicular drift and Coulomb collisions has a tendency to become a uniform mixing process, as $s_b/s_{bc}(\geq 1)$ increases. Namely, the stochastic process which is characterized by non-diffusivity (diffusion exponent $\alpha \sim 0$), uniform distribution, statistical stationarity, and Markovianity after the correlation time $\tau_{corr} \approx t_d$ which is estimated from the exponentially vanishing autocorrelation coefficient: $A(t,t') \sim A(\tau = t' - t) \sim \exp(-t/\tau_{corr})$. A clear uniform mixing process is obtained for $s_b/s_{bc} \gg 1$. When the regular structures exist inside stochastic sea, the magnetic field stochasticity appears as one of the strange diffusive processes in the long time limit. Within the stochastic sea with regular structures the magnetic stochasticity appears as a strange diffusive process characterized by non-diffusivity, uniform like broad distribution, statistical stationarity and power-law autocorrelation coefficient: $A(t,t') \sim A(\tau = t' - t) \sim \tau^c$ with a positive constant c. On the other hand, near the overlapping threshold with $s_b/s_{bc} \sim 1$, where the regular structures become more significant, the magnetic field stochasticity appears as a strange diffusive process with subdiffusivity ($\alpha < 1$), distribution far from uniform and Gaussian, statistical non-stationarity. Sticking of the magnetic field lines to or around regular structures inside the stochastic region leads to the space and time correlations compared with uniform mixing process, so that in these strange processes non-Markovianity may be suggested.

The uniform mixing process and the strange processes are related to the non-locality. Particles tied to the stochastic magnetic field lines easily spread out in the radial direction and reach up to the boundary, so that the radial displacement δr is prescribed by the radial width of the stochastic region w_{st} : $\delta r \sim w_{st}$, leading to the non-locality of the

radial diffusion where $\delta r/a \leq \delta r/w_{st} \leq 1$ with the minor radius a as the scale length of the system.

The deviation of the particle orbits by the collisionless perpendicular drift motion from the stochastic magnetic field qualitatively do not change the above mentioned statistical properties of the radial diffusion of particles tied to stochastic magnetic field lines, except for generation of the small correlation of $A(t,t')$ after τ_{corr} for $s_b/s_{bc} \gg 1$. Hence, it is concluded that the stochastic properties of the collisionless particle radial diffusion are almost all determined by those of the stochastic magnetic field lines. The reason is due to the fact that the parallel drift velocity of particles along the stochastic magnetic field is quite larger that the perpendicular drift velocity. The fast parallel drift motions along the stochastic magnetic field themselves make the stochastic radial displacement quite larger than that due to the slow perpendicular drift motions.

In the presence of the Coulomb collisions, the Coulomb collisions interrupts the fast parallel motion along the stochastic magnetic field lines. The range of the collision frequency considered here is from the neoclassical plateau regime with $\nu/\nu_t < 1$, to Pfirsch-Schlüter regime with $\nu/\nu_t > 1$ and $\nu/\nu_t \gg 1$, where ν_t is the transit frequency of particles in the regular magnetic field. Since $\tau_c < \langle t_b \rangle$ and $\tau_c < t_s$ hold, the long time limit is defined as $t > \max(t_s, \tau_c) = t_s$ for $s_b/s_{bc} \geq 1$, and as $t \gg \max(\langle t_b \rangle, \tau_c) = \langle t_b \rangle$ for $s_b/s_{bc} < 1$, where τ_c is the collision characteristic time, defined as $\tau_c = 1/\nu$. As $s_b/s_{bc}(\geq 1)$ increases, both the Liapunov length L_K and the parallel correlation length $L_{||}$ become shorter with keeping the inequality $L_\perp \ll L_K \ll L_{||}$. The significance of collisional scattering of parallel drift motions for $s_b/s_{bc} \geq 1$ are qualitatively determined by the relative magnitude of the mean free path λ_{mfp} to characteristic lengths of the stochastic magnetic field lines: $L_\perp, L_K$, and $L_{||}$, especially the relative magnitude between λ_{mfp} and L_K is important. When $\lambda_{mfp} \ll L_K$, the collisional interruption of the parallel drift along the stochastic magnetic field lines becomes significant. In opposite, when $\lambda_{mfp} \gg L_K$ particles spread out in the radial direction along the stochastic magnetic field lines before they suffer significant scattering due to collisions. Thus, the collisions become significant as s_b/s_{bc} decreases for a fixed ν/ν_t or as ν/ν_t increases for a fixed s_b/s_{bc}. Before overlapping with $s_b/s_{bc} < 1$, $\langle l_e(t) \rangle$ is always negative, thus the collisional scattering are more significant that after overlapping with $s_b/s_{bc} \geq 1$. So, as ν/ν_t decreases and as s_b/s_{bc} increases, the particle radial diffusion reflects the statistical properties of the magnetic field stochasticity, and behaves as a strange diffusive process with subdiffusivity, profile neither uniform nor Gaussian, statistical stationarity. The autocorrelation coefficient is power-law like, non-stationary, $A(t,t') \equiv A(t, \tau = t' - t)$, and non-locality of the stochastic process still remains by reflecting fast parallel motion along the stochastic magnetic field lines. The Markovianity is still open question. In opposite limit, namely, in the region with $\nu/\nu_t \gg 1$ and $s_b/s_{bc} \leq 1$, the collisional scattering of parallel drift motions becomes so significant that the stochastic radial particle displacements are created not by parallel drift motion-

s along the stochastic field lines, but by the collisional scattering of the perpendicular drift motions, leading to Wiener process through recovering the locality of the stochastic process.

The normal diffusivity with time independent diffusion coefficient is obtained only in the Wiener domain, where locality of the diffusion is ensured. In other processes, time dependent diffusion coefficient in subdiffusive process or non-diffusivity are obtained, where the locality of the diffusion process is not ensured. In the present situations with radially bounded stochastic magnetic region, the subdiffusivity appears associated with the non-locality of the stochastic process. In such a non-local process, the diffusion coefficient defined by the time derivative of the second cumulant does not have the clear physical meaning, or rather the second cumulant itself is a good indicator of the process but not sufficient. Note that the diffusion coefficient is introduced through standard phenomenological Fick's law based on the locality of the diffusion process, hence if the locality is not ensured, than such a Fick's law does not hold as it is. Additionally, the time development of the second cumulant for $s_b/s_{bc} \geq 1$ and $\nu/\nu_t = 0$, indicated the universality of the short time ($t < t_d$) dynamical relaxation phase (ballistic phase). However, in the long time limit ($t > t_s$) process appears as a strange diffusive process when the fast exponentiation of the stochastic magnetic field lines is suppressed by the stikness to the regular structures within the radially bounded stochastic region, or the uniform mixing in the absence of regular structures. These aspects suggest reconsideration of the radial diffusion process from the viewpoint of the general Brownian motion and non-local transport theory.

Tables

Table 1: The maximum deviation of the autocorrelation coefficients, $|y|$, from the Wiener value $y = 0$ in the banana, plateau and Pfirsch-Schlüter regimes, with respect to the different starting times t/τ_s.

t/τ_s	$\nu/\nu_t = 0.0045$	$\nu/\nu_t = 0.45$	$\nu/\nu_t = 4.5$
0.5	0.2014	0.1009	0.0772
1	0.1753	0.0548	0.0744
2	0.1157	0.0383	0.0729
3	0.0970	0.0426	0.0438
5	0.0553	0.0181	0.0251

Table 2: The average value of the deviation y from the Wiener one $\langle y \rangle = 0$ in the banana, plateau and Pfirsch-Schlüter regimes, respectively.

t/τ_s	$\nu/\nu_t = 0.0045$	$\nu/\nu_t = 0.45$	$\nu/\nu_t = 4.5$
0.5	0.0407	0.0050	0.0190
1	0.0567	0.0137	0.0274
2	0.0525	0.0061	0.0275
3	0.0416	0.0122	0.0162
5	0.0283	0.0001	0.0115

Table 3: The values of the diffusion exponent α in the long time limit in the parameter space $(s_b/s_{bc}, \nu/\nu_t)$.

$\nu/\nu_t \backslash s_b/s_{bc}$	0.33	1.3	3.3	33
$0(v_{d\perp} = 0)$	*osc.* ~ 0.0	0.40	0.01	0.02
$0(v_{d\perp} \neq 0)$	*osc.* ~ 0.0	0.29	0.01	0.02
0.45	0.73	0.63	0.30	0.07
4.5	0.97	0.92	0.52	0.12
45	1.07	1.00	1.04	0.22

Table 4: The values of the effective diffusion coefficient $D(t)$,D_{pw} and $\Delta D(\%)$ in the long time limit in $(s_b/s_{bc}, \nu/\nu_t)$ parametric space. In the circumstancies when ΔD becomes enormously high (e.g. $\geq 100\%$) the system behaviour is noted as the exponentially like. Note that in the presence of collisions $D(t)$ and D_{pw} are normalized by the corresponding neoclassical value D_{nc}.

$\nu/\nu_t \backslash s_b/s_{bc}$	0.33	1.3	3.3	33
$0(v_{d\perp}=0)$	osc.	0.079	0.26	0.60
	osc.	0.18	3.3	100
		(1%)	(exp.)	(exp.)
$0(v_{d\perp}\neq 0)$	osc.	0.042	0.26	0.62
	osc.	0.13	3.3	80.0
		(10%)	(exp.)	(exp.)
0.45	4.08	4.7	67.1	93.0
	5.2	7.7	190	1170
	(7.5%)	(6.5%)	(15%)	(11%)
4.5	1.2	2.2	14.0	38.1
	1.2	2.5	25.	270.
	(0.6%)	(2.7%)	(7.2%)	(5.0%)
45	1.01	1.10	1.85	4.5
	0.96	1.02	1.8	20.
	(2%)	(2.3%)	(0.1%)	(3%)

Table 5: The time behaviour of the autocorrelation coefficient in the parametric space $(s_b/s_{bc}, \nu/\nu_t)$.

$\nu/\nu_t \backslash s_b/s_{bc}$	0	0.33	1.3	3.3	33
$0(v_{d\perp}=0)$		osc.	P_{osc}	P_{st}	E
$0(v_{d\perp}\neq 0)$		osc.	P_{osc}	P_{st}	E_{corr}
0.45	P_W	P_f	P_f	P_f	P_f
4.5	P_W	P_W	P_f	P_f	P_f
45	P_W	P_W	P_W	P_W	P_f

Table 6: The values of the $C_1(t)$ in the long time limit.

$\nu/\nu_t \backslash s_b/s_{bc}$	0.33	1.3	3.3	33
$0(v_{d\perp}=0)$	1.5×10^{-4}	5.7×10^{-3}	-5×10^{-3}	-6×10^{-3}
$0(v_d\neq0)$	2.0×10^{-4}	6.2×10^{-3}	-6.5×10^{-3}	-5×10^{-3}
0.45	2.0×10^{-5}	1.4×10^{-3}	2.0×10^{-4}	-6.0×10^{-3}
4.5	-3.0×10^{-5}	1.1×10^{-3}	8.0×10^{-4}	-4.0×10^{-3}
45	3.0×10^{-4}	2.9×10^{-3}	1.1×10^{-3}	-1.0×10^{-3}

Table 7: The values of γ_3 in the long time limit in $(s_b/s_{bc}, \nu/\nu_t)$ parametric space.

$\nu/\nu_t \backslash s_b/s_{bc}$	0.33	1.3	3.3	33
$0(v_{d\perp}=0)$	osc.	0.60	-0.08	-0.13
$0(v_{d\perp}\neq0)$	osc.	0.60	-0.02	-0.18
0.45	0.0	0.70	-0.20	-0.11
4.5	0.05	0.25	-0.15	-0.15
45	0.045	0.10	0.02	-0.17

Table 8: The kurtosis in the long time limit in $(s_b/s_{bc}, \nu/\nu_t)$ space.

$\nu/\nu_t \backslash s_b/s_{bc}$	0.33	1.3	3.3	33
$0(v_{d\perp}=0)$	osc.	1.8	-0.95	-1.15
$0(v_{d\perp}\neq0)$	osc.	1.7	-0.95	-0.85
0.45	-0.05	3.0	-0.15	-1.1
4.5	-0.05	1.7	1.4	-1
45	-0.1	0.02	0.6	-0.8

Table 9: The type of statistical process.

$\nu/\nu_t \backslash s_b/s_{bc}$	0	0.33	1.3	3.3	33
$0(v_{d\perp}=0)$			S_{osc}	S_{st}	U
$0(v_{d\perp}\neq0)$			S_{osc}	S_{st}	U_{corr}
0.45	W	S	S	S	S
4.5	W	W	S	S	S
45	W	W	W	W_P	S

Table 10: The relation of the characteristic times in $(s_b/s_{bc}, \nu/\nu_t)$ parametric space: $\langle t_b \rangle/\tau_c$ for $s_b/s_{bc} = 0.33$, and t_d/τ_c for $s_b/s_{bc} > 1$. The time $\langle t_b \rangle$ is the characteristic time for trapping by island, τ_c is the collisional characteristic time, and t_d is the magnetic field decorrelation time.

$\nu/\nu_t \backslash s_b/s_{bc}$	0.33	1.3	3.3	33
0.45	1.6	120	20	18
4.5	16	1200	200	180
45	160	12000	2000	1800

Table 11: The ordering of the characteristic lengths: $L_{||}$ the parallel characteristic length, $L_\perp$ the perpendicular characteristic length, L_K the Liapunov length, and λ_{mfp} the mean free path; with respect to $s_b/s_{bc} \geq 1$ and $\nu/\nu_t > 0$ parameter space.

$\nu/\nu_t \backslash s_b/s_{bc}$	1.3	3.3	33
0.45	$L_\perp \ll \lambda_{mfp} \ll L_K \ll L_{||}$	$L_\perp \ll \lambda_{mfp} < L_K \ll L_{||}$	$L_\perp \ll L_K \ll \lambda_{mfp} < L_{||}$
4.5	$L_\perp \ll \lambda_{mfp} \ll L_K \ll L_{||}$	$L_\perp \ll \lambda_{mfp} \ll L_K \ll L_{||}$	$L_\perp \ll \lambda_{mfp} < L_K \ll L_{||}$
45	$L_\perp < \lambda_{mfp} \ll L_K \ll L_{||}$	$L_\perp < \lambda_{mfp} \ll L_K \ll L_{||}$	$L_\perp < \lambda_{mfp} \ll L_K \ll L_{||}$

References

[1] Klimontovich Yu. L. *Statistical Theory of Open Systems* (Kluwer Academic Publishers, 1995)

[2] Krilov N. S. *The Foundations of Statistical Physics* (Princeton University Press, Guildford, Surrey, 1979)

[3] Montroll E. W. and Shlesinger M. F. *Nonequilibrium Phenomena II: From Stochastics to Hydrodynamics* (Eds. Lebowitz J. L. and Montroll E. W., 1984)

[4] Balescu R. *Matter out of Equilibrium* (Imperial Collage Press, 1997)

[5] Gardiner C. W. *Hanbook of Stochastic Methods for Physics, Chemistry and the Natural Sciences* (Springler-Verlag, 1983)

[6] Bouchand J-P and Georges A. *Physics Reports* **195** No.4& 5 (1990) 127

[7] MacKay R. S., Meiss J. D. and Percival I. C. *Physica* **13D** (1984) 55

[8] Zaslavsky G. M. and Edelman M. *Chaos* **7** No.1 (1997) 159

[9] Shlesinger M. F., Zaslavsky G. M. and Klafer J. *Nature* **31** (1993) 363

[10] Klafter J., Shlesinger M. F. and Zumofen G. *Physics Today* (1996) 33

[11] Hinton F. L. and Hazeltine R. D. *Rev. Mod. Physics* **48** (1976) 309

[12] Hirshman S. P. and Sigmar V. D. *Nuclear Fusion* **21** (1981) 1079

[13] Lihtenberg A. J. and Lieberman M. A. *Regular and Chaotic Dynamics* (Springer-Verlag, 1992)

[14] Kadomtsev B. B. and Podguse O. P. *Plasma Physics and Controlled Nuclear Fusion Research* **1** (1979) 649

[15] Rechester A. B. and Rosenbluth M. N. *Phys. Rev. Lett.* **40** (1978) 38

[16] Kromers J. A., Oberman C. and Kleva R. G. *Journal of Plasma Physics* **30** (1983) 11

[17] Ishichenko M. B. *Plasma Physics and Controlled Fusion* **33** No.7 (1991) 795

[18] Wang H-D, Vlad M, Vandau E. E., Spineanu F, Misquich J. H. and Balescu R *Phys. Rev. E* **51** No.5 (1995) 4844

[19] Vanden E. E. and Balescu R. *Phys. Plasmas* **3** No.3 (1995) 815

[20] Balescu R., Wang H-D and Misquich J. H. *Phys. Plasmas* **1** (1994) 3826

[21] Balescu R. *Phys. Rev. E* **51** No.5 (1995) 4807

[22] Vandan E. E. and Balescu R. *Phys. Plasmas* **3** No.3 (1996) 874

[23] Rax J. M. and White R. B. *Journal of Plasma Physics* **68** No.10 (1992) 1523

[24] Boozer A. H. and White R. B. *Phys. Rev. Lett.* **49** No.11 (1982) 786

[25] White R. B. *Statistical Physics and Chaos in Fusion Plasma* (John Wiley, 1984)

[26] Boozer A. H. and Kuo-Petravic G. 1981 *Phys. Fluids* 24 (1981) 851

[27] Tabet R., Saifoani D., Dezairi A. and Raonak A. *Eur. Phys. J.* **AP4** (1998) 329

[28] Oudyoudine A., Saifoauri D., Dezairi A. and Raonak A. *J. Phys. III France* **17** (1997) 1045

[29] Balescu R. *Physical Review E* **55** No.3 (1997) 2465

[30] Van-Kampen N. G. *Stochastic Processes in Physics and Chemistry* (North-Holland, 1981)

[31] Dubkov A. A. and Malakhov A. N. *Radiophys. Quantum Electron.* **19** (1977) 833

[32] Maluckov A., Nakajima N., Okamoto M., Murakami S. and Kanno R. *Research report Nifs Series*-689 (2001)

[33] Feller W. *An Introduction to Probability Theory and Its Applications* **I,II** (John Wiley and Sons, 1966)

[34] Zaslavsky G. M. and Chirikov B. V. *Soviet Physics Uspekhi* **14** No.5 (1972) 549

[35] Littlejohn R. G. *Journal of Plasma Physics* **29** (1983) 111

[36] White R. B. *in Magnetic Reconnection and Turbulence* (ed. by Dubois M. A., Gresillon D. and Bussac M. N., Les Editions de Physique, Orsay, 1985)

[37] Littlejohn R. G. *Phys. Fluids* **24** (1981) 1730

[38] D'haesleer W. D., Hitchon W. N. G., Collen J. D., and Shohet J. L. *Flux Coordinates and Magnetic Field Structure* (Springer-Verlag, 1991)

[39] Boozer A. H. *Phys. Fluids* **24** (1981) 1999

[40] White R. B., Boozer A. H., and Hay R. *Phys. Fluids* **25** No.3 (19982) 575

[41] Hazeltine R. D. and Meiss J. D. *Plasma Confinement* (Addison-Wesley Publishing Company, 1992)

[42] White R. B. *Theory of Tokamak Plasma* (North-Holland, 1989)

[43] Wakasa A., Murakami S., Maassberg H., Beidler C. D., Nakajima N., Watanabe K., Yamada H., Okamoto M., Oikawa Sh. and Itagaki M. *JPFR SERIES* **3** (2001) in press

[44] Lotz W. and Nührenberg J. *Phys. Fluids* **31** (1988) 2984

[45] Abramowitz M. and Stegun A. I. *Handbook of Mathematical Functions* (Dover Publications, Inc., New York, 1972) 772

[46] Benettin G., Galgani L. and Strelcyn J-M *Physical Review A* **14** No.6 (1976) 2338